Dissertation
submitted to the
Combined Faculties of the Natural Sciences and Mathematics
of the Ruperto-Carola-University of Heidelberg. Germany
for the degree of
Doctor of Natural Sciences

Put forward by
Moritz Tillmann Boeckel
born in: Friedberg(Hessen), Germany
Oral examination: June 8^{th} 2011

A Little Inflation at the Cosmological QCD Phase Transition

Referees: Professor Jürgen Schaffner-Bielich
Professor Michael G. Schmidt

Topic in German

In dieser Dissertation untersuche ich ein neues Szenario welches im frühen Universum für die Quantenchromodynamik (QCD) einen starken Phasenübergang erster Ordnung bei nicht verschwindender Baryonendichte ermöglicht und diskutiere mögliche beobachtbare Konsequenzen. Nach Einführungen in wichtige Aspekte der zugrunde liegenden Felder der QCD und der Kosmologie diskutiere ich die Möglichkeit einer kurzen inflationären Phase am kosmologischen QCD Phasenübergang. Ein starker Baryogenese-Mechanismus is notwendig um die benötigte Baryonasymmetrie der Größenordung eins voraussetzen zu können, eine Möglichkeit wäre dabei die sogenannte Affleck-Dine Baryogenese die ebenfalls diskutiert wird. Die zweite Kernannahme dieses "kleine Inflation"-Szenarios ist ein quasistabiler QCD-Vacuumzustand der eine kurze Periode der exponentiallen Expansion verursacht und dabei das Verhältnis von Baryonen zu Photonen auf den Heute beobachteten Wert verdünnt. Die kosmologischen Auswirkunge sind unter anderem eine direkte Modifikation der primordialen Dichtefluktuationen bis zu einer Massenskala der dunklen Materie von $M_{med} \sim 1M_{\odot}$, eine Änderung in der spektralen Steigung bis zu $M_{max} \sim 10^6 M_{\odot}$, Produktion von starken primordialen Magnetfeldern und eines Gravitationswellen-Spektrums das von zukünftigen Pulsarlaufzeit-Gravitationswellen-Detektoren beobachtet werden könnte.

Topic in English

In this thesis I explore a new scenario that allows for a strong first order phase-transition of quantum chromodynamics (QCD) at non-negligible baryon density in the early universe and its possible observable consequences. After an introduction to important aspects of the underlying fields of QCD and cosmology I discuss the possibility of a short inflationary phase at the cosmological QCD phase transition. A strong mechanism for baryogenesis is needed to start out with a baryon asymmetry of order unity, e.g. as provided by Affleck-Dine baryogenesis which is also discussed within the thesis. The second main assumption for this "little inflation" scenario is a quasistable QCD-vacuum state that leads to a short period of exponential expansion consequently diluting the net baryon to photon ratio to today's observed value. The cosmological implications are among other things direct effects on primordial density fluctuations up to length scales corresponding to an enclosed dark matter mass of $M_{med} \sim 1M_{\odot}$, change in the spectral slope up to $M_{max} \sim 10^6 M_{\odot}$, production of strong primordial magnetic fields and a gravitational wave spectrum that could be observed by future pulsar timing gravitational wave detectors.

Acknowledgements

I would like to thank all the people who have directly or indirectly supported me during the last three and a half years and without whom this work could not have been completed.

First of all I would like to thank my professor Jürgen Schaffner-Bielich for supporting and supervising my doctoral thesis. The basic ideas that lead to this thesis were developed with him during many interesting discussions and without his continuous support the thesis could not have taken shape.

Furthermore I want to thank our compact stars and cosmology group for a warm and pleasant working atmosphere. I would like to thank Irina Sagert, Giuseppe Pagliara, Andreas Lohs, Debarati Chatterjee, Simon Weissenborn, Bruno Mintz and Basil Sa'd. Special thanks go to the two other cosmo-guys Rainer Stiele and Simon Schettler for countless discussions about many problems related to the thesis. I am also very grateful to Matthias Hempel for numerous chats about complicated topics that often helped a lot in improving my understanding.

I am indebted to my second supervisor professor Michael Schmidt for interesting discussions about the thesis and related topics.

Tina Straße cannot be thanked enough for always being a good friend next door whenever I was in need of one. Additional thanks go to her, Soniya Savant and Sandeep Botla for making our Dossenhome such a great place to live. I also want to thank Ilja Doroschenko for many laughs and unfortunately far too few encounters in the last years. Furthermore I want to thank all the other people that made my time in Heidelberg unforgettable, most importantly Florian Marhauser, Julia Schaper, Katja Weiß and Florian Freundt.

And last but not least I am deeply grateful to my parents and my siblings for their love, support and encouragement throughout the years. They always had an open ear and were ready to help in any situation.

Contents

Chapter 1

Introduction

The standard models of cosmology and particles physics provide excellent descriptions of the universe from an early stage up to the present day. In the last two decades a wealth of observations has confirmed many predictions of the theory hot big bang while on the other hand opening up many new questions, for example about the nature of dark matter and dark energy. However, there are still some long standing questions unanswered like the origin and size of the asymmetry between matter and antimatter, the source of magnetic fields in galaxies or the existence of gravitational waves.

An important prediction of these standard models are a set of phase transitions most notably the electroweak phase transition and the phase transitions of quantum chromodynamics (QCD). The former taking place at temperatures about 200 GeV is nowadays assumed to be a crossover at least without including physics beyond the standard model. The latter transition from the quark-gluon plasma to a hadron gas should have happened at a temperature of about $T_{QCD} \approx 150 - 200$ MeV merely 10^{-5} sec after the big bang. The cosmic QCD phase transitions was extensively discussed in the 80s and 90s by numerous authors [1, 2, 3, 4, 5, 6] mostly with a focus on magnetic field production and the generation of baryon inhomogeneities that could affect big bang nucleosynthesis. At the time it was commonly assumed that the phase transition was of first order allowing for nucleation and bubble collisions that would provide an environment in which magnetic fields, gravitational waves and baryon inhomogeneities could be generated.

Lattice gauge theory calculations have shown in the last decade that the phase transitions of QCD at zero baryon density are most probably only a rapid crossovers [7, 8]. This is relevant for the early universe since in standard cosmology the baryon asymmetry is tiny $\eta_B = n_B/s \sim 10^{-9}$, where n_B is the net baryon density and s the entropy density, as deduced from later stages in the evolution of the universe. Thus the common notion became that the cosmological QCD phase transition occurred in conditions that made a first order phase transition very unlikely. A sketch of a possible QCD phase diagram is depicted in figure 4.1 along with the commonly accepted path the universe took during and after the transition. The universe started out in the upper left and moved along the temperature axis from the chirally symmetric quark gluon plasma through a crossover transition to the chirally broken hadron gas phase. At this point one might ask if there is a simple scenario with the cosmological QCD phase transition being first order without violating the constraint of a small baryon asymmetry in the later evolution of the universe. The

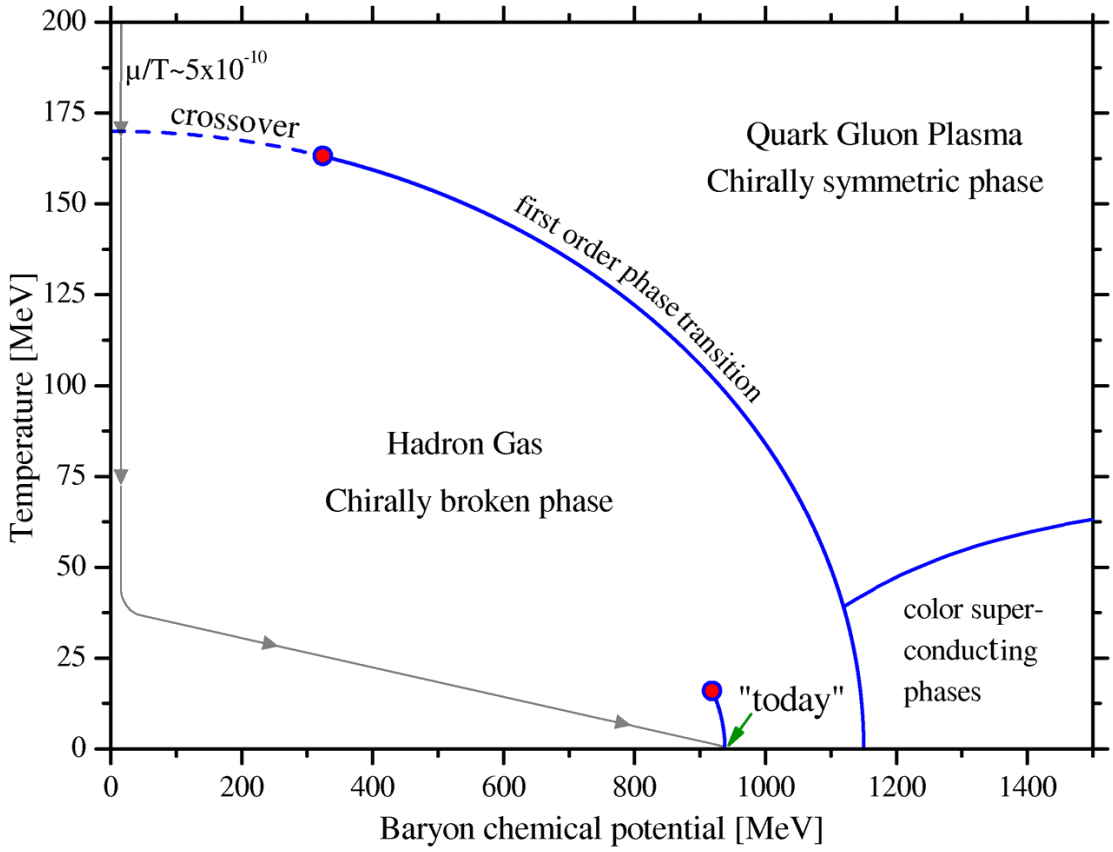

Figure 1.1: Sketch of a possible QCD-phase diagram with the commonly accepted standard evolution path of the universe as calculated e.g. in [9] depicted by the grey path.

little inflation scenario which is the topic of this thesis [10, 11, 12] allows for such a first order QCD phase transition in the early universe without being in contradiction to present cosmological observations. After introductions to the relevant aspects of QCD and cosmology we will return to this question and outline how a little inflationary phase would allow a cosmological QCD phase transition to be first order and what the implications would be.

This work is organized as follows:

The basics of QCD are introduced in the second chapter. We will discuss the most important basics of chiral symmetry with an emphasis on symmetries and effective models. In particular we will explain the structure of the linear sigma model with quarks and its extension with a dilaton field.
In the third chapter we will first quickly discuss the basics of cosmology. Then

we will explain in detail the theory of linear density perturbations in cosmology with focus on a certain gauge that we will use later on. Furthermore we discuss standard inflation and baryogenesis with an emphasis on the mechanism of Affleck-Dine baryogenesis.
Finally in chapter four we introduce the "little inflation" scenario in contrast to the standard picture of the cosmological QCD phase transition. Then we will examine constraints on the duration of such a little inflationary phase before we discuss the issue of nucleation. We will examine the differences for small scale density perturbations and possible implications for structure formations. Furthermore changes to dark matter physics, the generation of magnetic fields and gravitational waves will be topics to be discussed in the context of this new scenario.

Chapter 2

QCD

Three quarks for Muster Mark!
Sure he has not got much of a bark
And sure any he has it's all beside the mark.

– James Joyce, *Finnegans Wake*

2.1 Introduction

It has been widely accepted for several decades that quantum chromodynamics (QCD) is the correct theory describing the strong nuclear interaction. The first important step towards the understanding of the strong interaction was probably done by Yukawa in 1935. He theorized that the protons and neutrons interact via the exchange of a massive virtual field quantum explaining why the nuclear forces are short range. The uncertainty principle would allow the creation of such a field quantum if

$$\Delta E \Delta t = mc^2 \Delta t \sim \hbar \tag{2.1}$$

here c is the speed of light and $\hbar$ is Planck's constant[1]. Since the range of the nuclear interaction is roughly $r \approx 1$fm this suggests a lifetime of

$$\Delta t \sim \frac{r}{c} \approx \frac{1}{200\text{MeV}}. \tag{2.2}$$

This means that one should expect a field quantum with a mass of

$$mc^2 \approx \frac{\hbar c}{r} \approx 200\text{MeV}. \tag{2.3}$$

When the strongly interacting π-meson was discovered by Perkins in 1947 with a mass of ~ 140 MeV this seemed to give strong support for Yukawa's theory[2].

When more and more mesons were discovered in the 1950s and 60s it became clear that the pion was not special at all apart from being the lightest meson. Furthermore scattering experiments showed that pion exchange could not properly describe high energy proton-neutron interactions and could not account for the strong interaction among pions themselves. Hadrons turned out to be the observed physical degrees of freedom of the strong interaction at low temperatures and density but not the elementary constituents of the strong interaction. In 1964 Murray Gell-Mann [13] and George Zweig [14, 15] independently found a system to categorize the previously chaotic zoo of hadrons with what Gell-Mann called the Eightfold Way[3] due to the underlying SU(3) symmetry that has eight independent generators. In the following decade the quantum field theory behind this symmetry, QCD, was developed that introduced quarks and gluons as fundamental degrees of freedom. QCD has two remarkable properties: confinement, which denotes that

[1] Later on we will use natural units throughout this thesis so $c = \hbar = k_B = 1$ if not stated differently.

[2] For some time the muon (discovered in 1936) was sometimes interpreted to be the field quantum of the strong interactions because its mass seemed to match the expectation with ~ 100 MeV until it became clear that it does not interact strongly.

[3] A reference to the Noble Eightfold Path in Buddism.

at low energies the quarks inside a hadron cannot be separated because the force between them increases linearly with distance. And secondly asymptotic freedom, which means that at very high momentum (and small distances) the interactions between quarks and gluons become weaker and weaker until they can be treated as quasi-free particles. Thus if matter is heated and/or compressed sufficiently strong interactions should become weaker and weaker until a new state of matter is formed in which the individual quarks are no longer associated to a fixed bound state but can travel rather freely. This deconfined and asymptotically free phase of strongly interacting matter is called Quark-Gluon Plasma (QGP). It should have been present in the early universe at sufficiently high temperatures as we will discuss later. It might still exist in the present universe in certain types of compact stars called quark or hybrid stars [16] and it can most probably be produced in heavy ion collisions[4]. The latter discovery was announced after experiments at the SPS at CERN in 2000 and later on also at the Relativistic Heavy-Ion Collider (RHIC) located at Brookhaven National Laboratory.

QCD is based on the invariance under the non-abelian SU(3) gauge transformations. Let us now have a look at the Lagrange density of QCD and then discuss some of its properties.

$$\mathcal{L}_{QCD} = \sum_f \left[\bar{\psi}_f \left(\not{D} - m_f\right) \psi_f\right] - \frac{1}{4} G^a_{\mu\nu} G^{a\mu\nu} \tag{2.4}$$

Here the interactions are hidden both in the covariant derivative D^μ as well as in the square of the field strength tensor $G^a_{\mu\nu}$

$$\begin{aligned} \not{D} &= i\gamma^\mu \left(\partial_\mu - ig\mathcal{A}_\mu\right) \\ G^a_{\mu\nu} &= \partial_\mu \mathcal{A}^a_\nu - \partial_\nu \mathcal{A}^a_\mu - igf^{abc}\left[\mathcal{A}^b_\mu, \mathcal{A}^c_\nu\right] \\ \mathcal{A}_\mu &= T^a A^a_\mu \end{aligned} \tag{2.5}$$

Here A^a_μ are the eight color gauge fields, m_f are the quark masses, γ^μ are the Dirac gamma-matrices, f^{abc} are the $SU(3)$ structure constants and T^a are the generators of the gauge transformations. The quark fields ψ_f come in the six flavors up, down, strange, charm, bottom and top and carry one of three color charges. The gluon fields are mostly characterized by their color index[5] $a = 1, ..., 8$. This Lagrangian describes the strong interactions between quarks via the exchange of

[4] See for example the review of Boyanovsky et al. [17] that compares the QCD phase transition in the big bang with the "little bang" in the laboratory.

[5] For a $SU(N_c)$ gauge theory there are $N_c^2 - 1$ independent gauge fields.

gluons that carry strong charge themselves. The latter is in contrast to the gauge field of quantum electrodynamics (QED), the photon, that does not carry electric charge, hence gluons can interact among themselves. The non-abelian structure of the QCD-Lagrangian is hidden in the product of the gluon field strength tensor that includes a self-interaction term arising from the non-vanishing commutator $\left[\mathcal{A}^b_\mu, \mathcal{A}^c_\nu\right]$. Thus three - and four-gluon interactions are possible that are absent for QED, where any interaction requires a charged fermion to be present.
Unfortunately this Lagrangian cannot be easily used to explain low energy properties of the strong interactions. The main reason is the running coupling constant of QCD [18, 19], i.e.

$$\alpha_s^2(p) = \frac{g^2(p)}{4\pi} \approx \frac{1}{\beta_0 \ln\left(\frac{p^2}{\Lambda^2_{\mathcal{QCD}}}\right)} \tag{2.6}$$

which is the equivalent of the fine structure constant in QED, is too large to allow a perturbative treatment in terms of Feynman diagrams at low energies. Here $\beta_0 = \frac{1}{4}(11 - 2N_f/3)$ and $\Lambda_{\mathcal{QCD}} \approx 220\text{MeV}$ is the QCD energy scale. At an energy of 500 MeV the coupling constant is still very large $\alpha_s(500\text{MeV}) \approx 0.5$ and only at very high energies it approaches so low values that perturbative expansions should converge quickly, e.g. $\alpha_s(90\text{GeV}) \approx 0.12$ [18, 19].
There are two main ways to address the mentioned difficulties, the first are lattice gauge theory approaches to QCD that try to solve the theory on a discretized spacetime [20, 21]. These approaches are mostly limited to vanishing baryon densities and require enormous amounts of computer power but progress in recent years has be steady. The second one are effective models [22] that try to mimic QCD by building Lagrangians that incorporate one or even several of its symmetries. The hope is that if one fits such an Lagrangian to important experimental constraints one may end up with a model that is reasonably close to full QCD to make meaningful predictions. We will follow the latter way and first examine several important symmetries of QCD before we will show how they may be represented in an effective description.

2.2 Noethers Theorem and Conserved Currents

To be able to discuss the important properties of QCD it is necessary to remind ourselves of the connection between symmetries of a theory and its conserved currents and charges. In this context it is common to consider the Lagrange density $\mathcal{L}(\Phi_\alpha, \partial_\mu \Phi_\alpha)$ of a given field $\Phi_\alpha(x)$ [23, 24, 25]. The action S is defined via the 4-volume Integral of the Lagrange density (or Lagrangian)

$$S = \int \mathcal{L}(\Phi_\alpha, \partial_\mu \Phi_\alpha)\, d^4x \tag{2.7}$$

Now let us consider a transformation of the fields

$$\Phi_\alpha(x) \rightarrow \Phi'_\alpha(x) = e^{-i\Omega^i_{\alpha\beta}\omega^i}\Phi^\beta(x) \tag{2.8}$$

where the $\Omega^i_{\alpha\beta}$ are the generators and ω^i are the parameters of the transformation [26]. Now for simplicity let us assume an infinitesimal transformation

$$\Phi_\alpha \rightarrow \Phi'_\alpha = \Phi_\alpha + \delta\Phi^i_\alpha \approx \left(1 - i\Omega^i_{\alpha\beta}\omega^i\right)\Phi_\alpha \tag{2.9}$$

$$\partial_\mu\Phi_\alpha \rightarrow (\partial_\mu\Phi_\alpha)' = \partial_\mu\Phi_\alpha + \delta(\partial_\mu\Phi_\alpha) \tag{2.10}$$

Using this we can calculate the variation of the Lagrangian

$$\begin{aligned}
\delta\mathcal{L} &= \mathcal{L}(\Phi'_\alpha, (\partial_\mu\Phi_\alpha)') - \mathcal{L}(\Phi_\alpha, \partial_\mu\Phi_\alpha) \\
&\approx \overbrace{\mathcal{L}(\Phi_\alpha, \partial_\mu\Phi_\alpha) + \frac{\partial\mathcal{L}}{\partial\Phi_\alpha}\delta\Phi^i_\alpha + \frac{\partial\mathcal{L}}{\partial(\partial_\mu\Phi_\alpha)}\delta(\partial_\mu\Phi_\alpha)} - \mathcal{L}(\Phi_\alpha, \partial_\mu\Phi_\alpha) \\
&\approx \frac{\partial\mathcal{L}}{\partial\Phi_\alpha}\delta\Phi^i_\alpha + \frac{\partial\mathcal{L}}{\partial(\partial_\mu\Phi_\alpha)}\partial_\mu(\delta\Phi^i_\alpha)
\end{aligned} \tag{2.11}$$

In the step from the second to the third line we have used that ∂_μ and δ commute on the linear level. Now let us use this result for the variation of the action

$$\begin{aligned}
\delta S &= \int d^4x \left(\frac{\partial\mathcal{L}}{\partial\Phi_\alpha}\delta\Phi^i_\alpha + \frac{\partial\mathcal{L}}{\partial(\partial_\mu\Phi_\alpha)}\partial_\mu(\delta\Phi^i_\alpha)\right) \\
&= \int d^4x \left(\left(\frac{\partial\mathcal{L}}{\partial\Phi_\alpha} \overbrace{-\partial_\mu\frac{\partial\mathcal{L}}{\partial(\partial_\mu\Phi_\alpha)}}\right)\delta\Phi^i_\alpha + \partial_\mu\left(\frac{\partial\mathcal{L}}{\partial(\partial_\mu\Phi_\alpha)}\delta\Phi^i_\alpha\right)\right)
\end{aligned} \tag{2.12}$$

The first bracket has to vanish because of the Euler-Lagrange equations of motion

$$0 = \frac{\partial\mathcal{L}}{\partial\Phi_\alpha} - \partial_\mu\frac{\partial\mathcal{L}}{\partial(\partial_\mu\Phi_\alpha)}. \tag{2.13}$$

Consequently for the action to be invariant the last term in (2.12) also has to vanish

$$0 = \partial_\mu \left(\frac{\partial \mathcal{L}}{\partial(\partial_\mu \Phi)} \delta \Phi^i_\alpha \right) = \omega^i \partial_\mu J^\mu_i. \tag{2.14}$$

This is obviously a conservation equation for the current

$$J^\mu_i = \frac{\partial \mathcal{L}}{\partial(\partial_\mu \Phi_\alpha)} \delta \Phi^i_\alpha = -i \frac{\partial \mathcal{L}}{\partial(\partial_\mu \Phi_\alpha)} \Omega^{\alpha\beta}_i \Phi_\beta \tag{2.15}$$

where the parameters ω^i have been pulled out of the definition of the currents to ensure that they are independent of the transformations. One may additionally define conserved charges Q_i via the volume integral of the zeroth component of the current

$$Q_i = \int_V J^0_i d^3x = -i \int_V \frac{\partial \mathcal{L}}{\partial(\partial_0 \Phi_\alpha)} \Omega^i_{\alpha\beta} \Phi^\beta d^3x \tag{2.16}$$

These results are nothing else but the well known Noether's theorem which states that every continuous symmetry of a theory described by a Lagrangian leads to a conserved current and consequently to a conserved charge. We will discuss several continuous symmetries in the course of this thesis, i.e. axialvector, vector and scale symmetries of QCD.

2.3 Chiral Symmetry

Chiral symmetry is a symmetry of the strong interactions that is motivated to a large part by the comparison of weak interaction processes involving only leptons (purely leptonic) and both hadrons and leptons (semileptonic). Let us compare the two decays

$$\mu^- \rightarrow \nu_\mu + e^- + \bar{\nu}_e \tag{2.17}$$
$$n \rightarrow p + e^- + \bar{\nu}_e \tag{2.18}$$

within classical Fermi theory of weak interactions. In both cases the interaction Lagrangian can be formulated in terms of a coupling of charged currents, for the purely leptonic decay (2.17)

$$\mathcal{L}_{lept} = \frac{4G_F}{\sqrt{2}} j^{\alpha+} j^-_\alpha \tag{2.19}$$

where $G_F \approx 1.17\ \mathrm{GeV}^{-2}$ is Fermi's constant and α is as usual a Minkowski 4-index. The currents $j^\pm_\alpha$ can be expressed as

$$j^+_\alpha = \frac{1}{2}\sum_\ell \bar{\nu}_\ell \gamma_\alpha (1-\gamma_5)\ell \qquad j^-_\alpha = \frac{1}{2}\sum_\ell \bar{\ell}\gamma_\alpha(1-\gamma_5)\nu_\ell \tag{2.20}$$

Here γ_α are the Dirac gamma matrices defined by the algebra $\{\gamma_\alpha, \gamma_\beta\} = 2g_{\alpha\beta}$ and $\gamma_5 = i\gamma_0\gamma_1\gamma_2\gamma_3$. The resulting interaction Lagrangian for the decay (2.17) then reads

$$\mathcal{L}_{lept,\mu} = \frac{G_F}{\sqrt{2}} \bar{\nu}_\mu \gamma^\alpha (1-\gamma_5)\mu\ \bar{e}\gamma_\alpha(1-\gamma_5)\nu_e \tag{2.21}$$

The factors of $(1-\gamma_5)$ reflect the fact that weak interactions are of the (V-A) vector - axialvector type, i.e. only left-handed neutrinos and right-handed antineutrinos are coupled weakly to other particles. This becomes clearer when realizing that the projection operators for left and right handed fields read $P_{R/L}\ell = (1 \pm \gamma_5)\ell = \ell_{R/L}$. Thus in the above Lagrangian the first projection operator actually projects the right handed part out of the anti-neutrino spinor to the left of it and the second projection operator projects the left-handed part out of the neutrino spinor to its right.

Now let us have a look at the $\beta-$decay (2.18), which also contains hadrons and is thus a bit more complex

$$\mathcal{L}_{hadr} = \frac{4G_F}{\sqrt{2}}(J^{\alpha+} j^-_\alpha + J^{\alpha-} j^+_\alpha) \tag{2.22}$$

Here $J^{\alpha+}$ denotes the hadronic current given by

$$J^{+}_{\alpha} = \frac{1}{2}\bar{p}\gamma_{\alpha}(g_V - g_A\gamma_5)n \tag{2.23}$$

where g_V and g_A denote the vector- and the axial-vector couplings, respectively. The Lagrangian for the beta decay (2.18) can consequently be written as

$$\mathcal{L}_{hadr,n} = \frac{G_F}{\sqrt{2}}\bar{p}\gamma^{\alpha}(g_V - g_A\gamma_5)n\ \bar{e}\gamma_{\alpha}(1-\gamma_5)\nu_e \tag{2.24}$$

These two relative coupling constants are necessary as compared to the purely leptonic case because protons and neutrons are composite particles. The fundamental weak interaction couples to the quarks inside the hadrons and thus there should be strong interaction corrections as compared to the case of weak interactions with free quarks. It seems natural that g_V and g_A could be very different from unity. The experimental results are thus quite surprising

$$g_V \approx 0.98 \qquad g_A \approx 1.28. \tag{2.25}$$

Thus the effective weak vector couplings of hadrons and leptons is surprisingly almost identical and even in the axial vector coupling shows only small hadronic corrections. If one invokes an additional symmetry of strong interactions that leads to conservation of vector- and axial-vector currents then the above experimental result can be understood quite naturally. We will outline the connection of the conservation of these currents to an important symmetry of QCD, chiral symmetry, in the next chapter. As a guide to further reading on chiral symmetry the review articles by Koch [27] and by Bentz et al. [28] and the book by Mosel [24] can be recommended.

2.3.1 Chiral Transformations

Let us have a look at the relevant transformations that reflect the axial- and vector-symmetries, i.e. the chiral transformations. We will examine a simple example of a system in which the vector-current is conserved while the axial-current is not conserved. Non-interacting fermions ψ with a mass m have exactly this property as we shall see. The Lagrangian reads

$$\mathcal{L} = \bar{\psi}(\not{p} - m)\psi = \bar{\psi}(i\gamma_{\mu}\partial^{\mu} - m)\psi \tag{2.26}$$

The vector- and axial-vector transformations Λ_V, Λ_A as expected from (2.8) are given by [24, 27]

$$\begin{aligned} \Lambda_V: \ \psi &\rightarrow e^{-i\frac{\vec{\tau}}{2}\vec{\Theta}}\psi \approx (1 - i\frac{\vec{\tau}}{2}\vec{\Theta})\ \psi, \\ \bar{\psi} &\rightarrow \bar{\psi}e^{i\frac{\vec{\tau}}{2}\vec{\Theta}} \approx \bar{\psi}\ (1 + i\frac{\vec{\tau}}{2}\vec{\Theta}) \end{aligned} \tag{2.27}$$

$$\begin{aligned} \Lambda_A: \ \psi &\rightarrow e^{-i\gamma_5\frac{\vec{\tau}}{2}\vec{\Theta}}\psi \approx (1 - i\gamma_5\frac{\vec{\tau}}{2}\vec{\Theta})\ \psi, \\ \bar{\psi} &\rightarrow \bar{\psi}e^{-i\gamma_5\frac{\vec{\tau}}{2}\vec{\Theta}} \approx \bar{\psi}\ (1 - i\gamma_5\frac{\vec{\tau}}{2}\vec{\Theta}) \end{aligned} \tag{2.28}$$

Here $\vec{\tau}$ is the vector of the Pauli spin matrices and $\vec{\Theta}$ is the parameter vector[6]. The above transformations are a representation of the symmetry group $SU(2)_V \times SU(2)_A$.

Applying the infinitesimal vector transformations to the Lagrangian (2.26) we find that

$$\mathcal{L} \xrightarrow{\Lambda_V} \mathcal{L}' \approx \bar{\psi}(1 + i\frac{\vec{\tau}}{2}\vec{\Theta})(i\gamma_\mu\partial^\mu - m)(1 - i\frac{\vec{\tau}}{2}\vec{\Theta})\psi \approx \bar{\psi}(i\gamma_\mu\partial^\mu - m)\psi = \mathcal{L} \tag{2.29}$$

Since they act on different spaces the $\gamma-$ and $\tau-$matrices can simply be commuted. The term that is quadratic in the small parameters $\vec{\Theta}$ is for consistency neglected in the last step. In other words even massive fermions are invariant under the vector-transformations (2.27). If we now compare the vector transformation law and the Lagrangian to our previous result (2.15) we consequently find the conserved vector current

$$\vec{V}_\mu = -i\frac{\partial\mathcal{L}}{\partial(\partial^\mu\psi)}\frac{\vec{\tau}}{2}\psi = \bar{\psi}\gamma_\mu\frac{\vec{\tau}}{2}\psi. \tag{2.30}$$

Now let us do the same exercise for the axial transformations

$$\begin{aligned} \mathcal{L} \xrightarrow{\Lambda_A} \mathcal{L}' &\approx \bar{\psi}(1 - i\gamma_5\frac{\vec{\tau}}{2}\vec{\Theta})(i\gamma_\mu\partial^\mu - m)(1 - i\gamma_5\frac{\vec{\tau}}{2}\vec{\Theta})\psi \\ &\approx \bar{\psi}(i\gamma_\mu\partial^\mu - m)\psi + 2im\bar{\psi}\gamma_5\frac{\vec{\tau}}{2}\vec{\Theta}\psi = \mathcal{L} + \delta\mathcal{L} \end{aligned} \tag{2.31}$$

where we have again dropped the term quadratic in the small parameters $\vec{\Theta}$. Therefore the axial symmetry is broken explicitly if $m \neq 0$, i.e. the Lagrangian itself is

[6]Note that the transformation law of $\bar{\psi}$ in (2.28) is often written incorrectly in the literature, probably originating from the standard paper on chiral symmetry by Koch Ref. [27] in equation (45) which would actually not lead to the axial symmetry being broken by a mass term but by the kinetic term of the Lagrangian. The transformation can be derived from the transformation of ψ and using $\bar{\psi} = \psi^\dagger\gamma_0$. Then one finds that $\bar{\psi}' = (\psi')^\dagger\gamma^0 \approx \left[(1 - i\gamma_5\frac{\vec{\tau}}{2}\vec{\Theta})\ \psi\right]^\dagger\gamma^0 = \psi^\dagger(1 + i\gamma_5\frac{\vec{\tau}}{2}\vec{\Theta})\ \gamma^0 = \psi^\dagger\gamma^0(1 - i\gamma_5\frac{\vec{\tau}}{2}\vec{\Theta}) = \bar{\psi}\ (1 - i\gamma_5\frac{\vec{\tau}}{2}\vec{\Theta})$. Here we have used that $(AB)^\dagger = B^\dagger A^\dagger$, that γ_5 and the Pauli matrices are Hermitian and that γ_5 anti-commutes with all other $\gamma-$matrices.

not invariant under the axial transformation in the presence of a mass term. Nevertheless if the mass m is small compared to the relevant energy scale then the axial current

$$\vec{A}_\mu = -i\frac{\partial \mathcal{L}}{\partial(\partial^\mu \psi)}\gamma_5 \frac{\vec{\tau}}{2}\psi = \bar{\psi}\gamma_\mu\gamma_5\frac{\vec{\tau}}{2}\psi \tag{2.32}$$

could still be approximately conserved. According to (2.12) and (2.15) the current will then obey the equation

$$\partial^\mu \vec{A}_\mu = 2im\bar{\psi}\gamma_5\frac{\vec{\tau}}{2}\psi \tag{2.33}$$

which can be understood as an approximate conservation equation. In one of the following sections dealing with the linear σ-model we will consider another type of symmetry breaking, i.e. spontaneous symmetry breaking that can appear even if the Lagrangian is invariant under the given transformation.

2.4 PCAC-relation

One of the most important relations of chiral symmetry is the partial conserved axial-vector (PCAC) relation which creates a connection between axial currents of the weak interaction and the strongly interacting pion fields. It is usually given in the form

$$\partial^\mu A^a_\mu(x) = f_\pi m_\pi^2 \pi^a(x) \qquad a = 1, 2, 3 \tag{2.34}$$

Here $A^a_\mu(x)$ is the weak axial-vector current, f_π is the pion decay constant and $\pi^a(x)$ is one of the pion fields according to its isospin index a. We will schematically deduce it from the weak decay of the pion[7]. We start from the matrix element for the weak pion decay

$$\langle 0 \mid A^a_\mu(x) \mid \pi^b(q) \rangle \tag{2.35}$$

where a and b are isospin indices. The form of the weak axial-vector current $A^a_\mu(x)$ is a priori unknown but because it must transform as a Lorentz vector it must be proportional to the pion momentum q^μ, since it is the only other 4-vector in the problem. The further space-time dependence of the matrix element can be deduced from from translational invariance

$$\langle 0 \mid A^a_\mu(x) \mid \pi^b(q) \rangle = \langle 0 \mid A^a_\mu(0) \mid \pi^b(q) \rangle e^{-iqx} \tag{2.36}$$

as explained in [24].

$$\langle 0 \mid A^a_\mu(x) \mid \pi^b(q) \rangle = -iC\delta^{ab} q_\mu e^{-iqx} \tag{2.37}$$

the constant of proportionality [8] C is nothing else but the pion decay constant that has been experimentally found to have a value of $f_\pi \simeq 92.4$ MeV. To put this in the form of a conservation law we take the 4-divergence of (2.37)

$$\langle 0 \mid \partial^\mu A^a_\mu(x) \mid \pi^b(q) \rangle = -f_\pi \delta^{ab} q^\mu q_\mu e^{-iqx} = -f_\pi \delta^{ab} m_\pi^2 e^{-iqx} \tag{2.38}$$

where we have used Lorentz invariance in the last step $q^\mu q_\mu = m_\pi^2$. The PCAC relation connects the conservation of the axial-vector current with the size of the pion mass. Since the pion mass is small (compared to hadronic scales of $\sim$ 1GeV) but non-zero the axial-vector current is only partially conserved.
Taking only the lowest mode of the free pion field $\pi(x) \approx e^{-iqx}$ (again up to a normalization) we can also deduce the axial current carried by the pion by applying the Klein-Gordon equation for the free pion field

$$\partial_\mu \partial^\mu \pi(x) = -m_\pi^2 \pi(x) \tag{2.39}$$

[7] A more rigorous derivation also for other mesons can be found in [29, 24]

[8] We neglect in (2.37) a necessary normalization factor of the plain wave for the sake of simplicity

Applying (2.39) to (2.37) we arrive at

$$\langle 0 \mid \partial^\mu A^a_\mu(x) \mid \pi^b(q)\rangle = f_\pi \delta^{ab} \partial_\mu \partial^\mu \pi^b(x) \tag{2.40}$$

If we compare this to equation (2.38) the axial vector current carried by the pion is found to be

$$A^a_\mu(x) = f_\pi \partial_\mu \pi^a(x) \tag{2.41}$$

A very important application of the PCAC-relation is the so-called Goldberger-Treiman relation which we will consider next.

2.5 Goldberger-Treiman Relation

Since it makes little sense to consider the PCAC-relation for pions without any interactions the most obvious generalization is to include nucleons into the consideration. The axial current of the nucleon reads

$$A^a_{\mu,N} = g_A \bar{\psi}_N \gamma_\mu \gamma_5 \frac{\tau^a}{2} \psi_N \tag{2.42}$$

as shown in equation (2.32). Here $\psi_N = \begin{pmatrix} \psi_{N,p} \\ \psi_{N,n} \end{pmatrix}$ is the 2-spinor of the proton and the neutron in isospin-space, γ_μ and γ_5 are the usual anti-commuting gamma-matrices and τ^a are the Pauli-matrices. The additional factor as compared to equation (2.32) has been experimentally found to be $g_A \approx 1.28$ due to renormalization of $A^a_{\mu,N}$ as discussed in section 2.3. Following section 2.4 we now consider the divergence of the nucleon current.

$$\begin{aligned} \partial^\mu A^a_{\mu,N} &= \partial^\mu \left(g_A \bar{\psi}_N \gamma_\mu \gamma_5 \frac{\tau^a}{2} \psi_N \right) \\ &= g_A \left(\bar{\psi}_N \gamma_\mu \overleftarrow{\partial}^\mu \gamma_5 \frac{\tau^a}{2} \psi_N + \bar{\psi}_N \gamma_\mu \partial^\mu \gamma_5 \frac{\tau^a}{2} \psi_N \right) \\ &= g_A \left(\bar{\psi}_N \gamma_\mu \overleftarrow{\partial}^\mu \gamma_5 \frac{\tau^a}{2} \psi_N - \bar{\psi}_N \gamma_5 \frac{\tau^a}{2} \gamma_\mu \partial^\mu \psi_N \right) \\ &= i g_A m_N \bar{\psi}_N \gamma_5 \tau^a \psi_N \end{aligned} \tag{2.43}$$

where we have used the anti-commutation relation $\{\gamma_\mu, \gamma_5\} = 0$ from the second to the third line and the Dirac equation for ψ_N and the adjoint Dirac equation for $\bar{\psi}_N$ in the last step [9]. Since m_N is sizable even compared to hadronic scales $A^a_{\mu,N}$ alone is not even approximately conserved. Still one might consider the combined axial current of pion and nucleon to be just the sum of both single currents

$$A^a_\mu = \underbrace{g_A \bar{\psi}_N \gamma_\mu \gamma_5 \frac{\tau^a}{2} \psi_N}_{\text{nucleon}} + \underbrace{f_\pi \partial_\mu \pi^a(x)}_{\text{pion}} \tag{2.44}$$

where we have used one of the results of section 2.4 for the pion axial current. If we now assume that the combined current (2.44) is conserved, i.e. $\partial^\mu A^a_\mu = 0$ we arrive at

$$\partial_\mu \partial^\mu \pi^a(x) + i g_A \frac{m_N}{f_\pi} \bar{\psi}_N \gamma_5 \tau^a \psi_N = 0 \tag{2.45}$$

[9] which directly give $\gamma_\mu \partial^\mu \psi_N = -i m_N \psi_N$ and $\bar{\psi}_N \gamma_\mu \overleftarrow{\partial}^\mu = i m_N \bar{\psi}_N$, respectively

which is a Klein-Gordon equation for a massless pion coupled to the nucleon field via the second term. Again we find that the axial current is only conserved in the limit of a vanishing pion mass. Using the PCAC-relation (2.34) instead of a completely conserved current introduces an additional term to (2.45) resulting in

$$\left(\partial_\mu \partial^\mu + m_\pi^2\right) \pi^a(x) + i g_A \frac{m_N}{f_\pi} \bar{\psi}_N \gamma_5 \tau^a \psi_N = 0 \tag{2.46}$$

Finally we can identify the constants in front of the interaction term with an effective pion-nucleon coupling constant to find the Goldberger-Treiman relation

$$g_{\pi NN} = g_A \frac{m_N}{f_\pi} \approx 12.7 \tag{2.47}$$

which is in remarkably good agreement with the experimentally found value $g_{\pi NN}^{exp} \approx 13.4$ when considering the relatively simple arguments and estimates used to derive it.

2.6 Linear σ-Model

The linear σ-model was first discussed by Gell-Mann and Levy [30] to model the axial vector current in the beta decay even before the first precursors of QCD were developed in the mid 60s. The idea was to write down a model of the nuclear-mesonic interactions that would incorporate approximately conserved vector- and axial-vector-currents as found in the weak decays[10] as discussed in section 2.3. The linear sigma model has been used by numerous authors with many different variations and extensions in the last decades, see [27, 31, 32, 33, 34] and references therein. The model includes the nucleon spinor[11] ψ, the $\vec{\pi}$-mesons and the σ-meson. One may find the behavior of the mesons under vector- and axial-vector-transformation by examining the structure of the state they represent [27], i.e.

$$\vec{\pi} = i\bar{\psi}_q \vec{\tau}\gamma_5 \psi_q \quad \text{and} \quad \sigma = \bar{\psi}_q \psi_q \tag{2.48}$$

where the index q was added to distinguish the quark spinor from the nucleon spinor that will appear later.

$$\begin{aligned} \Lambda_V: \ \vec{\pi} &\rightarrow \vec{\pi}' \approx \vec{\pi} + \vec{\Theta} \times \vec{\pi}, \\ \sigma &\rightarrow \sigma' = \sigma \end{aligned} \tag{2.49}$$

$$\begin{aligned} \Lambda_A: \ \vec{\pi} &\rightarrow \vec{\pi}' \approx \vec{\pi} + \vec{\Theta}\sigma, \\ \sigma &\rightarrow \sigma' \approx \sigma - \vec{\Theta}\vec{\pi} \end{aligned} \tag{2.50}$$

In other words the vector transformations correspond to a rotation with the angles $\vec{\Theta}$ in isospin-space, explaining why the $\vec{\pi}$ is transformed like a three component isovector while the isoscalar σ stays invariant. The axial transformations are more subtle and mix pion and sigma mesons. The next step would be to find terms that are invariant under both Λ_V and Λ_A. For the vector-transformations this is rather obvious since rotations preserve the norm of a vector so any potential that only uses terms quadratic in the meson fields will be invariant under the vector transformations, i.e.

$$\Lambda_V: \ \vec{\pi}^2 \rightarrow (\vec{\pi}')^2 = \vec{\pi}^2, \qquad \sigma^2 \rightarrow (\sigma')^2 = \sigma^2 \tag{2.51}$$

At the linear level the quadratic terms transform under the axial transformations in the following way

$$\begin{aligned} \Lambda_A: \ \vec{\pi}^2 &\rightarrow (\vec{\pi}')^2 \approx (\vec{\pi} + \vec{\Theta}\sigma)(\vec{\pi} + \vec{\Theta}\sigma) \approx \vec{\pi}^2 + 2\vec{\pi}\vec{\Theta}\sigma \\ \sigma^2 &\rightarrow (\sigma')^2 \approx (\sigma - \vec{\Theta}\vec{\pi})(\sigma - \vec{\Theta}\vec{\pi}) \approx \sigma^2 - 2\vec{\pi}\vec{\Theta}\sigma \end{aligned} \tag{2.52}$$

[10] The title of the publication was actually "The axial vector current in beta decay".

[11] actually many authors later replaced nucleons by quarks in their versions or extensions of the linear σ-model

where in the second step again the terms quadratic in $\vec{\Theta}$ have been dropped. Thus terms built up from $\vec{\pi}^2 + \sigma^2$ will be invariant both under Λ_V and Λ_A. This result can be directly used again to construct interaction terms between nucleons and mesons that also preserve both symmetries. Roughly speaking one may simply replace one of each meson field in the invariant term $\vec{\pi}^2 + \sigma^2$ by a corresponding nucleon term with the same transformation behavior. The terms of choice simply have the same structure as the mesons themselves as seen in equation (2.48) i.e.

$$g_S\bar{\psi}\psi\sigma + ig_S\bar{\psi}\gamma_5\vec{\tau}\psi\vec{\pi} \tag{2.53}$$

such that the change of first term under the axial transformation will exactly cancel the change of the second term. As one can see this requires a common scalar coupling constant g_S for both interaction terms.
The chirally invariant Lagrangian of the sigma model reads

$$\mathcal{L} = \frac{1}{2}\left(\partial_\mu\pi\right)^2 + \frac{1}{2}\left(\partial_\mu\sigma\right)^2 + \bar{\psi}\left[i\partial\!\!\!/ - g_S(\sigma + i\gamma_5\vec{\tau}\cdot\vec{\pi})\right]\psi - U_S(\pi,\sigma) \tag{2.54}$$

with the chirally symmetric potential

$$U_S(\pi,\sigma) = \frac{\lambda}{4}(\sigma^2 + \pi^2 - f_\pi^2)^2 \tag{2.55}$$

where f_π is the pion decay constant. The reason behind this constant in the potential is located in the interaction term $g_S\sigma\bar{\psi}\psi$. From the Goldberger-Treiman relation we learned that $g_{\pi NN}/g_A f_\pi = m_N = g_S f_\pi$ such that the interaction between mesons and the nucleon generates the nucleon mass. For this to be realized the vacuum expectation value of the σ-field must be $\langle\sigma\rangle = f_\pi$ which is provided by potential (2.55). The pion-nucleon interaction term cannot generate the nucleon mass since the pion is a pseudoscalar particle, i.e. it changes sign under parity transformations and is thus required to have a vanishing expectation value in the vacuum $\langle\pi\rangle = 0$. In figure 2.1 this so called "mexican-hat" potential is shown as a function of π and σ. In contrast to the Lagrangian the vacuum expectation value is not invariant under axial transformations[12] since (2.50) rotates the pion and the sigma into each other. Such a situation is usually denoted as *spontaneous symmetry breaking* , i.e. the systems ground state does not exhibit the same symmetries as the Lagrangian.

The next question to ask is do the mesons also acquire a mass in the ground state like the nucleon does? The physical pion and sigma particles should be

[12] while it is invariant under Λ_V since σ is invariant anyways and the rotation of $\langle\vec{\pi}\rangle = 0$ according to equation (2.49) does not do anything.

identified with perturbations around the ground state, their mass will then be given by the curvature of the potential at that point. A bosonic mass then should have the structure $\frac{1}{2}m^2\phi^2$ such that the second derivative with respect to the field evaluated in the ground state should give the mass squared[13]

$$\left.\frac{\partial^2 U_S}{\partial\phi^2}\right|_{vac} = m^2 \tag{2.56}$$

Applying this to the given potential we find

$$\left.\frac{\partial^2 U_S}{\partial\sigma^2}\right|_{vac} = \left(\lambda(\sigma^2+\pi^2-f_\pi^2)+2\lambda\sigma^2\right)\Big|_{vac} = 2\lambda f_\pi^2 = m_\sigma^2 \tag{2.57}$$

$$\left.\frac{\partial^2 U_S}{\partial\pi^2}\right|_{vac} = \left(\lambda(\sigma^2+\pi^2-f_\pi^2)+2\lambda\pi^2\right)\Big|_{vac} = 0 = m_\pi^2. \tag{2.58}$$

Thus the pion is massless while the σ acquires a finite vacuum mass. The pions are in this case the so-called Goldstone bosons of the system. According to the Goldstone-theorem any continuous symmetry of a Lagrangian that is broken spontaneously in the ground state will lead to such massless excitations, for more details see for example [24, 35] and references therein. Pionic excitations correspond to moving he system around in the circular flat valley in the potential as depicted in figure 2.1. The massive sigma meson corresponds to radial excitations that "cost energy" in contrast to the pionic ones. Now we know that the axial current is only partially conserved and that the pion actually has a comparably small but non-vanishing mass of $m_\pi \approx 139$ MeV. The next step should thus be to change the potential such that it breaks the axial symmetry explicitly by introducing a finite mass for the pion while keeping the vacuum expectation value the same. The easiest and most common way to do this is to introduce a term linear in σ since this will preserve the vector symmetry according to (2.49) while explicitly breaking the axial symmetry (2.50). The potential of choice is thus

$$U_B(\pi,\sigma) = \frac{\lambda}{4}(\sigma^2+\pi^2-f^2)^2 - H\sigma \tag{2.59}$$

The parameter f is no longer equal to f_π which is necessary to keep the vacuum expectation values at $\langle\pi\rangle = 0$ and $\langle\sigma\rangle = f_\pi$. Consequently at this point in the

[13] We will later on examine the more complicated case model in which additional coupling terms spoil this simple picture. In general the second derivatives with respect to the fields in the ground state only represent the particle masses if all mixed second derivatives vanish such that the Hessian matrix is already diagonal.

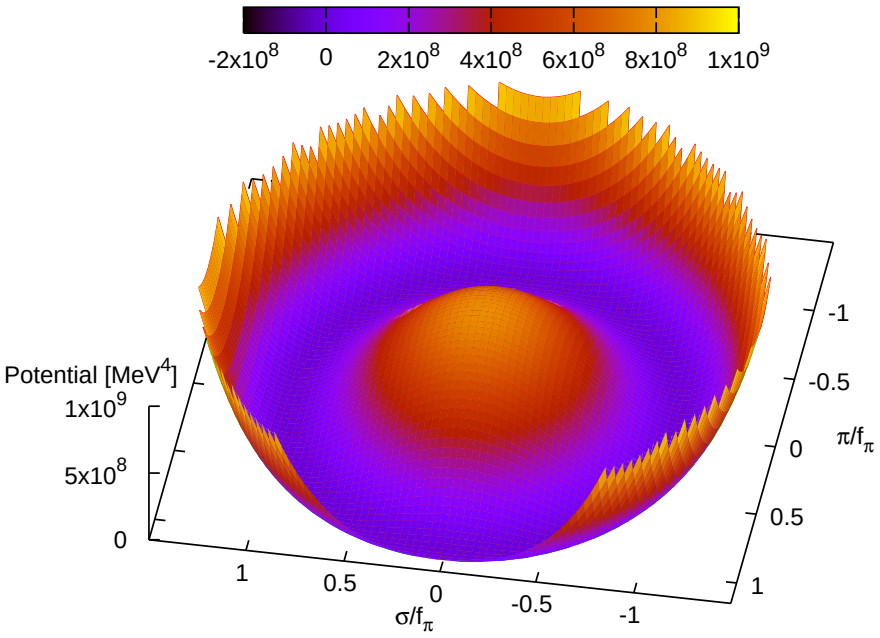

Figure 2.1: Potential of the sigma model without explicit chiral symmetry breaking

potential the first derivatives with respect to the fields should vanish

$$\begin{aligned} \left.\frac{\partial U_B}{\partial \sigma}\right|_{vac} &\stackrel{!}{=} 0 = \left(\lambda\sigma(\sigma^2+\pi^2-f^2)-H\right)\big|_{vac} \\ &= \lambda f_\pi (f_\pi^2 - f^2) - H \qquad (2.60) \\ \left.\frac{\partial U_B}{\partial \pi}\right|_{vac} &\stackrel{!}{=} 0 = \left(\lambda\pi(\sigma^2+\pi^2-f^2)+2\lambda\pi^2\right)\big|_{vac} = 0 \qquad (2.61) \end{aligned}$$

The first condition can be exploited later to find H while the second one is trivially fulfilled. Now let us repeat the calculation of the meson masses to find additional constraints on the parameters.

$$\begin{aligned} \left.\frac{\partial^2 U_B}{\partial \sigma^2}\right|_{vac} &= \left(\lambda(\sigma^2+\pi^2-f^2)+2\lambda\sigma^2\right)\big|_{vac} \\ &= \lambda(3f_\pi^2 - f^2) = m_\sigma^2 \qquad (2.62) \\ \left.\frac{\partial^2 U_B}{\partial \pi^2}\right|_{vac} &= \left(\lambda(\sigma^2+\pi^2-f^2)+2\lambda\pi^2\right)\big|_{vac} \\ &= \lambda(f_\pi^2 - f^2) = m_\pi^2 \qquad (2.63) \end{aligned}$$

We can eliminate λ by combining (2.62) and (2.63) to find

$$f^2 = \frac{m_\sigma^2 - 3m_\pi^2}{m_\sigma^2 - m_\pi^2} f_\pi^2. \tag{2.64}$$

Using this result the parameter λ can now be found from either (2.62) or (2.63) to be

$$\lambda = \frac{m_\sigma^2 - m_\pi^2}{2f_\pi^2}. \tag{2.65}$$

Finally H can be fixed by replacing f^2 and λ by the above results in (2.60) giving the simple result

$$H = \frac{m_\sigma^2 - m_\pi^2}{2f_\pi^2} f_\pi \left(f_\pi^2 - \frac{m_\sigma^2 - 3m_\pi^2}{m_\sigma^2 - m_\pi^2} f_\pi^2 \right) = m_\pi^2 f_\pi. \tag{2.66}$$

Thus we could break the axial symmetry and introduce a non-vanishing pion mass

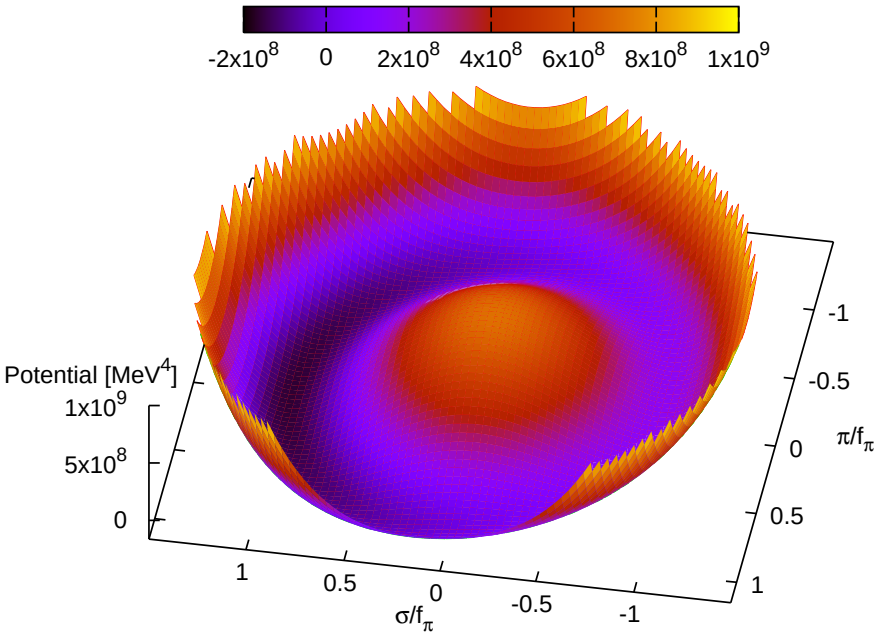

Figure 2.2: Potential of the linear sigma model with explicit chiral symmetry breaking, one can see the potential is slightly deeper in the true vacuum $\langle\pi\rangle = 0, \langle\sigma\rangle = f_\pi$.

while keeping the vacuum expectation value of the meson fields and consequently also the nucleon mass at the same value. The resulting potential is depicted in figure 2.2 where one can clearly see there is only one minimum of the potential

located at $\langle\pi\rangle = 0$ and $\langle\sigma\rangle = f_\pi$ and going around the circle will "cost energy" due to the small but finite pion mass. In both figures λ is kept fixed to allow easier visual comparison[14]. The pions are sometimes called pseudo-Goldstone bosons in this situation to distinguish from the idealized situation with no explicit breaking of the axial symmetry.

[14]In figure 2.1 $m_\sigma = 860$ MeV with $m_\pi = 0$ and in figure 2.2 $m_\sigma \approx 871$ MeV with $m_\pi = 139$ MeV both resulting in $\lambda \approx 43.3$

2.7 The Bag-Model

To explore some of the aspects of the QCD phase transition it can be useful to have a relatively simple model including a first order phase transition. This is provided by the MIT-bag model (see ref.[36, 37, 17]) that includes a first order phase transition from the deconfined to the confined phase. The pressure and energy density above the critical temperature are then given by a free gas plus a vacuum contribution.

$$p_H = g_H \frac{\pi^2}{90} T^4 - B \qquad \epsilon_H = g_H \frac{\pi^2}{30} T^4 + B \tag{2.67}$$

Here g are the effective degrees of freedom[15] and the subscripts H and L here denote the high and the low temperature phase, respectively. In the low temperature phase pressure and energy density are given by

$$p_L = g_L \frac{\pi^2}{90} T^4 \qquad \epsilon_L = g_L \frac{\pi^2}{30} T^4 \tag{2.68}$$

The phase transition is fixed by the condition of equal pressure at equal temper-

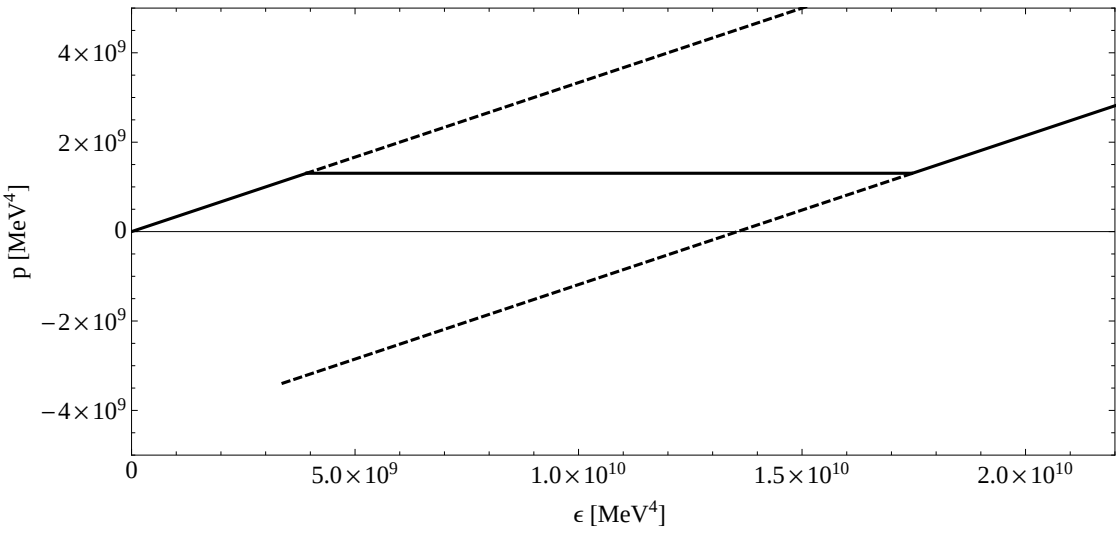

Figure 2.3: Pressure as a function of the energy density in the Bag model for $g_H = 51.25$, $g_L = 14.25$, $T_c = 170$ MeV. Dashed lines show unstable branches, i.e. at the same temperature the other phase has a higher pressure.

ature (and chemical potential). To meet this condition the bag constant has to be

[15]The number of effective bosonic degrees of freedom, i.e. fermionic degrees of freedom are weighted with an additional factor of 7/8

chosen accordingly as a function of the degrees of freedom g_H, g_L in the high and the low temperature phase and by the critical temperature T_c

$$B = \frac{T_c^4 (g_H - g_L)\pi^2}{90} \tag{2.69}$$

For example for a particle composition[16] with $g_H = 51.25$, $g_L = 14.25$ and $T_c = 170$ MeV one finds $B^{1/4} \approx 241$ MeV. In figure 2.3 the pressure of the Bag model is shown as a function of the energy density. The solid line shows the phase with the highest pressure at the same temperature. Dashed lines correspond to metastable branches where the pressure is lower than in the other phase. The high temperature phase ends at $\epsilon_H = B = -p_H$. The horizontal line at constant pressure is the phase transition

[16] This corresponds to having two massless quark flavors with $7/8 \cdot 2 \cdot 2 \cdot 2 \cdot 3 = 21$ degrees of freedom (DoF) and 16 DoF from the eight gluons. Both phases additionally include 2 DoF for the photons, $7/8 \cdot 2 \cdot 2 \cdot 2 = 7$ DoF for $e^{\pm}$,$\mu^{\pm}$ and $7/8 \cdot 2 \cdot 3 = 5.25$ DoF for the three neutrino families.

2.8 Scale Symmetry

An important property of any high energy Lagrangian is its behavior under scale transformations[17], which are space-time transformations of the form

$$x_\mu \to x'_\mu = \lambda x_\mu \qquad \lambda > 0 \tag{2.70}$$

If a theory contains no dimensionful parameters, such as particle masses, one would expect it to be invariant under such transformations. All fundamental constants should be unaffected by (2.70), e.g. the speed of light is invariant as space and time coordinates are scaled by the same amount. The transformation of a general field $\phi(x)$ (boson or fermion) then reads [38]

$$\phi(x) \to \phi'(x) = U(\lambda)\phi(\lambda x) \tag{2.71}$$

where $U(\lambda)$ is an element of the abelian Lie group of dilatations. The elements of a Lie-group with a single parameter can be expressed in the following form [23]

$$U(\lambda) = e^{-i\alpha\hat{L}} = e^{\ln(\lambda)\hat{D}} \tag{2.72}$$

where $\alpha = \ln(\lambda)$ is the group parameter and $\hat{L}$ is the generator of the Group. The form of $U(\lambda)$ may be derived from the requirements that $U(\lambda_1\lambda_2) = U(\lambda_1)U(\lambda_2)$ and $U(1) = 1$ (see e.g. [39]). $\hat{D}$ is in general a diagonalizable matrix and we will only care about its eigenvalues κ that take the form $\frac{d}{2} - 1$ for bosons and $\frac{3}{2}\left(d/2 - \frac{1}{2}\right)$ for fermions where d is the number of space-time dimensions. Now we may consider an infinitesimal transformation of the field $\phi(x) \to \phi'(x) = \phi(x) + \delta\phi$ where

$$\begin{aligned} \delta\phi &= \left.\frac{\partial\phi}{\partial\alpha}\right|_{\alpha=0} \delta\alpha + \mathcal{O}(\delta\alpha^2) \\ &\approx \delta\alpha(\hat{D} + x_\mu\partial^\mu)\phi(x) \\ &= \begin{cases} \delta\alpha(1 + x_\mu\partial^\mu)\phi(x) & \text{for bosons} \\ \delta\alpha(\frac{3}{2} + x_\mu\partial^\mu)\phi(x) & \text{for fermions} \end{cases} \end{aligned} \tag{2.73}$$

Similarly one finds for the complete Lagrangian of the theory

$$\frac{\delta\mathcal{L}}{\delta\alpha} = (4 + x_\mu\partial^\mu)\mathcal{L} \tag{2.74}$$

For dimensional reasons the infinitesimal transformations of the field derivatives follow directly from (2.73) to fulfill (2.74) for canonical scale-free kinetic terms as

[17] sometimes also called dilatations

we will see later

$$\delta(\partial^\mu\phi) \;=\; \begin{cases} \delta\alpha(2 + x_\nu\partial^\nu)\partial^\mu\phi(x) & \text{for bosons} \\ \delta\alpha(\frac{5}{2} + x_\nu\partial^\nu)\partial^\mu\phi(x) & \text{for fermions} \end{cases} \tag{2.75}$$

or in other words their eigenvalues are given by $\kappa + 1$. The important question now is when exactly is the action $S = \int dx^4\mathcal{L}$ invariant under (2.70) and (2.71)? This is fulfilled if $(4 + x_\mu\partial^\mu)\mathcal{L}$ is nothing else but a divergence term, i.e. equal to $\partial^\mu\left(x_\mu\mathcal{L}\right)$ since

$$\int_V dx^4\partial^\mu\left(x_\mu\mathcal{L}\right) = \int_{S(V)} dn^\mu\left(x_\mu\mathcal{L}\right) = 0 \tag{2.76}$$

if the surface is taken to infinity. n^μ is a 4-vector orthogonal to the surface $S(V)$. Now we may calculate when the difference between (2.74) and (2.76) vanishes to find a criterion for scale invariance of a given Lagrangian.

$$\begin{aligned}
& \int dx^4\left[\partial^\mu\left(x_\mu\mathcal{L}\right) - \frac{\delta\mathcal{L}}{\delta\alpha}\right] \\
= \;& \int dx^4\left[4\mathcal{L} + x_\mu\partial^\mu\mathcal{L} - \sum_i \frac{\partial\mathcal{L}}{\partial\phi_i}\delta\phi_i - \sum_i \frac{\partial\mathcal{L}}{\partial(\partial_\mu\phi_i)}\delta(\partial_\mu\phi_i)\right] \\
= \;& \int dx^4\left[4\mathcal{L} + x_\mu\partial^\mu\mathcal{L} - \sum_i \frac{\partial\mathcal{L}}{\partial\phi_i}\left(\kappa_i + x_\mu\partial^\mu\right)\phi_i - \sum_i \frac{\partial\mathcal{L}}{\partial(\partial_\mu\phi_i)}(\kappa_i + 1 + x_\nu\partial^\nu)\partial^\mu\phi_i\right] \\
= \;& \int dx^4\Bigg[4\mathcal{L} + x_\mu\partial^\mu\mathcal{L} - x_\mu\underbrace{\sum_i\left(\frac{\partial\mathcal{L}}{\partial\phi_i}\partial^\mu\phi_i + \frac{\partial\mathcal{L}}{\partial(\partial_\nu\phi_i)}\partial^\mu(\partial^\nu\phi_i)\right)}_{\partial^\mu\mathcal{L}} \\
- \;& \sum_i\left(\frac{\partial\mathcal{L}}{\partial\phi_i}\kappa_i\phi_i + \frac{\partial\mathcal{L}}{\partial(\partial_\nu\phi_i)}(\kappa_i + 1)\partial^\nu\phi_i\right)\Bigg] \\
= \;& \int dx^4\left[4\mathcal{L} - \sum_i\left(\frac{\partial\mathcal{L}}{\partial\phi_i}\kappa_i\phi_i + \frac{\partial\mathcal{L}}{\partial(\partial_\nu\phi_i)}(\kappa_i + 1)\partial^\nu\phi_i\right)\right]
\end{aligned}$$

where we have used that $\partial^\mu x_\mu = 4$ in the first step and inserted (2.73) and (2.75) in the second step. Since scale invariance should not depend on the size of the volume we can omit the integration and finally obtain

$$4\mathcal{L} - \sum_i\left(\frac{\partial\mathcal{L}}{\partial\phi_i}\kappa_i\phi_i + \frac{\partial\mathcal{L}}{\partial(\partial_\nu\phi_i)}(\kappa_i + 1)\partial^\nu\phi_i\right) \begin{cases} = 0 & \text{scale invariance} \\ \neq 0 & \text{broken scale symmetry} \end{cases} \tag{2.77}$$

With the result (2.77) it is straightforward to check that canonical kinetic and potential terms are scale invariant. Let's look at some examples, e.g. the Lagrangian of a non-interacting Dirac field

$$\mathcal{L} = \bar{\psi}\left(i\gamma^\mu\partial_\mu - m\right)\psi \tag{2.78}$$

for which we find that

$$\begin{aligned} & 4\mathcal{L} - \sum_i \left(\frac{\partial\mathcal{L}}{\partial\phi_i}\kappa_i\phi_i + \frac{\partial\mathcal{L}}{\partial(\partial_\nu\phi_i)}(\kappa_i+1)\partial^\nu\phi_i\right) \\ = \;& 4\bar{\psi}\left(i\gamma^\mu\partial_\mu - m\right)\psi + \frac{3}{2}m\bar{\psi}\psi - \frac{3}{2}\bar{\psi}\left(i\gamma^\mu\partial_\mu - m\right)\psi - \frac{5}{2}\bar{\psi}i\gamma^\mu\partial_\mu\psi \\ = \;& -m\bar{\psi}\psi \neq 0 \end{aligned} \tag{2.79}$$

Which means that the Lagrangian (2.78) is only scale invariant for vanishing particle mass. Now let's check the Lagrangian of the linear-σ model[18]

$$\begin{aligned} \mathcal{L} &= \frac{1}{2}\left(\partial_\mu\pi\right)^2 + \frac{1}{2}\left(\partial_\mu\sigma\right)^2 + \bar{\psi}\left[i\partial\!\!\!/ - g(\sigma + i\gamma_5\vec{\tau}\cdot\vec{\pi})\right]\psi \\ &- \frac{\lambda}{4}(\sigma^2+\pi^2)^2 + \frac{k_0}{2}(\sigma^2+\pi^2) + f_\pi m_\pi^2\sigma \end{aligned} \tag{2.80}$$

In which case one finds with some bookkeeping [19] that

$$\begin{aligned} & 4\mathcal{L} - \sum_i \left(\frac{\partial\mathcal{L}}{\partial\phi_i}\kappa_i\phi_i + \frac{\partial\mathcal{L}}{\partial(\partial_\nu\phi_i)}(\kappa_i+1)\partial^\nu\phi_i\right) \\ = \;& 2\left(\partial_\mu\pi\right)^2 + 2\left(\partial_\mu\sigma\right)^2 + 4\bar{\psi}\left[i\partial\!\!\!/ - g(\sigma + i\gamma_5\vec{\tau}\cdot\vec{\pi})\right]\psi - \lambda(\sigma^2+\pi^2)^2 + 2k_0(\sigma^2+\pi^2) \\ + \;& 4f_\pi m_\pi^2\sigma - 2\left(\partial_\mu\pi\right)^2 - 2\left(\partial_\mu\sigma\right)^2 + \bar{\psi}gi\gamma_5\vec{\tau}\cdot\vec{\pi}\psi + \bar{\psi}g\sigma\psi + \frac{3}{2}\bar{\psi}\left[g(\sigma + i\gamma_5\vec{\tau}\cdot\vec{\pi})\right]\psi \\ - \;& \frac{3}{2}\bar{\psi}\left[i\partial\!\!\!/ - g(\sigma + i\gamma_5\vec{\tau}\cdot\vec{\pi})\right]\psi - \frac{5}{2}\bar{\psi}i\partial\!\!\!/\psi + \lambda\pi^2(\sigma^2+\pi^2) + \lambda\sigma^2(\sigma^2+\pi^2) \\ - \;& k_0\pi^2 - k_0\sigma^2 - f_\pi m_\pi^2\sigma \\ = \;& k_0(\sigma^2+\pi^2) + 3f_\pi m_\pi^2\sigma \neq 0 \end{aligned} \tag{2.81}$$

which means that in this case the scale symmetry is broken by two terms. Explicitly broken scale symmetry from the k_0-term is actually a flaw of the most simple linear sigma model. The term that is responsible for chiral symmetry breaking does also break the scale symmetry which is expected but it does not scale like a mass term[20]. We will later see how these flaws can be cured in the dilaton-quark-meson model by introduction of the dilaton-field.

[18] note that we use a slightly different notation that is closer to the one used later on in section (2.10)

[19] the terms in the sums are first ordered according to the term they originate from and then according to $\pi, \sigma, \psi, \bar{\psi}$

[20] a fermionic mass term should have scaling dimension 3 and therefore only result in $f_\pi m_\pi^2\sigma$ in this case, whereas a bosonic mass term should have scaling dimension 2 and result in $2f_\pi m_\pi^2\sigma$

2.9 Trace Anomaly

The energy momentum tensor $T^{\mu\nu}$ is usually defined via

$$T^{\mu\nu} = \frac{\partial \mathcal{L}}{\partial(\partial_\mu \phi)} \partial^\nu \phi - \mathcal{L} g^{\mu\nu} \tag{2.82}$$

But the energy momentum tensor is actually not unique since energy momentum conservation only requires $\partial_\mu T^{\mu\nu} = 0$. Thus gradient terms of the type $\partial_\lambda f^{\lambda\mu\nu}$ with $f^{\lambda\mu\nu} = -f^{\mu\lambda\nu}$ may be added without changing the 4-momentum of the system [40]. One may find modified energy-momentum tensor $\Theta^{\mu\nu}$ that is connected with the conservation of scale symmetry [41]

$$j^\mu_D = x_\nu \Theta^{\mu\nu} \tag{2.83}$$

Thus the system will be scale invariant if

$$\partial_\mu j^\mu_D = (\partial_\mu x_\nu)\Theta^{\mu\nu} + x_\nu \underbrace{\partial_\mu \Theta^{\mu\nu}}_{=0} = g_{\mu\nu}\Theta^{\mu\nu} = \Theta^\mu_\mu = 0 \tag{2.84}$$

where we have used energy momentum conservation. Thus $\Theta^{\mu\nu}$ is chosen such that its trace vanishes just if the system is scale invariant.
Examining the QCD Lagrangian (2.4)

$$\mathcal{L}_{QCD} = \sum_f \left[\bar{\psi}_f \left(\not{D} - m_f\right) \psi_f\right] - \frac{1}{4} \mathcal{G}_{a\mu\nu} \mathcal{G}^{\mu\nu}_a \tag{2.85}$$

we find at first glance that it is invariant under scale transformations for $m_f = 0$. The kinetic term, the quark gluon interaction term as well as the gluon self-interaction term are all invariant on the classical level because they have scaling dimension four. However on the quantum level this symmetry is broken as found by Collins et al. [42] and the corresponding anomalous trace of the energy-momentum tensor can be derived from renormalization group calculations to be

$$\Theta^\mu_\mu = \frac{\beta_{QCD}(g)}{2g} \left\langle G^a_{\mu\nu} G^{\mu\nu}_a \right\rangle \tag{2.86}$$

where β_{QCD} is the beta-function of QCD, g is the strong coupling constant. The beta-function describes the change of the coupling g under change of the energy scale μ

$$\beta_{QCD}(g) = \mu \frac{\partial g}{\partial \mu} \tag{2.87}$$

To lowest order in the coupling β_{QCD} has been computed to be

$$\beta_{QCD} = -\frac{33 - 2N_f}{48\pi^2} g^3 \tag{2.88}$$

Now we may compare this result to the trace anomaly of the bag model, for which we first need the energy momentum tensor that is of the free-gas type

$$\Theta^{\mu\nu} = \begin{pmatrix} \epsilon & 0 & 0 & 0 \\ 0 & p & 0 & 0 \\ 0 & 0 & p & 0 \\ 0 & 0 & 0 & p \end{pmatrix} \tag{2.89}$$

Using equations (2.67), (2.68) this means that the trace anomaly will simply be

$$\Theta^{\mu}_{\mu} = \epsilon - 3p = \begin{cases} 4B & \text{for } T > T_c \\ 0 & \text{for } T < T_c \end{cases} \tag{2.90}$$

Thus one may connect the vacuum energy with the gluon condensate

$$\epsilon_V \sim B \sim \left\langle G^a_{\mu\nu} G^{\mu\nu}_a \right\rangle \tag{2.91}$$

In the next section we will use this result to fix some of the properties of the dilaton quark meson model.

2.10 Dilaton Quark Meson Model

To describe the dynamics of the phase transition and especially the impact on density perturbations it is essential to have a reasonable thermodynamic description of the chirally restored quark phase. For this we use the quark meson model with a dilaton field, which incorporates chiral symmetry breaking as well as the trace anomaly of QCD. This model has been discussed by numerous authors [43, 44, 45, 46] to describe nuclear matter. It has the interesting property that for a wide range of parameters the high temperature phase does only disappear in the $T \to 0$ limit [47], which is necessary to get an equation of state of the "wrong vacuum" that can be used to model inflation. We will apply a simplified version of the Lagrangian used in [45] and stick closely to their notation, while we do not include the ω-meson for simplicity and use quarks instead of nucleons as degrees of freedom. The Lagrangian includes the linear σ-model first introduced by [30] which incorporates the scalar isovector π-field with the σ-field as its chiral partner. Furthermore we include the isoscalar dilaton field χ that incorporates the scale anomaly and thus a non-trivial vacuum of QCD.

2.10.1 Lagrangian and Basic Thermodynamics

The Lagrangian of the dilaton quark meson model reads

$$\mathcal{L} = \frac{1}{2}\left(\partial_\mu \pi\right)^2 + \frac{1}{2}\left(\partial_\mu \sigma\right)^2 + \frac{1}{2}\left(\partial_\mu \chi\right)^2 + \bar{\psi}\left[i\partial\!\!\!/ - g(\sigma + i\gamma_5 \vec{\tau}\cdot\vec{\pi})\right]\psi - U(\pi,\sigma,\chi) \quad (2.92)$$

with the potential

$$\begin{aligned} U(\pi,\sigma,\chi) &= \frac{\lambda}{4}(\sigma^2+\pi^2)^2 - \frac{k_0}{2}\left(\frac{\chi}{\chi_0}\right)^2(\sigma^2+\pi^2) \\ &- f_\pi m_\pi^2 \sigma \left(\frac{\chi}{\chi_0}\right)^2 + k_1\left(\frac{\chi}{\chi_0}\right)^4 + \frac{1}{4}\chi^4 \ln\frac{\chi^4}{\chi_0^4} \end{aligned} \quad (2.93)$$

In this potential appropriate powers of χ/χ_0 have been inserted to render the Lagrangian scale invariant except for the two terms that are supposed to break scale symmetry. In equation (2.81) we have seen that in the ordinary linear sigma model the quadratic k_0 term will lead to a breaking of scale symmetry which is no longer the case here. As we shall have see the chiral symmetry breaking term still breaks the scale symmetry as does the logarithmic term in χ. We will discuss this in more detail after we have outlined the most important aspects of the model.
After integrating out the quark degrees of freedom [33] one arrives at an effective

mesonic Lagrangian

$$L(\pi,\sigma,\chi) = \frac{1}{2}\left(\partial_\mu\pi\right)^2 + \frac{1}{2}\left(\partial_\mu\sigma\right)^2 + \frac{1}{2}\left(\partial_\mu\chi\right)^2 - U(\pi,\sigma,\chi) - \Omega_{\bar{q}q}(T,\mu,m_q) \quad (2.94)$$

with the quark-antiquark potential reading

$$\Omega_{\bar{q}q}(T,\mu,\sigma) = -\frac{\nu_q TV}{2\pi^2}\int_0^\infty dpp^2\left[\ln\left(1+e^{-\beta(E_q-\mu)}\right) + \ln\left(1+e^{-\beta(E_q+\mu)}\right)\right] \quad (2.95)$$

with the quasiparticle quark energy $E_q = \sqrt{p^2+m_q^2}$. The effective quark mass is on the mean field level determined by

$$m_q^2 = g^2\sigma^2 \quad (2.96)$$

The mean field values of the glueball and the meson fields in the vacuum are $\langle\chi\rangle = \chi_0, \langle\sigma\rangle = \sigma_0 = f_\pi$ and $\langle\pi\rangle = 0$. The full thermodynamic potential is then given by

$$\Omega(T,\mu,\pi,\sigma,\chi) = (U(\pi,\sigma,\chi) - U_{vac})V + \Omega_{\bar{q}q}(T,\mu,\sigma) \quad (2.97)$$

Where U_{vac} is subtracted to make sure $\Omega(0,0,0,f_\pi,\chi_0) = 0$, yielding

$$U_{vac} = \frac{\lambda}{4}f_\pi^4 - \frac{k_0}{2}f_\pi^2 - f_\pi^2 m_\pi^2 + k_1 \quad (2.98)$$

Ω/V exhibits two minima, the first one is located at[21] $\sigma \sim 0$ and $\chi \sim 0$ and a second one at $\sigma \sim f_\pi$ and $\chi \sim \chi_0$. The former corresponds to the chirally restored phase with a low effective mass while the second one is the chirally broken phase with a large effective mass. If the scalar coupling is sufficiently large the both minima are present in the low temperature limit, although the chirally broken phase is energetically favored. As the authors of Ref. [46] have found the chirally restored phase will undergo a crossover to restored scale symmetry at much higher temperatures if the density is non-zero, i.e. the maximum moves towards $\chi \sim 0$. Note that we do not fix the effective quark mass in the vacuum via the Goldberger-Treiman relation because the model is set up to describe quarks in the high temperature chirally restored phase. We will later on fix the model parameters using the more relevant value of the vacuum energy and the masses of the sigma meson and the

[21] at least at low densities and high temperatures, see e.g. Ref. [46]

dilaton. The constants k_0 and k_1 are determined by the conditions

$$\begin{aligned} \left.\frac{\partial\Omega/V}{\partial\sigma}\right|_{vac} &= 0 = \lambda f_\pi^3 - k_0 f_\pi - f_\pi m_\pi^2 \\ &\rightarrow k_0 = \lambda f_\pi^2 - m_\pi^2 \end{aligned} \tag{2.99}$$

$$\begin{aligned} \left.\frac{\partial\Omega/V}{\partial\chi}\right|_{vac} &= 0 = -\frac{k_0}{\chi_0} f_\pi^2 - \frac{2 f_\pi^2 m_\pi^2}{\chi_0} + \frac{4k_1}{\chi_0} + \chi_0^3 \\ &\rightarrow k_1 = \frac{f_\pi^2}{4}\left(2m_\pi^2 + k_0 - \frac{\chi_0^4}{f_\pi^2}\right) \\ &= \frac{f_\pi^2}{4}\left(m_\pi^2 + \lambda f_\pi^2 - \frac{\chi_0^4}{f_\pi^2}\right) \end{aligned} \tag{2.100}$$

The equations of motion are found by minimizing the thermodynamic potential with respect to σ and χ.

$$\frac{\partial\Omega/V}{\partial\sigma} = 0 = \lambda\sigma^3 - k_0\left(\frac{\chi}{\chi_0}\right)^2\sigma - f_\pi m_\pi^2\left(\frac{\chi}{\chi_0}\right)^2 + g\rho_S \tag{2.101}$$

$$\frac{\partial\Omega/V}{\partial\chi} = 0 = -k_0\frac{\chi}{\chi_0^2}\sigma^2 - 2f_\pi m_\pi^2\sigma\frac{\chi}{\chi_0^2} + \chi^3\left(\frac{4k_1}{\chi_0^4} + 1 + \ln\frac{\chi^4}{\chi_0^4}\right) \tag{2.102}$$

These equations can reduced to a one dimensional problem by solving for χ explicitly

$$\chi = \chi_0\left(\frac{\lambda\sigma^3 + g\rho_S}{k_0\sigma + m_\pi^2 f_\pi}\right)^{1/2} \tag{2.103}$$

The scalar density is defined by

$$\rho_S = \frac{g\nu_q}{2\pi^2}\int_0^\infty dp p^2\frac{m_q}{E_q}\left[\frac{1}{e^{\beta(E_q-\mu)}+1} + \frac{1}{e^{\beta(E_q+\mu)}+1}\right] \tag{2.104}$$

The pressure is just

$$P(T,\mu) = -\frac{\Omega}{V} \tag{2.105}$$

the net baryon density is calculated as usual

$$\bar{n}_B(T,\mu,m_q) = \frac{\partial\Omega/V}{\partial\mu} = \frac{\nu_q}{2\pi^2}\int_0^\infty dp p^2\left[\frac{1}{e^{\beta(E_q-\mu)}+1} - \frac{1}{e^{\beta(E_q+\mu)}+1}\right] \tag{2.106}$$

The energy density is then given by

$$\begin{aligned}
\epsilon(T,\mu) &= \left(1 - T\frac{\partial}{\partial T} - \mu\frac{\partial}{\partial \mu}\right)\frac{\Omega}{V} = -P + T\frac{\partial P}{\partial T} + \mu\bar{n}_B \\
&= -P + T\frac{\nu_q}{2\pi^2}\int_0^\infty dp p^2 \left[\ln\left(1 + e^{-\beta(E_q-\mu)}\right) + \ln\left(1 + e^{-\beta(E_q+\mu)}\right)\right] \\
&\quad + \frac{\nu_q T^2}{2\pi^2}\int_0^\infty dp p^2 \left[\frac{E_q - \mu}{T^2(e^{\beta(E_q-\mu)}+1)} + \frac{E_q+\mu}{T^2(e^{\beta(E_q+\mu)}+1)}\right] + \mu\bar{n}_B \\
&= -P + (P + U(\pi,\sigma,\chi) - U_{vac}) \\
&\quad + \frac{\nu_q}{2\pi^2}\int_0^\infty dp p^2 E_q \left[\frac{1}{e^{\beta(E_q-\mu)}+1} + \frac{1}{e^{\beta(E_q+\mu)}+1}\right] - \mu\bar{n}_B + \mu\bar{n}_B \\
&= U(\pi,\sigma,\chi) - U_{vac} + \frac{\nu_q}{2\pi^2}\int_0^\infty dp p^2 E_q \left[\frac{1}{e^{\beta(E_q-\mu)}+1} + \frac{1}{e^{\beta(E_q+\mu)}+1}\right]
\end{aligned} \tag{2.107}$$

The entropy density can as usual be deduced from the Euler-equation

$$\epsilon = Ts - pV + \mu n_B \quad \rightarrow \quad s = \frac{\epsilon + p - \mu n_B}{T} \tag{2.108}$$

Calculating the speed of sound is a bit more involved but straightforward. By definition the speed of sound is the isentropic derivative of the pressure with respect to the energy density

$$c_s^2 = \left.\frac{\partial p}{\partial \epsilon}\right|_s \tag{2.109}$$

Isentropic means nothing else but

$$ds = \left.\frac{\partial s}{\partial T}\right|_\mu dT + \left.\frac{\partial s}{\partial \mu}\right|_T d\mu = 0 \tag{2.110}$$

Then we need the total differentials of the pressure and the energy density

$$dp = \left.\frac{\partial p}{\partial T}\right|_\mu dT + \left.\frac{\partial p}{\partial \mu}\right|_T d\mu = \left.\frac{\partial p}{\partial T}\right|_\mu dT - \left.\frac{\partial p}{\partial \mu}\right|_T \left.\frac{\partial s}{\partial T}\right|_\mu \left(\left.\frac{\partial s}{\partial \mu}\right|_T\right)^{-1} dT \tag{2.111}$$

$$d\epsilon = \left.\frac{\partial \epsilon}{\partial T}\right|_\mu dT + \left.\frac{\partial \epsilon}{\partial \mu}\right|_T d\mu = \left.\frac{\partial \epsilon}{\partial T}\right|_\mu dT - \left.\frac{\partial \epsilon}{\partial \mu}\right|_T \left.\frac{\partial s}{\partial T}\right|_\mu \left(\left.\frac{\partial s}{\partial \mu}\right|_T\right)^{-1} dT \tag{2.112}$$

where we have made use of equation (2.110) in the second step. The details on the required derivatives can be found in appendix 6.1.1. Multiplying both by $\left.\frac{\partial s}{\partial \mu}\right|_T$ we arrive at the speed of sound in the form

$$\left.\frac{\partial p}{\partial \epsilon}\right|_s = \frac{\left.\frac{\partial p}{\partial T}\right|_\mu \left.\frac{\partial s}{\partial \mu}\right|_T - \left.\frac{\partial p}{\partial \mu}\right|_T \left.\frac{\partial s}{\partial T}\right|_\mu}{\left.\frac{\partial \epsilon}{\partial T}\right|_\mu \left.\frac{\partial s}{\partial \mu}\right|_T - \left.\frac{\partial \epsilon}{\partial \mu}\right|_T \left.\frac{\partial s}{\partial T}\right|_\mu} = \frac{s \left.\frac{\partial s}{\partial \mu}\right|_T - n_B \left.\frac{\partial s}{\partial T}\right|_\mu}{\left.\frac{\partial \epsilon}{\partial T}\right|_\mu \left.\frac{\partial s}{\partial \mu}\right|_T - \left.\frac{\partial \epsilon}{\partial \mu}\right|_T \left.\frac{\partial s}{\partial T}\right|_\mu} \tag{2.113}$$

The remaining parameters χ_0 and λ are fixed via the QCD vacuum energy and the mass of the sigma meson.

2.10.2 Vacuum energy and the trace anomaly

As we have seen before in section 2.9 the trace anomaly of QCD relates the vacuum energy. In case of the dilaton quark meson model one may use this to fix the parameter χ_0 [44]. The scale breaking of the linear term in σ is altered as compared to (2.81) in the ordinary linear sigma model. According to equation (2.77) we find also find another scale breaking term

$$\begin{aligned} 4\mathcal{L} &- \sum_i \left(\frac{\partial \mathcal{L}}{\partial \phi_i} \kappa_i \phi_i + \frac{\partial \mathcal{L}}{\partial(\partial_\nu \phi_i)} (\kappa_i + 1) \partial^\nu \phi_i \right) \\ &= f_\pi m_\pi^2 \sigma + \chi^4 \simeq \chi^4 = 4\epsilon_{vac} \left(\frac{\chi}{\chi_0} \right)^4 \\ \rightarrow \epsilon_{vac} &= \frac{\chi_0^4}{4} \end{aligned} \tag{2.114}$$

We neglect the contribution from the first term representing the quark condensate for simplicity as done in [45, 39] because its contribution is much smaller than the one from the gluon condensate given by the second term[22]. QCD sum rules suggest $|\epsilon_{vac}| \approx (240 \text{ MeV})^4$ (see ref. [48]) while bag model estimates range from $(235 \text{ MeV})^4$ down to $(145 \text{ MeV})^4$ in the original paper of the MIT group [37]. This results in a possible range for the parameter

$$205 \text{ MeV} < \chi_0 < 339 \text{ MeV} \tag{2.115}$$

which we will use to limit the parameter space later on.

[22] For the parameters used later on the gluon condensate is about 80 times larger than the quark condensate.

2.10.3 Diagonalizing the mass matrix

Now we want to connect the parameters λ and χ_0 to the vacuum masses of the sigma meson, the pion and the glueball. For a single field the mass would simply be given by the curvature at the minimum of the potential in the vacuum but in for a Lagrangian with multiple fields one has to consider the matrix

$$M_{ij} = \left.\frac{\partial^2 U}{\partial\phi_i \partial\phi_j}\right|_{vac} \tag{2.116}$$

where $\phi_i = \pi, \sigma, \chi$. This matrix will in general not be diagonal and therefore the mathematical fields in the Lagrangian cannot be directly be connected to the physical fields but will rather be linear combinations thereof. For a more complicated Lagrangian e.g. with vector fields and isospin-hypercharge multiplets one would also have to take care that the other quantum numbers match those of a physical particle when constructing possible linear combinations.
In the given case the mass matrix has the following form

$$M_{ij} = \left.\begin{pmatrix} \frac{\partial^2 U}{\partial\pi^2} & \frac{\partial^2 U}{\partial\pi\partial\sigma} & \frac{\partial^2 U}{\partial\pi\partial\chi} \\ \frac{\partial^2 U}{\partial\sigma\partial\pi} & \frac{\partial^2 U}{\partial\sigma^2} & \frac{\partial^2 U}{\partial\sigma\partial\chi} \\ \frac{\partial^2 U}{\partial\chi\partial\pi} & \frac{\partial^2 U}{\partial\chi\partial\sigma} & \frac{\partial^2 U}{\partial\chi^2} \end{pmatrix}\right|_{vac} \tag{2.117}$$

The pion mass is already fixed to m_π by choice of the term $-f_\pi m_\pi^2 \sigma \left(\frac{\chi}{\chi_0}\right)^2$ and by construction of the chiral Lagrangian. The only $\pi-$dependent terms are quartic or quadratic in π and therefore any first derivative will vanish when using the vacuum condition $\langle\pi\rangle = 0$. In other words the matrix is already diagonal in the π-sector

$$M_{ij} = \left.\begin{pmatrix} \frac{\partial^2 U}{\partial\pi^2} & 0 & 0 \\ 0 & \frac{\partial^2 U}{\partial\sigma^2} & \frac{\partial^2 U}{\partial\sigma\partial\chi} \\ 0 & \frac{\partial^2 U}{\partial\chi\partial\sigma} & \frac{\partial^2 U}{\partial\chi^2} \end{pmatrix}\right|_{vac} \tag{2.118}$$

Thus we only need to find the solutions to the following eigenvalue problem

$$\left.\begin{pmatrix} \frac{\partial^2 U}{\partial\sigma^2} - m_i^2 & \frac{\partial^2 U}{\partial\sigma\partial\chi} \\ \frac{\partial^2 U}{\partial\chi\partial\sigma} & \frac{\partial^2 U}{\partial\chi^2} - m_i^2 \end{pmatrix}\right|_{vac} \begin{pmatrix} v_{i1} \\ v_{i2} \end{pmatrix} = 0 \tag{2.119}$$

The explicit solutions are rather lengthy and not very illuminating and can be found in the appendix in section 6.1.2. The two masses have a fixed ordering so it is obvious to connect the lighter excitation with the σ-meson.

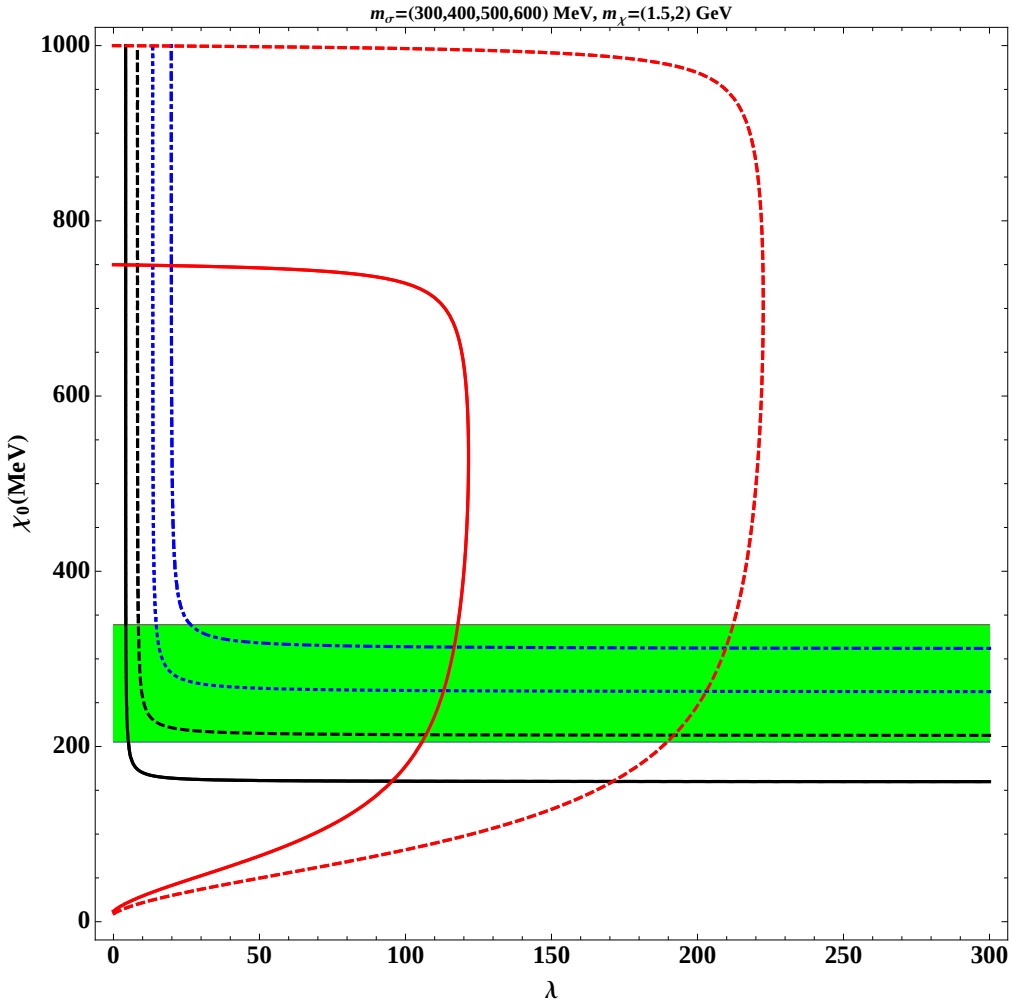

Figure 2.4: This plot shows the lines of constant mass for the two mass eigenstates in the $\chi_0 - \lambda$-parameter plane. The heavier solution is shown in red for masses of 1,5 GeV (solid) and 2 GeV (dashed) while the lighter solution is shown for masses of 300 MeV (solid black), 400 MeV (dashed black), 500 MeV (dotted blue) and 600 MeV (dashed-dotted blue).

The results in the $\lambda - \chi_0$-plane for several fixed masses are shown in figure 2.4. Intersection points mark viable parameter sets of the model. The green shaded region shows the allowed region from vacuum energy estimates (2.114), as one can plainly see this excludes the intersection points at high χ_0 and small values of λ.

2.10.4 Pressure and Equation of State

We choose a σ-mass of 642 MeV, a dilaton mass of 1.5 GeV and a vacuum energy of (236 MeV)^4 to achieve a reasonable critical temperature of 170 MeV for the phase transition at zero net density. The scalar coupling is chosen to be g = 7.5 which is approximately the limiting value above which the chirally restored phase is present even in the $T \to 0$ limit for the given parameters. In figure 2.5

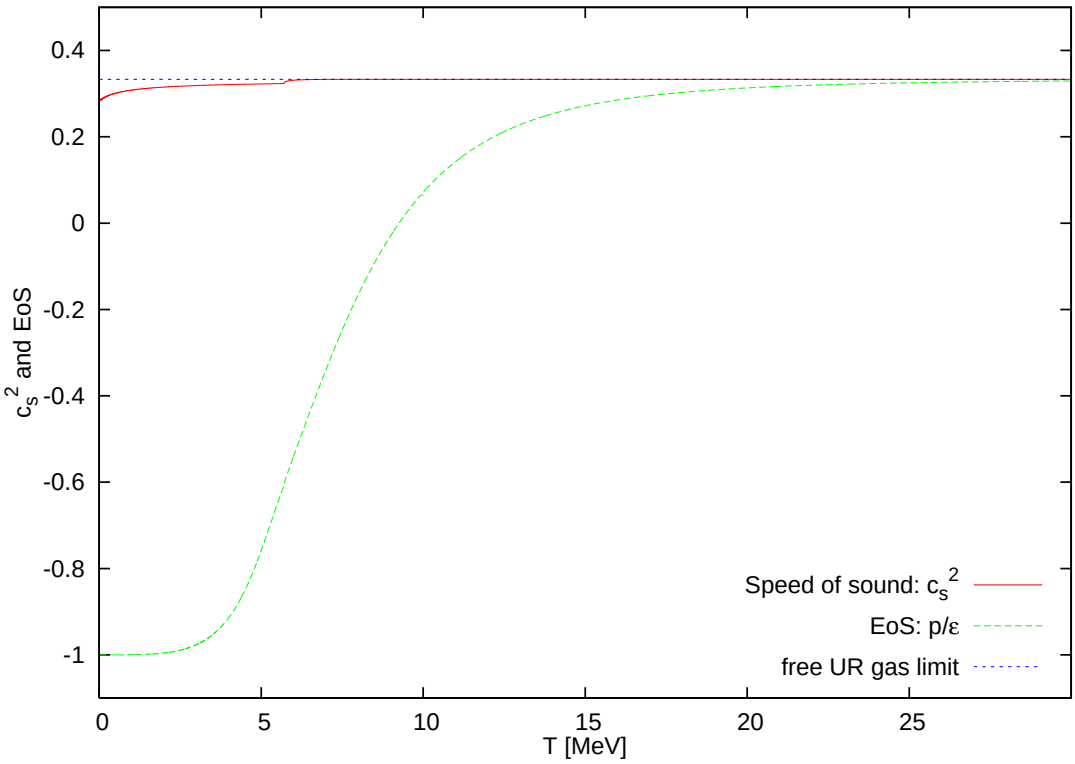

Figure 2.5: Square of the isentropic speed of sound and equation of state for the limiting case $\mu_B/T = 125.2$.

we show the resulting speed of sound and equation of state in the maximum case $\mu_{Bi}/T_i = 125.2$. As one could expect the speed of sound stays very close to the relativistic gas value of $c_s^2 = 1/3$ because the effective quark mass stays low in the chirally restored phase. The equation of state nicely interpolates from a relativistic gas ($w = 1/3$) to that of vacuum energy ($w = -1$). The small kink in the speed of sound at $T \sim 6$ MeV is caused by the merging of a third always metastable intermediate phase with the chirally restored phase which causes a sudden but small change in the effective mass. The existence of this third maximum in the pressure within this model has been discussed before for example by Mishustin

[43], it can also be seen in figure 2.6 at $\sigma \sim 0.5 f_\pi$. There we show the pressure as a function of the σ-field (or equivalently the effective mass) at the phase transition temperature $T = 10.1$ MeV and $\mu_B/T = 125.2$. The first minimum at $\sigma \sim 0$ is the chirally restored phase, the chirally broken phase is located at $\sigma \sim f_\pi$. The intermediate phase only appears close to the phase transition and never becomes the favored one. Note that at these temperatures and densities one may expect color-superconducting quark matter in one of many possible phases [49] which exceeds the scope of the current investigation but may be an interesting starting point for an alternative field theoretical description of the scenario. For comparison we

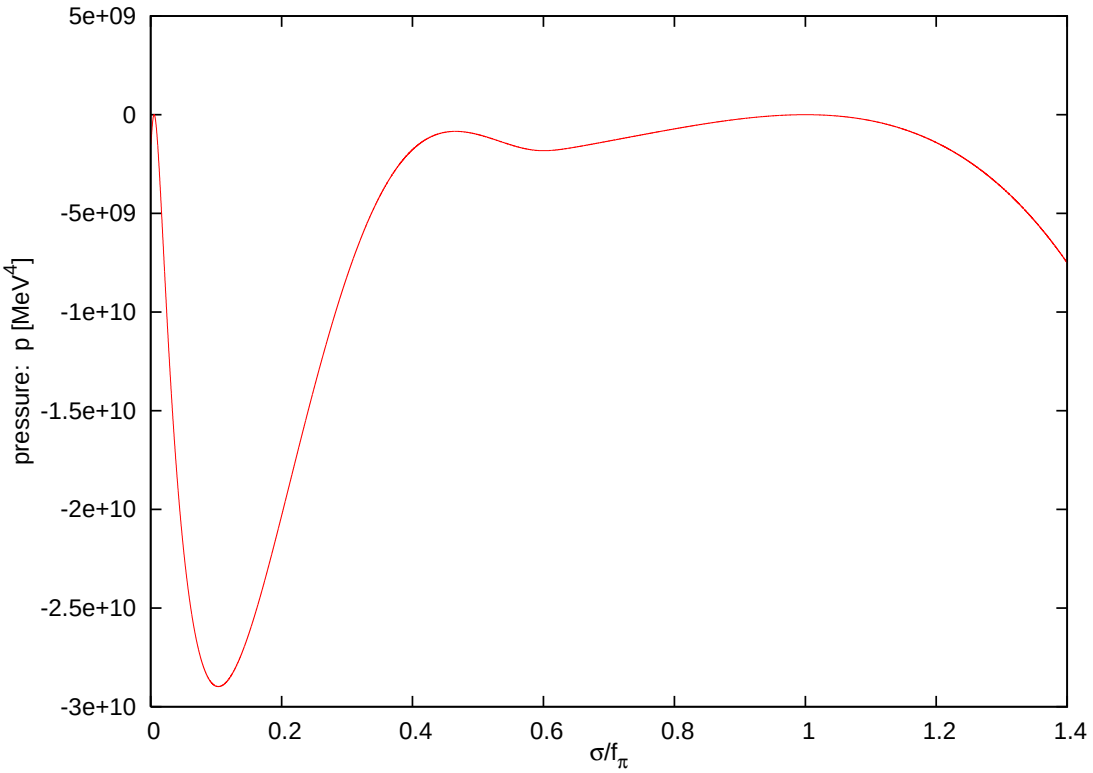

Figure 2.6: Pressure p as a function of the $\sigma-$field in units of f_π at the phase transition temperature $T = 10.1$ MeV and $\mu_B/T = 125.2$.

show the pressure at the phase transition temperature $T = 170$ MeV $\mu_B = 0$ in figure 2.7. As one can see the barrier between the chirally restored phase at $\sigma \sim 0$ and the chirally broken phase at $\sigma \sim 0.9 f_\pi$ is weaker by more than an order of magnitude as compared to the case at high density and low temperature showing that the phase transition actually becomes stronger. Figure 2.8 additionally shows a 3d map of the pressure for the $T = 10.1$ MeV and $\mu_B/T = 125.2$ case. Here one can see that the chirally restored phase does not have a restored scale symmetry

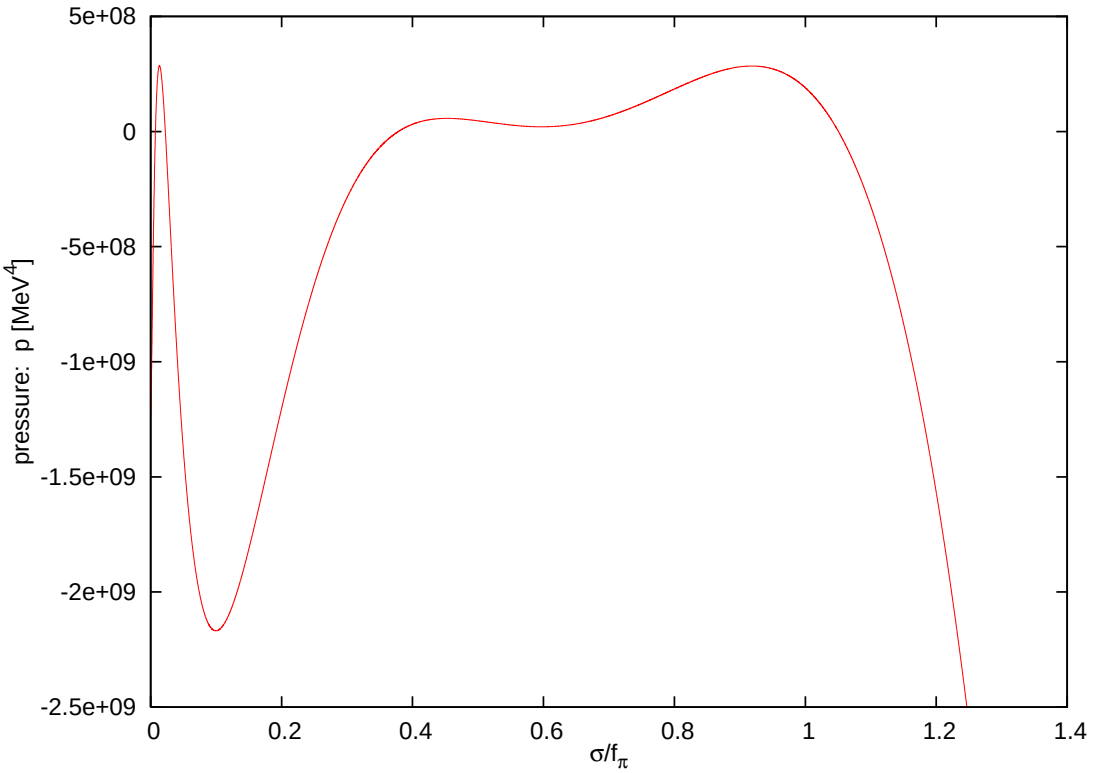

Figure 2.7: Pressure p as a function of the $\sigma-$field in units of f_π at the phase transition temperature $T = 170$ MeV and $\mu_B = 0$.

$\chi_0 \sim 0$ but rather $\chi \sim 0.8\chi_0$. As the authors of Ref. [46] have found the chirally restored phase will undergo a crossover to restored scale symmetry at much higher temperatures if the density is non-zero, i.e. the maximum moves towards $\chi \sim 0$. Finally in figure 2.9 the phase diagram of the dilaton-quark-meson model for temperature and baryochemical potential is shown. For the chosen model parameters the phase transition is first order everywhere. Furthermore as stated before the high temperature phase is meta-stable anywhere below the phase transition line and only disappears in the limit of vanishing temperature and chemical potential. At vanishing baryochemical potential the phase transition temperature is $T_c = 170$ MeV and at the other end one finds $\mu_c = 1272.18$ MeV for the high density zero temperature end of the phase transition line. In section 4.4 we will use the ϵ, p, c_s^2 and w of the chirally restored phase for our structure formation calculations in the little inflation scenario.

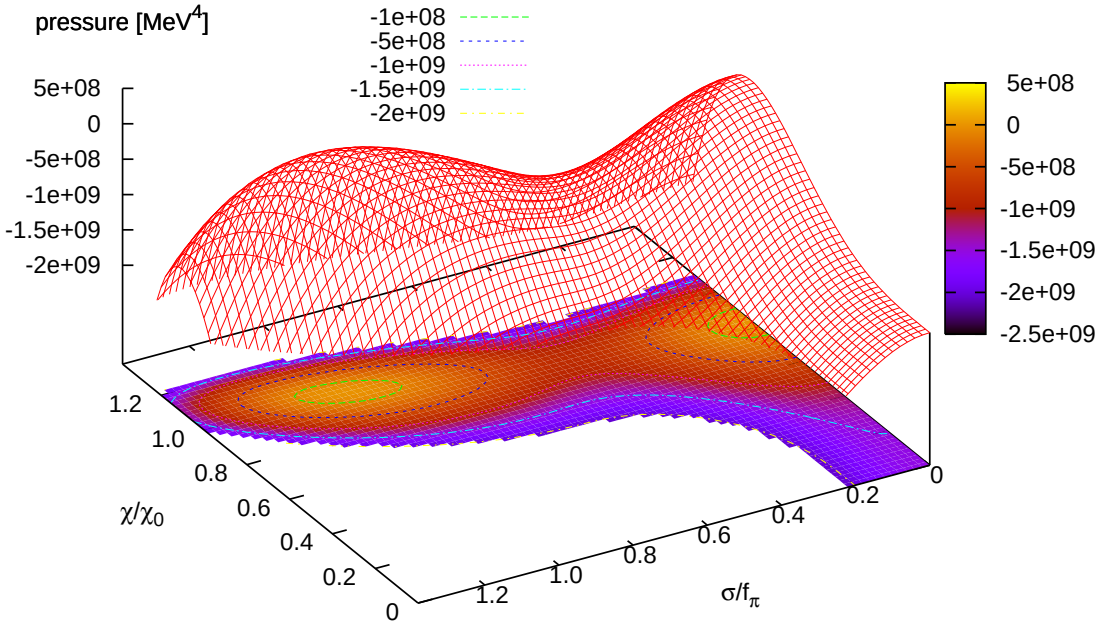

Figure 2.8: Pressure p as a function of the $\sigma-$ and $\chi-$fields in units of f_π and χ_0, respectively, at the phase transition temperature $T = 10.1$ MeV and $\mu_B/T = 125.2$.

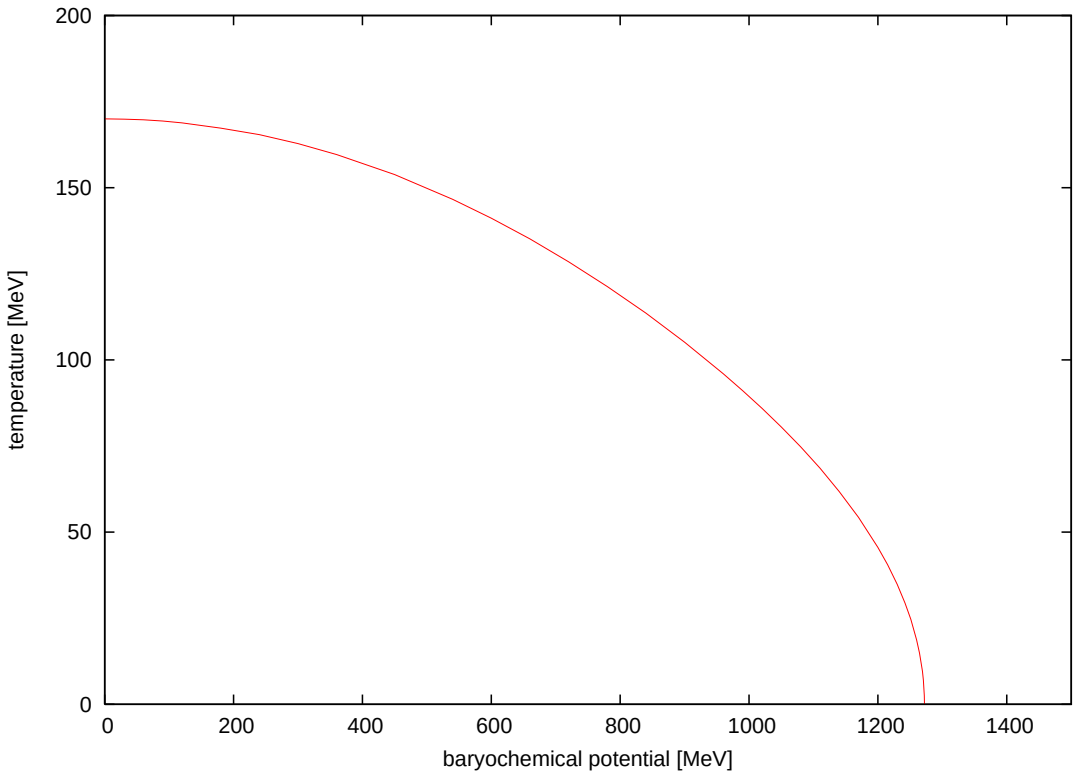

Figure 2.9: Phase diagram of the dilaton-quark-meson model for the previously mentioned parameters.

Chapter 3

Cosmology

These theories were based on the hypothesis that all matter in the universe was created in one *big bang* at a particular time in the remote past. It now turns out that [...] all such theories are in conflict with the observational requirements [...] to a degree that can hardly be ignored.

– Fred Hoyle, coining the expression "big bang" in 1949.

3.1 The homogeneous and isotropic FLRW-universe

Cosmology has gone a long way from the discovery of the Friedmann-Lemaître-Robertson-Walker (FLRW) solution to the Einstein equations to the present day high precision cosmology.
It all started in 1922 when Alexander Friedmann found the solution for an homogeneous and isotropic universe that was later independently discovered by the Belgian priest and physicist Georges Lemaître (in 1927) and by Howard Percy Robertson and Arthur Geoffrey Walker in the beginning of the 1930s.
The first observational evidence that supported the idea of an expanding universe was found in 1929 by the American astronomer Edwin Hubble. He observed variable stars named Cepeids that are believed to be good standard candles for distance measurements[1] and found what is today called the linear Hubble law

$$v = H_0 \cdot d, \qquad v \ll c \tag{3.1}$$

where v is the recessional velocity, H_0 is the present Hubble "constant"[2], d the distance to the object and c the speed of light. The linear Hubble law (3.1) shows that two objects move away from each other at a speed proportional to their distance. If we now assume that this held true for all times it means that all objects originated from one point at a time $t_H = H_0^{-1}$ which gives us an estimate for the age of the universe. As we shall see later the Hubble "constant" is in fact time dependent and was larger at earlier times, therefore the universe did not originate in one point and H_0^{-1} is only by chance a good estimate of the actual age of the universe.
The existence of a large amount of non-luminous dark matter was first deduced from observations of the Coma cluster in 1933 [51, 52] by Fritz Zwicky. He used the virial theorem to show that the velocity dispersion[3] is too large for the system to be stable unless the potential energy (and therefore also the mass of the cluster) is much larger than inferred from counting the visible galaxies. The nineteen thirties also saw the discovery of the dutch astronomer Jan Oort who found that stars inside the Milky Way seemed to move at too high rotational velocities [53] which indicated that mass was also missing on galactic scales[4].

[1] They are very bright and show a dependence of the period of variability with their total luminosity

[2] It is noteworthy that Hubbles initial results for H_0 ($\sim$500 km/(s Mpc)) were actually an order of magnitude larger than present day results ($\sim$ 70 km/(s Mpc)) indicating that he came to the right conclusion only by chance [50].

[3] that allows an estimate of the mean kinetic energy of galaxies in the cluster

[4] This was shown to be true also for the Galaxy M33 by Louise Volders in 1959 [54].

Observational data was inconclusive for several decades and cosmology saw many competing theories the most important one perhaps being the steady-state universe and the hot big bang. In short the steady-state universe assumed that the cosmos had always been in the present form and was consequently after Hubble's observations in need of an universal perpetual source of matter and energy to explain why the observed expansion had not lead to an empty universe. This theory was developed by Bondi, Gold and Hoyle in the late 1940s mostly on contradiction to the theory of a hot big bang. Hoyle actually coined the expression "big bang" to mock these theories he deemed wrong[5]. The big bang theory states that the universe started in a hot dense state and has expanded ever since, cooling down and evolving into the presently observed universe.

The observation that decided which theory was wrong finally came in 1965 with the fortunate discovery of the cosmic microwave background radiation (CMBR) by Arno Penzias and Robert Wilson[6].

Within the big bang theory the CMBR originates from an early hot stage in the evolution of the universe, when it was approximately 380 000 years old. At that time the universe had cooled down to temperatures where first helium and then hydrogen could recombine with the free electrons and the universe became transparent to photons. This transpired at a temperature of around 3000 K ($\sim$ 0.3 eV) well below the ionization temperature of hydrogen of 150000 K ($\sim$13.6 eV). Due to the large number of $\sim 1.7 \cdot 10^9$ photons per baryon any recombined H-Atom was instantly reionized until the temperature of the the photon-baryon plasma had sufficiently dropped due to expansion. Recombination strongly reduced the number of charged particles and thus increased the mean free path of photons rapidly until photons and baryons basically ceased scattering and the universe became transparent. As a side remark: the photons emitted by the recombining hydrogen and helium atoms did not create the CMBR as sometimes falsely suggested. The total energy density (including the rest mass) of baryons and radiation was roughly equal at that point and thus each baryon emitting a fraction of 13.6 eV/1GeV $\sim 10^{-8}$ of its energy in form of radiation was practically negligible. In other words the already present primordial radiation decoupled after recombination and we can

[5]The corresponding quote can be found on the title page of this chapter.

[6]The two were at the time actually just trying to calibrate a new radio antenna for their employer AT&T Bell Laboratories. They could not get rid of a constant noise that seemed to come from every direction and thus seemed to be a local problem with the antenna. They were unable to find the source of the problem, until the group of Robert Dicke at the close by Princeton University heard of the issue and realized that Penzias and Wilson must have found what they were just starting to look for, the cosmic microwave background radiation.

today observe the surface of last scattering of these photons. The temperature has dropped to merely 2.7 Kelvin ($\sim 2.3 \cdot 10^{-4}$ eV) due to the redshift caused by the cosmic expansion.

The discovery of the CMBR was the nail in the coffin of the steady state universe since it seemed extremely unnatural to have a uniform blackbody spectrum from every direction if the universe was infinitely old. This would either require the radiation to be emitted locally or abandoning the cosmological principle[7]. Thus after it was established by follow-up observations that the microwave background radiation was indeed a blackbody spectrum support for the steady state universe crumbled and Penzias and Wilson were awarded the Nobel Prize for their discovery in 1978.

Already in the 1940s Ralph Alpher and George Gamow [55] pioneered another very important and successful cornerstone of modern cosmology, big bang nucleosynthesis (BBN). The theory of BBN gives explanations for the observed abundances of light elements in the universe in contrast to competing theories that tried to explain the observed chemical distribution by stellar processes alone[8]. The first important result of BBN is that ^{4}He makes up $\sim 24\%$ of the baryonic mass while the rest consists almost entirely of ^{1}H. BBN furthermore predicts that other stable light isotopes only contribute in tiny fractions, most importantly deuterium ^{2}H, ^{3}He, ^{7}Li and ^{6}Li.

The high fraction of ^{4}He cannot be explained by stellar processes alone unless the universe was much older but then significant fractions of other elements would also be expected. From stellar evolution models one may only expect about 1% of hydrogen being processed to ^{4}He in the given time of ~ 10 billion years. Big bang nucleosynthesis occurred during a short period in the early universe from temperatures of 1 MeV down to 30 keV at about 1 sec. to 100 sec. after the big bang. Weak interactions kept neutrons and protons in β-equilibrium down to a temperature of 0.8 MeV until they became ineffective and the ratio of protons to neutrons froze out at a value of $n_n/n_p = e^{-\Delta m/T} = e^{-1.29/0.8} \approx 0.2$ where n_n and n_p are the number densities of neutrons and protons, respectively, and $\Delta m = 1.29$ MeV is their mass difference.

[7] That states that our position in the universe is not special in any way. Thus any observation above a sufficiently large length scale should be independent of the observer's location in the universe.

[8] Until the 60s this theory proposed in large parts by G.Burbidge, M.Burbidge, Fowler and Hoyle [56] was actually more popular partly because BBN only worked in the context of the not yet accepted big bang theory, as the name obviously suggests. Only when it became clear that stellar processes alone could not account for the large fraction of ^{4}He that observations showed in stars, the interstellar medium and the solar system BBN started to become the favored theory for the origin of the light elements.

The basic nuclear reactions of BBN that lead to ^{4}He all need deuterium as an intermediate step which resulted in the so called "deuterium bottleneck". Because of the high number of photons per baryon any deuterium nucleus was destroyed instantly by photodisintegration until the temperature dropped below ∼100 keV and the density of photons with sufficient energy[9] was strongly suppressed. Free neutrons are unstable with a lifetime of 886 seconds, thus about 10% of the neutrons decayed until ^{2}H could be produced in sufficient amounts to render the fusion reactions that lead to ^{4}He effective and store the surviving neutrons.

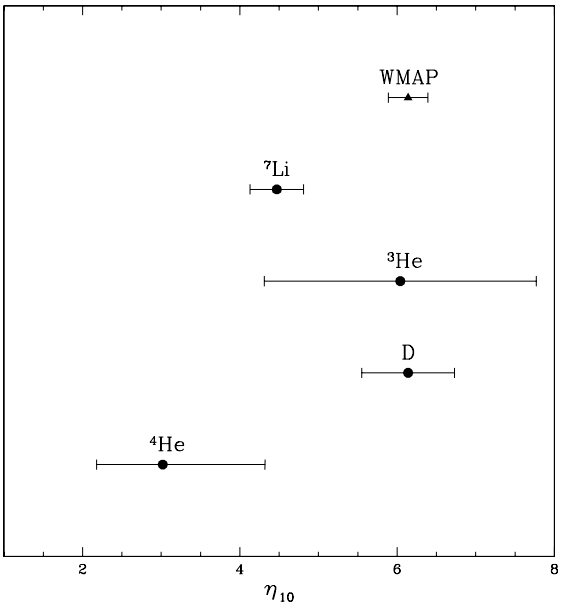

Figure 3.1: *Scaled baryon to photon ratio* $\eta_{10} = 10^{10}\eta_B$ *deduced from different primordial abundances of light elements and from WMAP, taken from* [57].

The most important unknown parameter for BBN clearly is the ratio of baryon density to entropy

$$\eta_B = \frac{n_B}{s} \tag{3.2}$$

that we will encounter time and again throughout this thesis. The big acceptance of BBN results from the fact that the observed abundances of ^{4}He, ^{3}He and D can be explained with an almost unique set of cosmological parameters, e.g. see figure 3.1 that shows the expected value of η_B from different observed primordial element abundances[10]. For a very detailed review of primordial nucleosynthesis see for example Ref. [57].

Comparison of big bang nucleosynthesis calculations to the observed abundances of light nuclei also allowed to quantify the mean density of baryonic matter in the universe for the first time. Once independent measurements of the total mass density (for example by observations of galaxy clusters) became available a discrepancy started to emerge. The observed amount of visible and dark matter did not coincide with the amount of

[9] The binding energy of deuterium is 2.2MeV.

[10] The error bars show the 1σstandard deviations. Within 2σ the ^{4}He results also agree with the other four results $1.7 \leq \eta_{10}(^4\text{He}) \leq 6.4$

[11] The issues of the constant galactic rotation curves and the high velocity dispersion of galaxy clusters were already known at that time but either could in principle be explained by various types of baryonic dark matter like brown dwarfs, black holes and planets.

baryons in the universe and non-baryonic dark matter became a serious possibility[11].

The 1970s and 80s saw the important work of the American physicist Vera Rubin [58, 59] who showed for a good sample of spiral galaxies that the rotational velocities in the outer parts are too high to be explained by the visible matter alone. This gave strong support for the existence of dark matter while its nature remained shrouded.

The COBE satellite finally measured the CMBR from space in 1990 finding that it represents by far the best blackbody spectrum ever measured[12] as can be seen in figure 3.1. Furthermore the COBE satellite also found tiny temperature anisotropies on top of the black body spectrum ($\delta T/T \approx 10^{-4}$), but the satellite was not specially constructed for this task and the additional instruments could only measure these fluctuations down to an angular scale of $\sim 1^\circ$. The temperature fluctuations

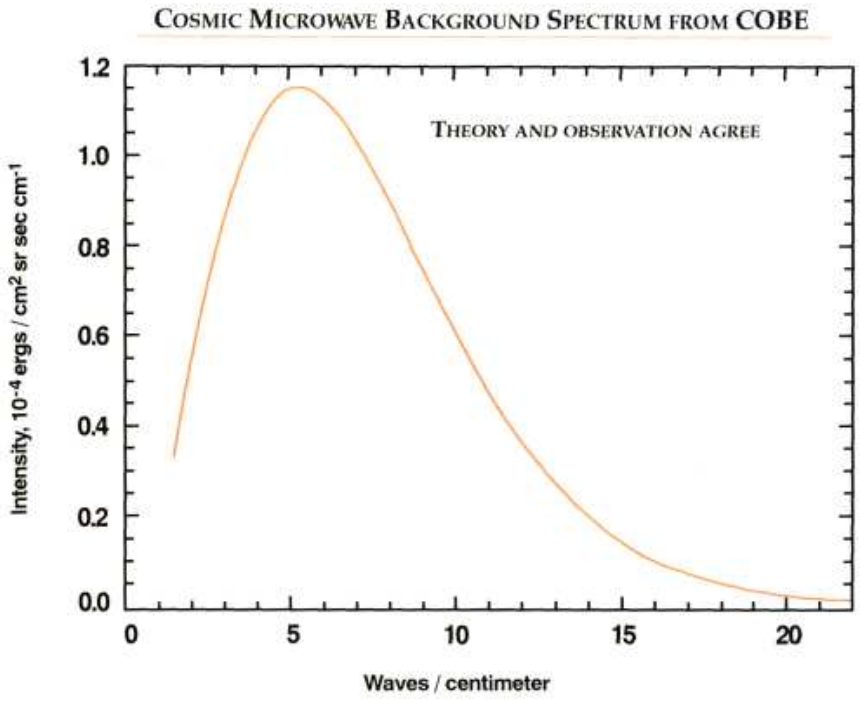

Figure 3.2: *Almost perfect blackbody spectrum of the of the CMBR as measured by the FIRAS experiment onboard the COBE satelite [61], errorbars are much smaller than the line width. Figure taken from [62].*

of the CMBR are believed to originate from quantum fluctuations that were mag-

[12]See for example Ned Wright's cosmology tutorial [60] where the COBE spectrum is shown with 400σ-errorbars that are still quite small.

nified by 50-60 orders of magnitude in spacial size and stretched even beyond the size of the observable universe today. The process responsible for this is called inflation which has become a cornerstone of the modern cosmological paradigm that solves several pressing problems of the original theory of the hot big bang. We will have a short overview of the topic in section 3.2 also in preparation of the main topic of the thesis. The fluctuations in the CMBR represent a snapshot of the inhomogeneities in the universe when it was about a factor 1100 smaller then today. These inhomogeneities are believed to have seeded all the presently observed large scale structures in the universe. It was clear that the knowledge of the spectrum of fluctuations would allow insights into many cosmological parameters that were only poorly known. It took another decade after COBE until in 2003 the WMAP-Satellite mission started. This satellite was in contrast to COBE dedicated to measure the CMBR anisotropies since the bulk properties were already known. Figure 3.3 shows the five year data full-sky map of the temperature anisotropies in the CMBR after subtraction of the strong galactic foreground and the dipole contribution as measured by WMAP [63]. Even by eye one may see

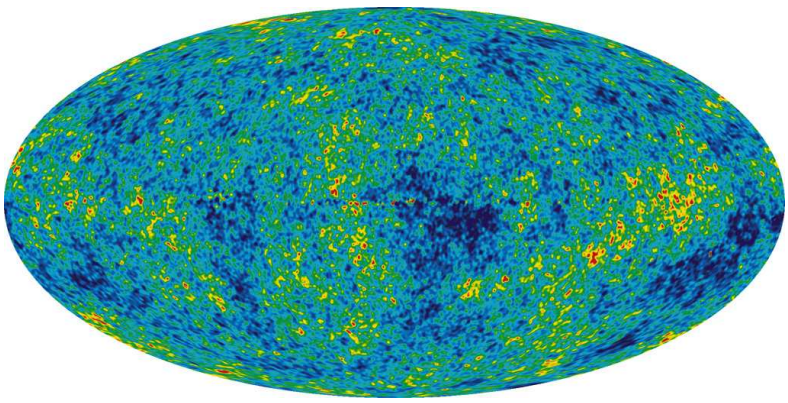

Figure 3.3: *Full-sky map of the temperature anisotropies in the CMBR after subtraction of the strong galactic foreground and the dipole contribution. Figure taken from the WMAP webpage* [63].

that there is a preferred size of the temperature fluctuations that turned out to have an angular diameter of roughly 1°. One may also see this in corresponding angular power spectrum as shown in figure 3.4. The various peaks are imprints of the by acoustic oscillations in the hot photon-baryon plasma during decoupling. The first peak corresponds to the sound horizon at recombination or in other words the oscillation with the largest possible wavelength. Thus each patch of one square degree in the sky corresponds to a Hubble volume at the point when the CMBR

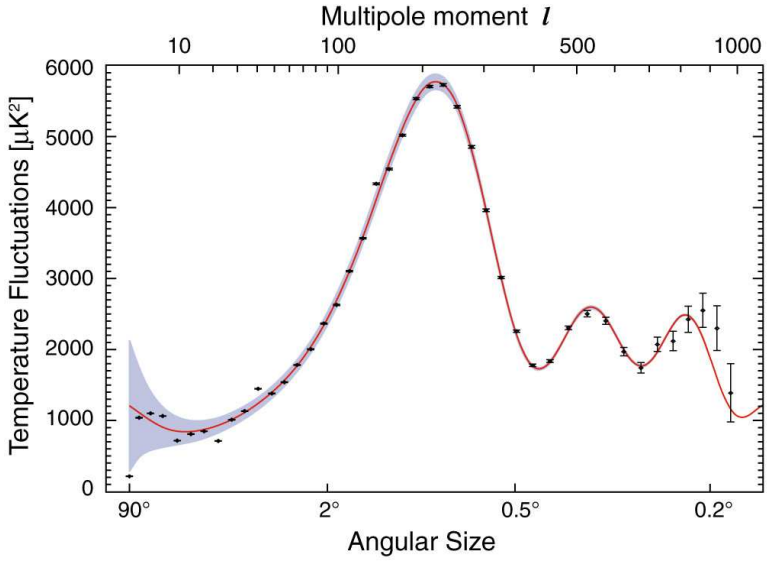

Figure 3.4: *Angular power spectrum of temperature fluctuations in the CMBR from the 5-year data release of the WMAP-satellite. Figure taken from the WMAP webpage [63].*

froze out, we will later on in section 3.2.2 discuss why this is actually a curious observation. From the position and relative amplitude of the different peaks one may deduce the geometry of the universe (i.e. the sign and size of the curvature-term in the Friedmann equations), the ratio of baryons to entropy η_B, the total amount of matter (baryonic and dark matter) and several other cosmological parameters. There were actually several other important advances from an observational point observations apart from the CMBR that lead to the combined Λ-CDM paradigm in cosmology. Perhaps the most important discoveries in this context not yet mentioned were the observed large scale distribution of structure of matter in the universe and the measurement of the late time acceleration of the cosmic expansion. Together all these observations have been strongly indicating that the universe is spacially flat today and mainly consists of two unknown components, non-baryonic dark matter ($\sim 25\%$) and dark energy ($\sim 70\%$). Ordinary baryonic matter seems to contribute only by 5% to the total energy budget of the universe[13], where about 90% of that is in the form of galactic and intergalactic gas. Dark matter seems to consist of non-relativistic particles that at most interact weakly with standard model particles[14]. We will later on assume dark matter to be non-relativistic and non-interacting already at the QCD-phase transition. Dark energy is mostly

[13]The contributions from photons and neutrinos seem to be negligible

[14]nevertheless even a very strong dark matter self-interaction cannot be excluded presently, see for example [64, 65]

characterized by having a negative pressure that drives the accelerated late time expansion of the universe and is in the most simple realizations only a cosmological constant corresponding to a fixed vacuum energy. Since dark energy is only relevant for late time cosmology we will neglect it for all later considerations but the basics ideas of accelerated expansion can also be found in section 3.2 about inflation.
Next we may first review some basic concepts of cosmology to gain the tools for the following discussions, especially for the treatment of cosmological perturbations.

3.1.1 FLRW-metric and the Friedmann equations

At early times as well as presently on large scales the universe the universe is highly homogeneous and isotropic and can be described using the well known Friedmann-Lemaître-Robertson-Walker (FLRW) line-element

$$ds^2 = {}^{(0)}g_{\mu\nu}dx^\mu dx^\nu = dt^2 - a^2(t)\gamma_{ij}dx^i dx^j = a^2(\eta)\left(d\eta^2 - \gamma_{ij}dx^i dx^j\right) \tag{3.3}$$

where ${}^{(0)}g_{\mu\nu}$ denotes the unperturbed background metric tensor, a is the scale parameter, γ_{ij} is the spacial 3x3 part of ${}^{(0)}g_{\mu\nu}$ and η is the conformal time defined by $dt = a\, d\eta$. The spacial part of the metric is given by

$$\gamma_{ij} = \frac{\delta_{ij}}{\left[1 + \frac{K}{4}\left(x^2 + y^2 + z^2\right)\right]^2} \tag{3.4}$$

with K being the curvature parameter that defines the geometry, i.e. $K < 0$ for a hyperbolic, $K = 0$ for a flat or $K > 0$ for a closed three dimensional space[15]. To find the equations of motion that describe the FLRW universe one has to solve the Einstein equations

$$G^\mu_\nu = R^\mu_\nu - \frac{1}{2}\delta^\mu_\nu R = 8\pi G T^\mu_\nu \tag{3.5}$$

Here G^μ_ν is the Einstein tensor, R^μ_ν is the Ricci tensor, $R \equiv R^\mu_\mu$ is the Ricci scalar, G is Newtons constant and T^μ_ν is the energy momentum tensor. Using the above metric one arrives at only two independent equations, namely the 0-0 equation and the i-i equation

$$\frac{a'^2}{a^4} + \frac{K}{a^2} = \frac{8\pi G}{3}T^0_0 \tag{3.6}$$

$$\frac{a''a}{a^4} + \frac{K}{a^2} = -\frac{4\pi G}{3}T^\mu_\mu \tag{3.7}$$

Here and in the following upper primes denote derivatives with respect to conformal time η, i.e. $x' = \frac{dx}{d\eta}$, overdots denote derivatives with respect to coordinate time

[15] to be more precise it defines if a three dimensional hypersurface at constant conformal time η has the mentioned geometries

t, i.e. $\dot{x} = \frac{dx}{dt}$. Introducing the Hubble parameter $H \equiv \frac{\dot{a}}{a}$ as well as the conformal Hubble parameter $\mathcal{H} \equiv \frac{a'}{a} = aH$ one may find the more common versions of the Friedmann equations

$$H^2 + \frac{K}{a^2} = \frac{\mathcal{H}^2}{a^2} + \frac{K}{a^2} = \frac{8\pi G}{3} T_0^0 \tag{3.8}$$

$$\dot{H} = \frac{\mathcal{H}'}{a^2} = -\frac{4\pi G}{3}\left(T_\mu^\mu - 2T_0^0\right) \tag{3.9}$$

where (3.9) is found by subtracting (3.6) from (3.7). In the following we will restrict ourselves to ideal fluids where the energy momentum tensor can be given just in terms of the energy density ϵ, the pressure p and the four-fluid velocity u^μ in the form

$$T_\nu^\mu = (\epsilon + p)\, u^\mu u_\nu - p\delta_\nu^\mu \; (+\Lambda\delta_\nu^\mu) \tag{3.10}$$

Here we have included a possible contribution of a constant vacuum energy. In the rest frame of the fluid[16] this simplifies to $T_\nu^\mu = diag(\epsilon, -p, -p, -p)$. With this energy momentum tensor one arrives at the standard form of the Friedmann equations

$$H^2 = \left(\frac{\dot{a}}{a}\right)^2 = \frac{8\ \pi\ G}{3}\ \epsilon - \frac{K}{a^2} + \frac{\Lambda}{3} \tag{3.11}$$

$$\frac{\ddot{a}}{a} = -\frac{4\ \pi\ G}{3}\,(\epsilon + 3p) + \frac{\Lambda}{3} \tag{3.12}$$

Here Λ is the cosmological constant or vacuum energy. One may use an alternative equation instead of the second Friedmann equation, which can be deduced from energy-momentum conservation, i.e the covariant divergence of $T_{\mu\nu}$ vanishes:

$$D_\mu T^{\mu\nu} = \partial_\mu T^{\mu\nu} + \Gamma^\mu_{\mu\sigma} T^{\sigma\nu} + \Gamma^\nu_{\rho\sigma} T^{\rho\sigma} = 0 \tag{3.13}$$

where $\Gamma^\nu_{\rho\sigma}$ are the Christoffel connections that are given by the metric tensor and its derivatives [66, 67]. This results in

$$\frac{d\epsilon}{da} + 3\ \frac{\epsilon + p}{a} = 0 \tag{3.14}$$

Alternatively one may also use entropy conservation to find this equation of motion for the energy density or it may be derived by combining eqn. (3.11) and its time derivative with eqn. (3.12). Consequently the three equations (3.11), (3.12) and (3.14) are not independent and one may use any two of them. To solve this system of equations one additionally requires an equation of state $p(\epsilon)$, then one may

[16] Meaning the peculiar velocities vanish, i.e. $u^\mu = (1, 0, 0, 0)$.

already solve equation (3.14) for the dependence on the scale parameter a. For the most prominent contributions radiation, non-relativistic matter and vacuum energy the scaling can be easily found to be

$$\epsilon(a) \propto \begin{cases} a^{-4}, & p \;=\; \epsilon \;/\; 3, \quad \text{radiation} \\ a^{-3}, & p \;\approx\; 0, \quad \text{non-relativistic matter} \\ const., & p \;=\; -\;\epsilon, \quad \text{vacuum energy} \end{cases} \tag{3.15}$$

Next let us have a look on the curvature term in the first Friedmann equation (3.11). Clearly there exists a density for which the curvature term has to vanish and this critical density can easily found to be

$$\epsilon_{crit} = \frac{3H^2}{8\pi G} \tag{3.16}$$

If $\epsilon = \epsilon_{crit}$ the universe has a flat geometry (i.e. $K = 0$), for an overdense universe $\epsilon > \epsilon_{crit}$ thus $K > 0$ and the other way around for an underdense universe. It is common practice to define dimensionless energy densities normalized to the critical density

$$\Omega_i = \epsilon_i / \epsilon_{crit} \tag{3.17}$$

For example while vacuum energy is the dominant contribution to the total energy density $\epsilon_{crit} \propto H^2 = const.$ and therefore the normalized energy densities scale like

$$\Omega_X(a) \propto \begin{cases} a^{-4}, & \text{radiation} \\ a^{-3}, & \text{cold matter} \\ const., & \text{vacuum energy} \end{cases} \tag{3.18}$$

Next let us summarize the time dependence of the scale parameter for periods in which one of the previously addressed contributions dominate the energy budget as can be easily deduced[17] from the first Friedmann equation (3.11):

$$a(t) \propto \begin{cases} t^{1/2}, & \text{radiation} \\ t^{2/3}, & \text{cold matter} \\ e^{\,t\,H}, & \text{vacuum energy with } H = \sqrt{\Lambda/3} \end{cases} \tag{3.19}$$

We will conclude this section with quickly reviewing the scaling behavior of temperature and chemical potential (more details can be found also in [68, 69] also for

[17] See for example [66] for more details

non-relativistic particles). The Friedmann equation for a flat radiation dominated universe is given by

$$H^2 = \frac{8\pi^3 G}{90} g(T) T^4 \tag{3.20}$$

where $g(T)$ is effective number of relativistic bosonic[18] degrees of freedom. From equation (3.15) we can easily see that during periods where $g(T)$ is constant the temperature will scale as

$$T \propto \frac{1}{a} \tag{3.21}$$

The same can be shown for the scaling behavior of the chemical potential μ if one assumes a conserved net number of particles and antiparticles N in a comoving volume a^3

$$N = a^3 \bar{n} \quad \rightarrow \quad \bar{n} \propto \frac{1}{a^3}. \tag{3.22}$$

The net number density for a free gas of fermions is given by

$$\bar{n} = g(T) \frac{1}{6} \left(\mu T^2 + \frac{1}{\pi^2} \mu^3 \right) \tag{3.23}$$

Hence, the chemical potential μ has to scale like the temperature

$$\mu \propto \frac{1}{a} \tag{3.24}$$

to fulfill (3.22). Finally we may note a useful relation between the temperature and time by combining (3.20) and (3.19) to find that

$$\frac{t}{1 \text{ sec}} \sim \sqrt{\frac{g(1 \text{ MeV})}{g(T)}} \left(\frac{1 \text{ MeV}}{T} \right)^2 \tag{3.25}$$

Now we have the tools to discuss some of the thermal history of the early universe in the next section.

3.1.2 Thermal history of the early universe

We have already mentioned some of the most important milestones in the history of the universe such as big bang nucleosynthesis and the decoupling of the cosmic microwave background radiation. Now I shall try to give a brief overview of the thermal history of the universe. Most of this is basic textbook knowledge so we may refer to the books [66, 67, 70] where we do not explicitly mention that the topic will be discussed in more detail later on.

[18] Meaning that fermionic degrees of freedom are weighted with a factor of 7/8

The Planck scale at 10^{19} GeV is usually the earliest discussed in the evolution of the universe. At even higher energy scales and earlier times general relativity is definitely not applicable because the de Broglie wavelength of photons becomes smaller than their own Schwarzschild radius. Above 10^{15} GeV it is usually expected from grand unified theories (GUT) that the strong, the electromagnetic and the weak forces should unify. The electroweak phase transition happened at a temperature of about 100 GeV during which the weak gauge bosons $W^{\pm}, Z^0$, leptons and quarks acquired their masses through the Higgs mechanism. A phase of exponential expansion, inflation, is believed to have happened somewhere between the GUT and the electroweak scale, we will go into more detail about this in section 3.2. After inflation but at latest at the electroweak phase transition the asymmetry between matter and antimatter that allowed the existence of galaxies and stars in the later universe was created during baryogenesis. We will explain the basic principles and some possible mechanisms in section 3.4. At about 10^{-5} sec after the big bang and roughly 100 MeV temperature the (nearly massless) quarks and gluons were bound in massive hadrons, most notably protons and neutrons, in the course of the QCD phase transitions. This point is of course the most important one for this thesis and we will go into much more detail also about the standard picture for the QCD phase transition in chapter 4. At a temperature of a few MeV the three neutrino species subsequently decoupled[19] because weak interactions dropped out of equilibrium. Between 1MeV and 30 keV the light elements were synthesised during big bang nucleosynthesis (BBN) as previously discussed. Relativistic particles (here just called radiation) dominated the energy budget of the universe from the end of inflation on until at a temperature of about 1eV matter became the most abundant form of energy. We have already discussed the decoupling of the CMBR 380 000 years after the big bang. Since the universe was mostly neutral afterwards it entered the so called dark ages until the universe was reionized at a redshift of $z_{\mathrm{reion}} \sim 10$ [71] probably triggered by the first generation of stars that were born $\sim 10^8$ years after the big bang. The first galaxies appeared about 0.5 to 1 Gyr after the big bang. Today the universe has cooled down to a CMBR temperature of 2.7 K at a prime-age of 13.7 billion years. In figure 3.5 all of this is again summarized in graphical form.

[19] electron neutrinos decoupled sightly after muon- and tau-neutrinos because the latter could only interact via neutral current weak interactions since muons and taus had already annihilated at higher temperatures.

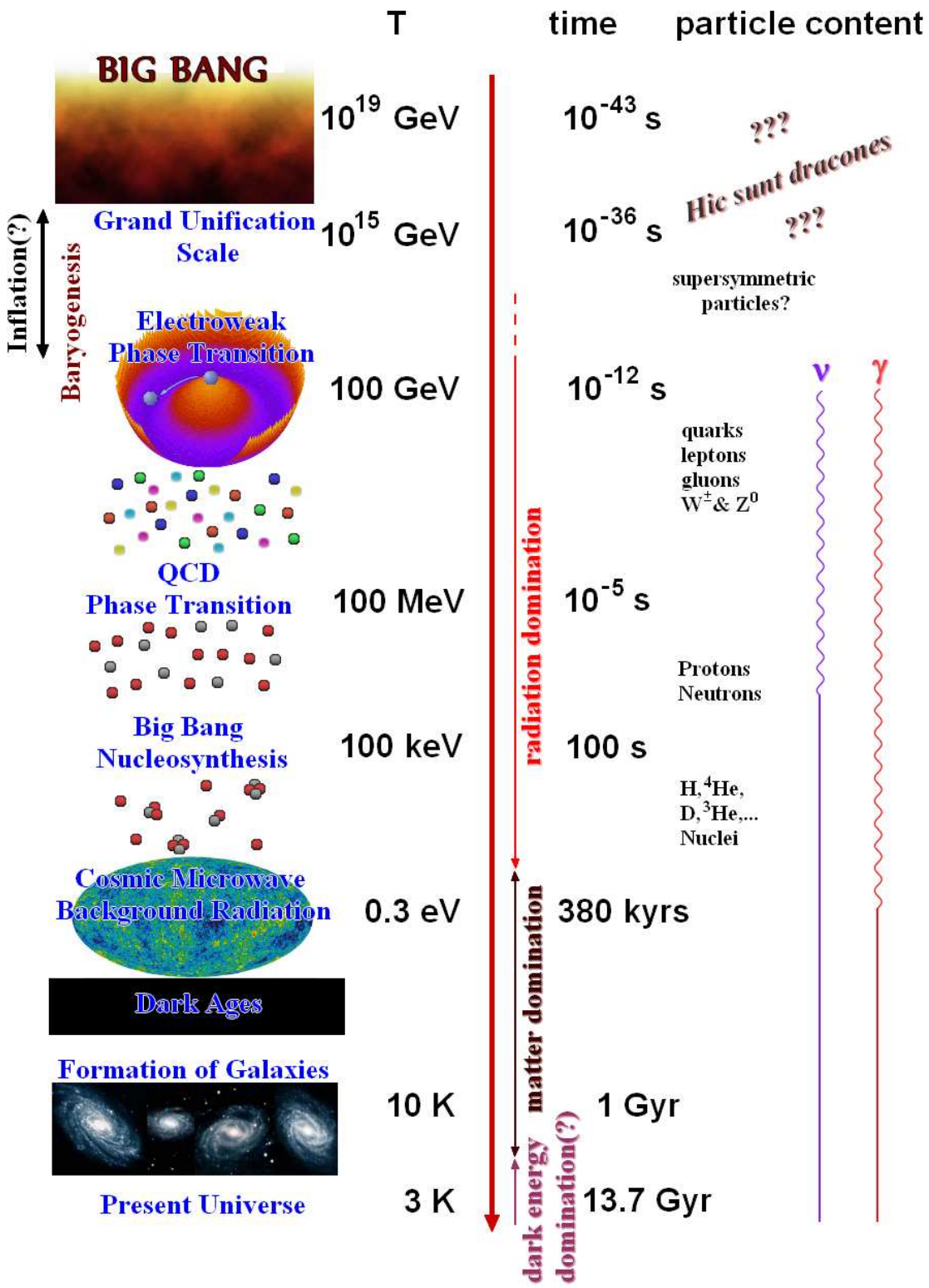

Figure 3.5: *Some of the most important milestones of the thermal history of the universe.*

3.2 Inflation

The theory of the hot big bang very successfully explains the cosmic expansion, the existence of the cosmic microwave background radiation, the observed redshifts of distant galaxies, and the observed primordial abundances of elements. Still several very curious properties of the universe stay unexplained. These are most prominent in the properties of the cosmic microwave background radiation. First of all observations of the first acoustic peak allowed to infer that the universe must be very close to being flat. For example the WMAP 7 year data alone tends towards a slight overdense universe but is consistent with a flat one $0.99 < \Omega < 1.27$ at 95% confidence [71]. Combining with any other observation like baryon acoustic oscillations[20] will clearly prefer a very flat universe $0.99 < \Omega < 1.01$ at 95% confidence. As we will see in the next section 3.2.1 this is a very unlikely situation in the basic big bang theory. The second observation that leads to concerns is the uniformity of the CMBR, i.e. why does the whole sky share the same temperature and a common spectrum of anisotropies if these regions were clearly not in causal contact when the CMBR decoupled? We will discuss the latter question in section 3.2.2.
We shall see that these characteristics of the universe are extremely unlikely within the standard big bang scenario, thus we will need to add something to the standard picture that will explain these observations quite naturally: inflation.

3.2.1 The flatness problem

As stated before the universe is apparently very close to being flat, which is actually a very unlikely situation and one may easily understand why. Let us have another look at the defining equation for the total energy density in units of the critical energy density

$$\Omega = \frac{\epsilon}{\epsilon_{crit}} = \frac{8\pi G\epsilon}{3H^2} = \frac{X\epsilon}{H^2} \tag{3.26}$$

where we have defined $X = 8\pi G/3$. Using this one may easily verify that the curvature term in the first Friedmann equation (3.11) can be rewritten to give

$$\frac{K}{Xa^2\epsilon_{crit}} = \Omega - 1 \tag{3.27}$$

[20] Baryon acoustic oscillations (BAO) denote the analogue of the anisotropies in the CMBR for baryonic matter. The acoustic oscillations in in the photon baryon plasma also created correlations between galaxies on scales of 100 Mpc that correspond to the sound horizon at freeze out of the CMBR.

Assuming a constant equation of state $p = w\epsilon$ we previously found that the energy density evolves as

$$\epsilon \propto a^{-3(1+w)} \tag{3.28}$$

Now we may calculate the logarithmic derivative of Ω with respect to a

$$\begin{aligned} \frac{d\Omega}{d\log a} &= a\frac{d\Omega}{da} = X\frac{-3(1+w)\epsilon\left(X\epsilon - \frac{K}{a^2}\right) - \epsilon\left(-3(1+w)X\epsilon + 2\frac{K}{a^2}\right)}{\left(X\epsilon - \frac{K}{a^2}\right)^2} \\ &= \frac{(1+3w)\epsilon\frac{K}{Xa^2}}{\left(\epsilon - \frac{K}{Xa^2}\right)^2} = \frac{(1+3w)\Omega(\Omega-1)}{(\Omega-(\Omega-1))^2} = (1+3w)\Omega(\Omega-1) \end{aligned} \tag{3.29}$$

Since $w \geq 0$ for any ordinary kind of matter this means that Ω will grow for $\Omega > 1$ and shrink for $\Omega < 1$. That is quite problematic since it means that a flat universe with $\Omega = 1$ is actually a unstable configuration that requires extremely fine tuned initial conditions to be stable up to the present day. If the universe at early times deviated even slightly from a flat geometry, that deviation would most certainly become large at late times. For example a universe with $\Omega = 1 \pm 0.01$ today

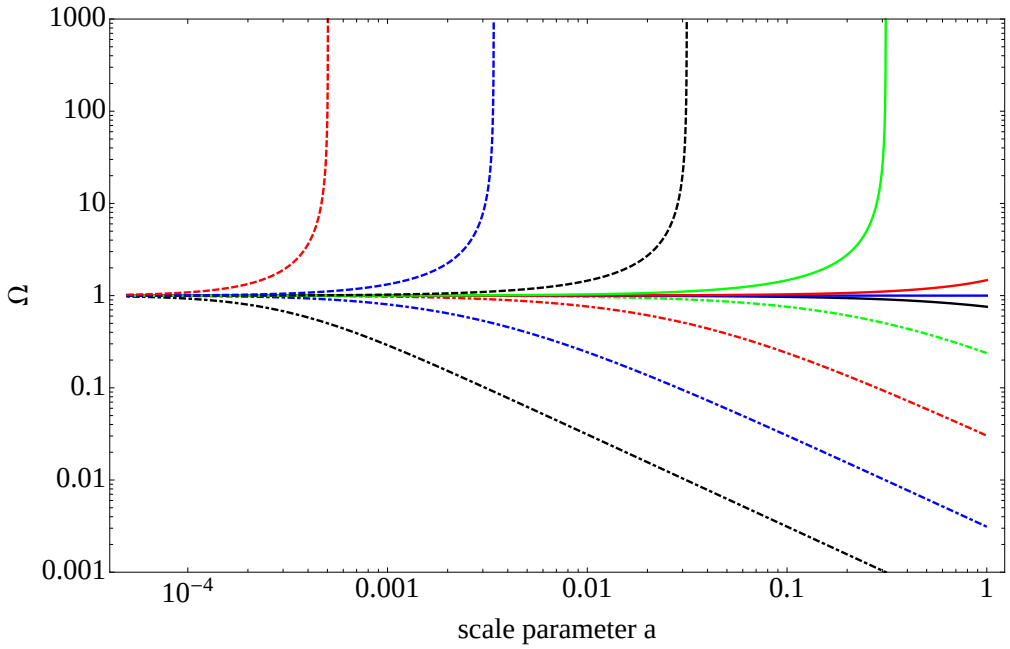

Figure 3.6: *Evolution of Ω as a function of the scale parameter for various quasi-flat initial conditions. All of them (except for an extremely small fraction) lead to vastly different universes then the one we observe today.*

requires at the time of recombination that $\Omega = 1 \pm 9 \cdot 10^{-6}$ and at nucleosynthesis $\Omega = 1 \pm 3 \cdot 10^{-17}$. Figure 3.6 shows the evolution of Ω for various quasi-flat initial

conditions where practically all of them lead to a radically different universe than we observe today. Basically all overdense initial conditions would have lead to a recollapse long ago while all underdense initial conditions would have left the universe void of enough matter to form stars and galaxies. This looks like a rather extreme case of fine tuning and is usually referred to as the flatness problem.

3.2.2 The horizon problem

The second major oddity about the CMBR is the apparent high degree of uniformity which is obvious by the existence of a common temperature for the whole sky. At first it may seem quite natural that the hot baryon-photon plasma was in thermal equilibrium in the early universe but it is on the contrary quite unnatural within the standard cosmological picture. We have seen that the anisotropies in the microwave background radiation show the most prominent variations on an angular scale of 1° which corresponds to the soundhorizon at decoupling. This also roughly agrees with the distance of 380000 light years a photon could have traveled since the big bang and thus with the size of a patch in the sky that was in causal contact back then. If two regions in the universe were separated by more then a horizon size at that point then they also could never haven been in thermal equilibrium before. To show this consider the physical distance d between two points that are at fixed comoving coordinates. The distance d will then just increase linearly with the scale factor:

$$d \propto a \tag{3.30}$$

Next one may examine the scaling behavior of the horizon that is proportional to the inverse of the Hubble parameter

$$d_H \propto H^{-1}. \tag{3.31}$$

One may easily find the general scaling of d/d_H after some algebra

$$\begin{aligned} \left(\frac{d}{d_H}\right)^2 &\propto a^2\left(X\epsilon - \frac{K}{a^2}\right) = Xa^2\epsilon_{crit}\left(\Omega - \frac{K}{Xa^2\epsilon_{crit}}\right) \\ &= Xa^2\epsilon_{crit}\left(\Omega - \Omega + 1\right) = \frac{|K|}{|\Omega - 1|} \end{aligned} \tag{3.32}$$

We have seen in equation (3.29) that

$$\frac{d|\Omega - 1|}{d\log a} > 0 \quad \text{for} \quad w > -\frac{1}{3} \tag{3.33}$$

which in turn means that

$$\frac{d}{d\log a}\left(\frac{d}{d_H}\right) < 0 \quad \text{for} \quad w > -\frac{1}{3}. \tag{3.34}$$

In other words the Hubble scale grows faster than any physical distance due to expansion. This means that any two points separated by a distance d today that are in causal contact now ($d/d_H < 1$) must have been separated by a distance larger than the horizon (i.e. $d/d_H > 1$) at earlier times. Specifically this means that scales that were not causally connected at recombination also could not have been in causal contact earlier and thus should not be in thermal equilibrium. However, we have seen that the CMBR shows a uniform temperature over the whole sky with only tiny variations on the level of $1 : 10^4$ and thus we have encountered what is often called the horizon problem.

3.2.3 The solution: Inflation

We have seen that both the flatness and horizon problem appear within standard cosmologies with a general content of matter and radiation where the global equation of state is $0 \leq w \leq 1/3$. The only solution within this context seems to be the very artificial initial condition that the universe started out almost perfectly flat and with a common temperature everywhere. The now commonly accepted solution came from Alan Guth in 1980 [72] and Andrei Linde [73] when they proposed the concept of inflation to solve these (and several other related or less severe[21]) problems. Putting it simple if the universe had a global equation of state $w < -1/3$ for a sufficiently long period then these problems can be avoided without the need for fine tuned initial conditions.

The most simple realization of Inflation is given by a constant vacuum energy that does not scale with the expansion of the universe. One easily finds that the Friedmann equation has the simple solution

$$H^2 = \left(\frac{\dot{a}}{a}\right)^2 = \frac{8\pi G}{3}\epsilon_V = \text{const.} \quad \rightarrow \quad a \propto e^{Ht} \tag{3.35}$$

In other words the expansion rate is constant while the actual physical distance between any two points increases exponentially with time. In this case both (3.29)

[21] For example the so-called monopole problem: in many grand unified extensions of the standard model magnetic monopoles are produced overabundantly in the early universe and in these theories it is difficult to understand why they did not overclose the universe and lead to a recollapse. Thus a mechanism to dilute their number density sufficiently to explain their absence today would be attractive. Similar problems might be posed by other early produced relics like for example topological defects and these would be solved in the same fashion.

and (3.34) change sign. The first point means that a flat universe becomes an attractor solution (Ω tends towards one) and if the inflationary period is long enough the universe can end up arbitrarily close to perfect flatness.
The second point means that the ratio of the physical distance between two points over the horizon size grows, thus arbitrarily large regions in space that were is causal contact before become fragmented into smaller and smaller patches of the universe that are still causally connected. Turning this around the whole presently observable universe could originate from a tiny region of the primordial universe that was in thermal equilibrium before the onset of inflation and got stretched beyond the size of our present universe.
In principle inflation can take place anywhere after the grand unification scale $T_{GUT} \sim 10^{15}$ GeV and the electroweak scale $T_{EW} \sim 200$ GeV. The physical length corresponding to the Hubble scale at the onset of inflation must be stretched at least to the size of the present universe, possibly much further. How long inflation has to last to solve the above problems depends on when it took place, i.e.

$$\theta \equiv \frac{a_f}{a_i} \gtrsim \frac{a_i}{a_0}\frac{H_i}{H_0} \sim \frac{T_0}{T_i}\frac{H_i}{H_0} \sim \begin{cases} 10^{24} \sim e^{55} & T_i = T_{GUT} \\ 10^{11} \sim e^{25} & T_i = T_{EW} \end{cases} \tag{3.36}$$

Here the indices i, f and 0 refer to the start of inflation, the end of inflation and to the present day, respectively. The flatness problem is solved at the same time because from equation (3.27) we can easily see that

$$\frac{|\Omega - 1|_f}{|\Omega - 1|_i} \sim \left(\frac{a_i}{a_f}\right)^2. \tag{3.37}$$

So that Ω will be extremely close to unity after inflation. Since today $|\Omega - 1| \lesssim 10^{-2}$ and

$$|\Omega - 1| \propto \begin{cases} a^2 & \text{radiation domination} \\ a & \text{matter domination} \end{cases} \tag{3.38}$$

one may easily do a conservative estimate for an inflation length to solve the flatness problem assuming $|\Omega - 1|_i \sim \mathcal{O}(1)$

$$\theta \gtrsim \begin{cases} 10^{28} \sim e^{64} & T_i = T_{GUT} \\ 10^{14} \sim e^{32} & T_i = T_{EW} \end{cases} \tag{3.39}$$

Of course the initial value for $|\Omega - 1|$ before inflation is unknown and could be smaller, thus one usually assumes an inflation length of 55-60 e-folds should suffice to solve both problems.

We have already seen that a cosmological constant caused by a nonzero vacuum energy results in an inflationary period. Still we know that inflation ended[22] so inflation must have had a dynamical cause. It is usually assumed that inflation was driven by at least one scalar field with a non-trivial vacuum state that gave a nearly constant contribution to the energy budget for a sufficiently long period of time. At the end of the inflationary period the scalar field settled into the true global minimum and released its energy into production of particles, a process called reheating during which also the entropy of the universe is vastly increased. We will later on recover the same process when turning to the little inflation scenario. We will now briefly discuss some basics of the inflationary mechanism but not go into too much detail since the "big inflation" is very different in terms of extend and consequences. Also several key simplifications that can be applied here are invalid if inflation does not last long enough. For more details on standard inflation one may refer to the standard textbooks by Mukhanov [67] and by Liddle and Lyth [70].

Let us assume a simple scalar Lagrangian of the type

$$\mathcal{L} = \frac{1}{2}\partial^\mu\phi\partial_\mu\phi - V(\phi) \tag{3.40}$$

with a resulting energy-momentum tensor

$$T^{\mu\nu} = \partial^\mu\phi\partial^\nu\phi - \mathcal{L}g^{\mu\nu}. \tag{3.41}$$

If one assumes a nearly homogenous background the gradient terms may be neglected[23] and one finds for the energy density and the pressure

$$\epsilon = \frac{\dot{\phi}^2}{2} + V(\phi) \qquad\qquad p = \frac{\dot{\phi}^2}{2} - V(\phi) \tag{3.42}$$

Consequently one directly finds that

$$H^2 = \frac{8\pi G}{3}\left(\frac{\dot{\phi}^2}{2} + V(\phi)\right) \tag{3.43}$$

This means that if the field is only slowly changing ($\frac{\dot{\phi}^2}{2} \ll V(\phi)$) and the potential term dominates then this will result in a constant Hubble parameter and an

[22] There is actually a whole class of models called eternal inflation in which inflation only locally ended but still goes on in other parts of the universe that are outside the observable universe, see Ref. [74] for a recent review on the topic.

[23] During inflation gradient terms will drop proportional to $\propto a^{-1}$ in contrast to the time derivative of ϕ and thus will become negligible anyways after a few e-folds.

inflationary equation of state

$$H^2 \approx \frac{8\pi G}{3} V(\phi) \qquad\qquad w = p/\epsilon \approx -1 \tag{3.44}$$

The equation of motion for the field may be found by calculating the covariant derivative of the energy momentum tensor $D_\mu T^{\mu\nu}$ as defined in equation (3.13) which results in

$$\ddot{\phi} + 3H\dot{\phi} + V' = 0 \tag{3.45}$$

where $V' = \frac{dV}{d\phi}$. Since the first time derivative of ϕ should already be small one may drop the second time derivative if the field is to be slowly varying

$$3H\dot{\phi} + V' \simeq 0 \tag{3.46}$$

This is usually called the slow roll approximation in which the field mostly evolves due to the Hubble friction term. In many models of inflation this is realized by a very flat potential such that the gradient of the potential is so low that the field will only roll towards the global minimum when the universe has expanded by many orders of magnitude. One may quantify the slow roll approximation in terms of several parameters that allow to categorize different models of inflation, the reader is referred to the standard textbooks on cosmology for more details [67, 70, 66] and to the reviews [75, 76] that give a broad overview of inflationary models.
Now we will shortly discuss one of the most important consequences of inflation: the generation of primordial density fluctuations. Not long after the initial publications on inflation by Guth and Linde it was realized independently by Guth [77], Starobinsky [78] and Hawking [79] that inflation could also explain the origin of primordial density fluctuations. These would be the seeds for all the structures in the universe from stars to superclusters of galaxies. The basic mechanism can be explained with a well known analogue from black hole physics, Hawking radiation. One may interpret vacuum fluctuations as the creation of virtual pairs of particles and antiparticles as allowed by the uncertainty principle. If such pairs are created next to a black hole horizon and one of the particles get trapped inside, then the other one becomes real and is emitted as part of a thermal Hawking radiation spectrum. For the inflationary scenario a similar picture may be used, a pair of a virtual particle and antiparticle may be separated by the exponential expansion before they can annihilate and thus become causally disconnected. Consequently they turn into classical excitations of the field.
In the next section we will introduce the basic concepts of structure formation but at this point we may already introduce the notion of scalar perturbations that are

the only components that may turn unstable and lead to the growth of structures. Decomposing the field into a constant part and a perturbation $\phi = \phi_0 + \delta\phi$ one may find after some steps starting from equation (3.45) an equation of motion for the perturbation $\delta\phi$ [76]

$$\ddot{\delta\phi} + 3H\dot{\delta\phi} + \left[\left(\frac{k}{a}\right)^2 + V''\right] = 0 \tag{3.47}$$

Here k is a comoving[24] wavenumber related to the momentum p (and the physical wavenumber k_{ph}) $p = k_{ph} = \frac{k}{a}$. For a sufficiently flat potential the mass term proportional to V'' can be neglected until $k_{ph} \ll H$ and the mode is already far outside the horizon and thus has become a classical fluctuation. In this case the amplitude of the field perturbation when its wavelength equals the horizon size will simply be given by

$$|\delta\phi|^2_{|k=aH} = \left(\frac{H}{2\pi}\right)^2 \tag{3.48}$$

This is not yet the amplitude of scalar perturbations, for that we first have to introduce the notion of a curvature perturbation in a simplified manner. During inflation the universe will quickly become flat to a very high accuracy as we have seen meaning that the curvature term in the Friedmann equation will only be a small perturbation

$$H^2 = \frac{8\pi G}{3}(\epsilon + \delta\epsilon) - \frac{\delta K}{a^2} \tag{3.49}$$

Subtracting the unperturbed background equation and dividing by it one finds that

$$\frac{\delta\epsilon}{\epsilon} = \frac{\delta K}{H^2 a^2} \tag{3.50}$$

This is a rather obvious result, namely that a local overdensity will cause a local positive curvature and vice versa. Related to that one usually introduces the curvature perturbation $\mathcal{R}$ via

$$\frac{\delta K}{a^2} = \frac{2}{3}\Delta\mathcal{R} \tag{3.51}$$

where Δ is the Laplacian. Within the slow roll approximation the curvature perturbation can be shown to depend on the field perturbation [67, 70, 66, 76]

$$\mathcal{R}(k) = \frac{\delta\phi(k)H}{\dot{\phi}} \tag{3.52}$$

[24] Meaning that is does not change with the expansion.

The power spectrum is then usually defined as[25]

$$\mathcal{P}_{\mathcal{R}}(k) = \frac{k^3}{2\pi^2}|\mathcal{R}(k)|^2 \tag{3.53}$$

Using equations (3.52) and (3.48) we find that

$$\mathcal{P}_{\mathcal{R}}(k) = \left(\frac{k^3}{2\pi^2}\frac{H^2}{\dot{\phi}^2}|\delta\phi|^2\right)_{|k=aH} \tag{3.54}$$

Finally one may find that the resulting spectrum is nearly scale invariant in the slow roll approximation

$$\mathcal{P}_{\mathcal{R}}(k) \propto \left(\frac{\mathcal{H}}{2\pi a}\right)^2 \left(\frac{k}{\mathcal{H}}\right)^{n_s-1} \tag{3.55}$$

The scalar spectral index $n_s \approx 1$, where one speaks of a scale invariant Harrison-Zeldovic spectrum for $n_s = 1$. Deviations from unity depend on the exact shape of the potential and may be quantified by the previously mentioned slow roll parameters. Indeed observations show such a spectrum of scalar density perturbations as shown for example by the newest seven year data release of the WMAP satellite [71] that found $n_s = 0.968 \pm 0.024$ (at 2σ confidence). Thus the inflationary model can also account for the production of the seeds for the large scale structures in the universe.

The short inflationary phase as discussed later on in this thesis is in many respects different to inflation as discussed here. We shall see that the "little inflation" cannot replace the "long" primordial inflationary phase and it will also be far too short to expect most of the estimates done here to apply there. The most important input we take from here is the shape of the spectrum of scalar density perturbations that will be used to investigate the impact of the little inflationary model on low scale structure formation.

In the next section we will discuss in a lot of detail the basic treatment of linear gravitational perturbations in an expanding background.

[25] Note that definitions differ in this point, especially on the normalization.

3.3 Structure Formation

3.3.1 Basics

One of the cornerstones of modern cosmology is the theory of structure formation that describes the evolution of the small inhomogeneities in the density of the primordial radiation and matter. As said these are believed to be created during Inflation and later on seed all the observable structures in the universe.
The treatment of gravitational perturbations in an expanding universe [26] is far from being a simple task and most work on the topic has been done only for small amplitude perturbations that can be dealt with by linearized theory. Once the perturbations become non-linear the only reliable tool is to further simplify the problem and solve it with n-body simulations with quasi-newtonian gravitation [27] on supercomputers. We will be concerned only with the former since we are dealing with an era of the cosmos during which the amplitudes of perturbations were still mostly linear.

3.3.2 Types of perturbations

The modern theory of cosmological perturbations was mostly developed in the 1980s starting with a pioneering work by Bardeen [80]. We stick mostly to the notation and derivation of [81] since it is the one most widely used in the literature. Where necessary we rely on [82], that is much denser and also covers the choice of gauge we will later work with.

$$g_{\mu\nu} = {}^{(0)}g_{\mu\nu} + \delta g_{\mu\nu} \tag{3.56}$$

One finds that there are 10 independent metric degrees of freedom in $\delta g_{\mu\nu}$ after taking care of symmetry constraints. These can be separated into three distinct types of perturbations, scalar, vector and tensor. This classification might be misleading in the sense that it does not denote the behavior under general coordinate transformation but merely how the degrees of freedom transform under three-space transformations on a constant-time hypersurface (see reference [83] for more on the topic). Therefore e.g. the perturbations denoted "scalar perturbations" are not invariant under general coordinate transformations as one might naively expect,

[26] from now on just cosmological perturbations.

[27] quasi-newtonian here means that the background still undergoes Hubble expansion but also the newtonian two-body force is usually softened for small distances to avoid unphysical behavior.

while "tensor perturbations" are on the other hand manifestly gauge invariant[28]. There is however a way to also construct such "gauge invariant" scalar perturbations and we will do so in section 3.3.4.

Scalar perturbations

$$g_{\mu\nu}^{(S)} = a^2(\eta) \begin{pmatrix} 2\alpha & -B_{|i} \\ -B_{|i} & -2\left(\varphi\gamma_{ij} + E_{|ij}\right) \end{pmatrix} \tag{3.57}$$

Here α, B, φ, E are spacetime dependent scalar functions. $B_{|i}$ denotes a covariant three dimensional derivative with respect to the background variable i [29], thus it becomes an ordinary 3-gradient for a flat background FLRW universe. Using (3.57) we can construct the corresponding line element

$$ds^2 = a^2(\eta)\left[(1+2\alpha)\,d\eta^2 - 2B_{|i}dx^i d\eta - \left[(1+2\varphi)\,\gamma_{ij} + 2E_{|ij}\right]dx^i dx^j\right] \tag{3.58}$$

The four independent functions correspond to 4 independent scalar degrees of freedom, but as we shall see later only 2 of these correspond to physical degrees of freedom. The other two are related to the freedom of gauge and would lead to a mixing with vector perturbations and contain unphysical gauge that need to be taken care of later on.

Vector perturbations

$$S_i^{|i} = F_i^{|i} = 0 \tag{3.59}$$

$$g_{\mu\nu}^{(V)} = -a^2(\eta) \begin{pmatrix} 0 & -S_i \\ -S_i & F_{i|j} + F_{j|i} \end{pmatrix} \tag{3.60}$$

Tensor perturbations

$$h_i^i = 0, \quad h_{ij}^{|j} = 0 \tag{3.61}$$

$$g_{\mu\nu}^{(T)} = -a^2(\eta) \begin{pmatrix} 0 & 0 \\ 0 & h_{ij} \end{pmatrix} \tag{3.62}$$

In the following we will only focus on the scalar part of the perturbations because they are the only ones that lead to gravitational instabilities and thus to the growth of structure. Vector and tensor perturbations generally decay over time, the latter might at least be observable in form of gravitational waves.

[28] meaning invariant under general infinitesimal coordinate transformations

[29] $B_{|i} \equiv D_i B$ with D_μ being the covariant derivative

3.3.3 Gauge transformations

In the case of general relativity a gauge transformation corresponds to changing the coordinates of physical spacetime and at the same time keeping the background coordinates unchanged. Now we want to consider how the scalar perturbations of the metric change under an infinitesimal change of coordinates

$$x^\mu \to \tilde{x}^\mu = x^\mu + \xi^\mu \tag{3.63}$$

The transformation (3.63) obviously transforms all three kinds of perturbations and will in general mix them. Therefore we need to disentangle which parts of (3.63) preserve the scalar nature of a perturbation. We may separate the spacial part of $\xi^\mu = (\xi^0, \xi^i)$ into a transverse and a longitudinal part

$$\xi^i = \xi^i_T + \xi^i_L = \xi^i_T + \gamma^{ij}\Xi_{|j} \tag{3.64}$$

The transverse vector is defined by the generalized condition to be solenoidal

$$\xi^i_{T|i} = 0 \tag{3.65}$$

where the analogue for a flat Minkowsky space would be $\vec{\nabla} \cdot \vec{\xi} = 0$. ξ^i_T only contributes to vector-like perturbations and therefore has to be excluded in the following to prevent any mixing of the classes of perturbations. The scalar Ξ is found as a solution to $\Xi^{|i}_{|i} = \xi^i_{|i}$ and gives the spacial part of the transformation that keeps the scalar nature of a perturbation unchanged in contrast to the transversal part[30].

So we are left with two functions Ξ and the temporal part ξ^0 to describe to gauge transformations for scalar perturbations. Note that the reduction to two functions does not reflect any fixing of a gauge it just specifies the nature of the perturbation degrees of freedom and ensures that no mixing of different types of perturbations takes place.

The scalar metric variables transform in the following way

$$\begin{aligned}
\phi &\to \tilde{\phi} = \phi - \frac{a'}{a}\xi^0 - \xi^{0\prime} \\
\psi &\to \tilde{\psi} = \psi + \frac{a'}{a}\xi^0 \\
B &\to \tilde{B} = B + \xi^0 - \Xi' \\
E &\to \tilde{E} = E - \Xi
\end{aligned} \tag{3.66}$$

[30] Here we deviate from the notation of [81] $\Xi \hat{=} \xi$ to clarify the difference from the 3-vector ξ^i

To fix a certain gauge one may now either directly choose two conditions to eliminate the gauge degrees of freedom [81] or one may introduce two new variables to eliminate one of the gauge degrees of freedom while at the same time allowing a clearer understanding of the gauge conditions later on [80, 82]. We will choose the latter way, namely to eliminate the dependence on spacial gauge transformations by a convenient choice of replacement variables for B and E [31].

3.3.4 Gauge invariant formalism

The variables of choice for our approach are

$$\chi \equiv -a\left(B - E'\right) \quad \text{and} \quad \kappa \equiv \frac{3}{a}\left(\mathcal{H}\phi - \psi'\right) + \frac{k^2}{a^2}\chi \tag{3.67}$$

here k is a comoving wavenumber defined via a Helmholtz-equation for χ, i.e. $\chi^{|i}_{|i} = -k^2\chi$. ϕ and ψ do already only change under temporal gauge transformations (3.66). So we only need to check if χ is invariant under spacial transformations, because then the same will be true for κ.

$$\chi \to \tilde{\chi} = -a\left(\tilde{B} - \tilde{E}'\right) = -a\left(B + \xi^0 - \Xi' - E' + \Xi'\right) \tag{3.68}$$

$$= -a\left(B - E' + \xi^0\right) \tag{3.69}$$

What is the physical meaning of the four metric perturbation variables ϕ, ψ, χ, κ? Choosing a frame in which the frame vector n^μ is orthogonal to three-space ($n^i = 0$) one finds that the three-space curvature $R^{(3)}$, the expansion Θ and the shear σ_{ij} of the frame vector have the following dependence on the perturbations [82]

$$\begin{aligned} R^{(3)} &= \frac{6K}{a^2} - 4\frac{k^2 - 3K}{a^2}\psi \\ \Theta &= 3\frac{\mathcal{H}}{a} - \kappa \\ \sigma_{ij} &= \chi_{|ij} - \frac{1}{3}\gamma_{ij}\chi^{|k}_{|k} \end{aligned} \tag{3.70}$$

Choosing $\kappa = 0$ corresponds to having an unperturbed Hubble flow, thus the name uniform expansion gauge. Choosing $\chi = 0$ leads to the more popular longitudinal or conformal Newtonian gauge as used in the well known review of Mukhanov, Feldman and Brandenberger [81].

[31] One may do so because the background is spacially homogenous [84, 82].

3.3.5 Uniform expansion gauge

We use uniform expansion gauge (UEG) that is free of unphysical gauge modes and has the two gauge invariant variables δ and $\hat{\psi}$, which can be identified with the density contrast and a quantity related to the fluid velocity in the subhorizon limit ($k_{\rm ph} \gg H$), respectively [6, 82]. For ideal fluids the evolution equations in UEG read

$$\dot{\epsilon} = -3H(\epsilon + \bar{\pi}) - \Delta\psi - 3H(\rho + p)\alpha \tag{3.71}$$

$$\dot{\psi} = -3H\psi - \bar{\pi} - (\rho + p)\alpha \tag{3.72}$$

which can be deduced from energy-momentum conservation and the three divergence of the Euler equation. Here $\epsilon \equiv \delta\rho$ and $\bar{\pi} \equiv \delta p$ denote the perturbation of the energy density and pressure, respectively, ψ is the potential of the momentum density $\vec{S}$, i.e. $\vec{\nabla}\psi = \vec{S}$. The latter is related to the fluid velocity v via $\psi k/a = (\rho + p)v$. Equations (3.71) and (3.72) apply for each decoupled ideal fluid, while all fluids are gravitationally linked via the perturbation of the lapse α and Einstein's R^0_0-equation

$$(\Delta + 3\dot{H})\alpha = 4\pi G(\rho + 3p) \tag{3.73}$$

Introducing dimensionless variables $\delta = \delta\rho/\rho$, $\hat{\psi} = k\psi/(a\rho)$ and the equation of state $w = p/\rho$ the UEG set of equations takes the form

$$\delta_i' = -\frac{3(c_{si}^2 - w_i)}{a}\delta_i + \frac{k}{\mathcal{H}a}\hat{\psi}_i - 3(1 + w_i)\frac{\alpha}{a} \tag{3.74}$$

$$\hat{\psi}_i' = -\frac{1 - 3w_i}{a}\hat{\psi}_i - c_{si}^2\frac{k}{\mathcal{H}a}\delta_i - (1 + w_i)\frac{k}{\mathcal{H}a}\alpha \tag{3.75}$$

$$\alpha = -\frac{\frac{3}{2}(1 + 3c_s^2)}{\left(\frac{k}{\mathcal{H}}\right)^2 + \frac{9}{2}(1 + w)}\,\delta \tag{3.76}$$

where the index i refers to an individual fluid each of which has a set of equations (3.74) and (3.75), $\mathcal{H} = Ha$ is the conformal Hubble parameter and $c_{\rm S}$ is the isentropic speed of sound. Slashes denote derivatives with respect to the scale parameter. All fluids are connected via the last equation for the perturbation of the lapse α. The mean density contrast, equation of state and speed of sound are calculated by

$$\delta = \frac{\sum_i \delta_i\rho_i}{\sum_i \rho_i},\ w = \frac{\sum_i p_i}{\sum_i \rho_i},\ c_s^2 = \frac{\sum_i c_{si}^2\delta_i\rho_i}{\sum_i \delta_i\rho_i} \tag{3.77}$$

Eqs. (3.74) and (3.75) apply to each decoupled fluid component i individually and the general relativistic analogue of the Poisson equation (3.76) connects them.

3.3.6 Analytic Solutions

Now let us discuss some simple analytic solutions to the above system of differential equations. Most importantly let us look at the growing super-horizon solutions in the case of a radiation dominated universe. First lets look at the radiation component:

$$\delta_R^{/} \simeq \frac{k}{\mathcal{H}a}\hat{\psi}_R + \frac{2}{a}\delta_R \tag{3.78}$$

$$\hat{\psi}_R^{/} \simeq \frac{1}{3}\frac{k}{\mathcal{H}a}\delta_R \tag{3.79}$$

Where we have used $c_s^2 = c_{sR}^2 = w = w_R = 1/3$ and $\alpha = -\delta_R/2$. Now we calculate the derivative of (3.78) with respect to the scale parameter keeping in mind that $k/(\mathcal{H}a) = const.$ during radiation domination.

$$\begin{aligned}\delta_R^{//} = \frac{k}{\mathcal{H}a}\hat{\psi}_R^{/} - \frac{2}{a^2}\delta_R + \frac{2}{a}\delta_R^{/} &= \frac{1}{3}\left(\frac{k}{\mathcal{H}a}\right)^2\delta_R - \frac{2}{a^2}\delta_R + \frac{2}{a}\delta_R^{/} \\ &\approx -\frac{2}{a^2}\delta_R + \frac{2}{a}\delta_R^{/}\end{aligned} \tag{3.80}$$

Where we have used equation (3.79) in the second step and neglected the term that is quadratic in the small quantity $k/\mathcal{H}$ in the third step. Given the form of the differential equations (3.80) and (3.79) it seems natural to assume a power law dependence of the solutions on $k/\mathcal{H} \propto a$

$$\delta_R \propto \left(\frac{k}{\mathcal{H}}\right)^{\beta} \tag{3.81}$$

Calculating the first and second derivatives we find

$$\delta_R^{/} = \frac{\beta}{a}\delta_R \tag{3.82}$$

$$\delta_R^{//} = -\frac{\beta}{a^2}\delta_R + \frac{\beta}{a}\delta_R^{/} \tag{3.83}$$

Consequently super-horizon solutions for δ_R and $\hat{\psi}_R$ are given by

$$\delta_R = A\left(\frac{k}{\mathcal{H}}\right)^2 \tag{3.84}$$

$$\hat{\psi}_R = \frac{A}{9}\left(\frac{k}{\mathcal{H}}\right)^3 \tag{3.85}$$

where A is a constant that fixes the amplitude at horizon entry.

Using these solutions we can now also find the evolution of the dark matter perturbations with $w_{DM} = c_{sDM}^2 = 0$

$$\delta'_{DM} \simeq -\frac{3}{a}\alpha = \frac{3}{2a}\delta_R \tag{3.86}$$

$$\hat{\psi}'_{DM} \simeq -\frac{1}{a}\hat{\psi}_{DM} - \frac{k}{\mathcal{H}a}\alpha = -\frac{1}{a}\hat{\psi}_{DM} + \frac{1}{2}\frac{k}{\mathcal{H}a}\delta_R \tag{3.87}$$

The solution for δ_{DM} is quickly found to be proportional to δ_R

$$\delta_{DM} = \frac{3}{4}A\left(\frac{k}{\mathcal{H}}\right)^2 = \frac{3}{4}\delta_R \tag{3.88}$$

For $\hat{\psi}_{DM}$ we need to make an educated guess

$$\hat{\psi}_{DM} = \frac{A}{6}\left(\frac{k}{\mathcal{H}}\right)^3 + B\frac{\mathcal{H}}{k} \tag{3.89}$$

Where the first term is the solution one would expect if just the second term in (3.87) was present and the second term of the ansatz would be the solution for the first term in (3.87) alone.

$$\Rightarrow \hat{\psi}'_{DM} = \frac{A}{2a}\left(\frac{k}{\mathcal{H}}\right)^3 - B\frac{\mathcal{H}}{ka} = \frac{2}{3}\frac{k}{\mathcal{H}a}\delta_R - \frac{1}{a}\hat{\psi}_{DM} \tag{3.90}$$

So the functional dependence is correct and we just need to change the prefactor in front of the growing mode. One may easily verify that

$$\hat{\psi}_{DM} = \frac{A}{8}\left(\frac{k}{\mathcal{H}}\right)^3 + B\frac{\mathcal{H}}{k} \tag{3.91}$$

solves equation (3.87). The decaying mode $\propto 1/a$ will quickly become irrelevant and is thus neglected in the following. Now let us summarize the solutions[32] we found

$$\delta_R = A\left(\frac{k}{\mathcal{H}}\right)^2 = \frac{4}{3}\delta_{DM} \tag{3.92}$$

$$\hat{\psi}_R = \frac{A}{9}\left(\frac{k}{\mathcal{H}}\right)^3 = \frac{8}{9}\hat{\psi}_{DM} \tag{3.93}$$

These solutions will set the relevant initial conditions for our numerical calculations later on.

[32]Note that in [6] it is incorrectly stated that $\hat{\psi}_R = \hat{\psi}_{DM}$ in this case which adds a small admixture of decaying modes.

Now we can also quickly derive the solutions for modes that are sufficiently subhorizon during radiation domination. In this case $k/\mathcal{H} \gg 1$ and the approximate equations of motion for the perturbations in the radiation read

$$\delta_R^{/} \simeq \frac{k}{\mathcal{H}a}\hat{\psi}_R - 4\frac{\alpha}{a} \tag{3.94}$$

$$\hat{\psi}_R^{/} \simeq -c_s^2\frac{k}{\mathcal{H}a}\delta_R - \frac{4}{3}\frac{k}{\mathcal{H}a}\frac{\alpha}{a} \tag{3.95}$$

$$\alpha \simeq 3\left(\frac{\mathcal{H}}{k}\right)^2\delta_R \tag{3.96}$$

Thus the terms proportional to α are suppressed and we may drop them. Taking the derivative of (3.80) with respect to a we then arrive at

$$\delta_R^{//} = \frac{k}{\mathcal{H}a}\hat{\psi}_R^{/} = -c_s^2\left(\frac{k}{\mathcal{H}a}\right)^2\delta_R \tag{3.97}$$

$$\hat{\psi}_R^{/} = -c_s^2\frac{k}{\mathcal{H}a}\delta_R \tag{3.98}$$

which is is simply a harmonic oscillator with the solutions

$$\delta_R = C\sin\left(c_s\frac{k}{\mathcal{H}}\right) + D\cos\left(c_s\frac{k}{\mathcal{H}}\right) \tag{3.99}$$

$$\hat{\psi}_R = -Cc_s\cos\left(c_s\frac{k}{\mathcal{H}}\right) + Dc_s\sin\left(c_s\frac{k}{\mathcal{H}}\right) \tag{3.100}$$

with C, D being constants. We will use the amplitude of the oscillations which is given by $(\delta_R^2 + \hat{\psi}_R^2/c_s^2)^{1/2}$ later on. Now let us turn to the dark matter side

$$\delta_{DM}^{/} \simeq \frac{k}{\mathcal{H}a}\hat{\psi}_{DM} \tag{3.101}$$

$$\hat{\psi}_{DM}^{/} \simeq -\frac{1}{a}\psi_{DM} \tag{3.102}$$

The solution for $\hat{\psi}_{DM}$ is obviously

$$\hat{\psi}_{DM} = \frac{E}{a} \tag{3.103}$$

which we may directly use to find δ_{DM}

$$\delta_{DM}^{/} = \frac{k}{\mathcal{H}a}\frac{E}{a} \tag{3.104}$$

$$\Rightarrow \delta_{DM}^{/} = F + E\frac{k}{\mathcal{H}a}\log a \tag{3.105}$$

with E, F also being constants. Thus during radiation domination subhorizon perturbations in radiation will oscillate with constant amplitude while matter perturbations will only grow logarithmically.

3.4 Baryogenesis

Our world is almost entirely made up of matter and even in the cosmos antimatter seems to be very rare and only occurs in very high energy processes like in supernovae, gamma-ray bursts or active galactic nuclei. There could in principle exist large domains of the universe that are entirely made up of antimatter and that would not differ in the emitted photons we would observe. Still the borders of such domains would emit strong diffuse annihilation-radiation where matter and antimatter would meet. The absence of such signals suggests that at least inside our own Hubble volume there are no such domains present and there really is a net surplus of matter over antimatter [85, 86, 87].
The conditions to generate a finite baryon asymmetry were first formulated systematically by Sakharov in 1967 [88]. These conditions read

Sakharov Criteria for Baryogenesis

- Baryon number violating processes
- C- and CP-violation
- Departure from thermal equilibrium

The first condition is rather obvious, if baryon number is always conserved then the universe must have already started out with all presently observed number of baryons. This is inconsistent with primordial inflation which is a cornerstone of modern cosmology as we have seen. An initial nonzero baryon asymmetry that could still provide $\eta_B^{today} \sim 10^{-9}$ after a standard inflation with a length of 60-65 e-folds would require $\eta_B^{initial} \gtrsim 10^{69-75}$, which is obviously a very extreme and unnatural initial condition. This also tells us that any viable baryogenesis mechanism must have transpired after primordial inflation.
The second condition is less obvious but can also be easily understood. Without C- and CP-violation the rate of any baryon number violating process would be equal to the rate of its inverse process producing antibaryon number and no net baryon number could be produced.
The third condition is more subtle but is also necessary. It is required because the baryon number operator changes sign under CPT transformation meaning its expectation value has to be zero if the system has an equilibrium density matrix. The reason for this is located in the fact that the density matrix will in equilibrium only depend on the Hamiltonian which is CPT invariant in any sensible theory.

This in turn means that only out of equilibrium the density matrix can allow for the generation of a non-zero expectation value of the baryon number.

t'Hooft pointed out already in 1976 there are so called sphaleron processes that arise at high temperatures due to anomalies in non-abelian gauge theories that can violate $B + L$ but conserve $B - L$ [89]. This special class of instanton tunneling processes[33] arises because for non-abelian gauge fields there is more than one configuration of the gauge field for which the field energy vanishes [90, 91]. These are connected by discrete gauge transformations that are labeled by the so called Chern-Simons number n_{cs}. Within the standard model these processes could be thermally excited above the mass of the weak gauge bosons $T \gtrsim 100\text{GeV} \sim M_W$ while for lower temperatures they are exponentially suppressed instantons. In Figure (3.7) such a periodical vacuum structure is sketched. Sphaleron processes will usually change baryon and lepton quantum numbers according to

$$\Delta B = \Delta L = N_f \Delta n_{cs} \quad \rightarrow \quad \begin{cases} \Delta(B - L) = 0 \\ \Delta(B + L) = 2N_f \Delta n_{cs} \end{cases} \tag{3.106}$$

where N_f is the number of families. These processes are important for several reasons, for once they can generate a baryon asymmetry if they are effective while the universe is out of equilibrium. This is the basic mechanism behind electroweak baryogenesis (see section 3.4.1). More importantly these processes will transfer net baryon asymmetry into net lepton asymmetry or vice versa which is most important for the mechanism of baryogenesis via leptogenesis (see section 3.4.2). Also this tells us that a viable baryogenesis mechanism should also violate $B - L$ to produce an asymmetry that will not be washed out by sphaleron processes later on.

There have been numerous approaches to baryogenesis, see e.g. [90] for an extensive overview, the most well known being probably electroweak baryogenesis, baryogenesis via leptogenesis and Affleck-Dine baryogenesis. We will only briefly address the first two and focus on explaining the third one in detail since it is the only one that can also produce a large baryon asymmetry as needed for the little inflation scenario as we shall see later on.

[33] Some authors clearly distinguish instantons as quantum tunneling between vacua while sphalerons are the thermally activated counterpart and not a special class of the former. However, the terminology in the literature is not unique in this point.

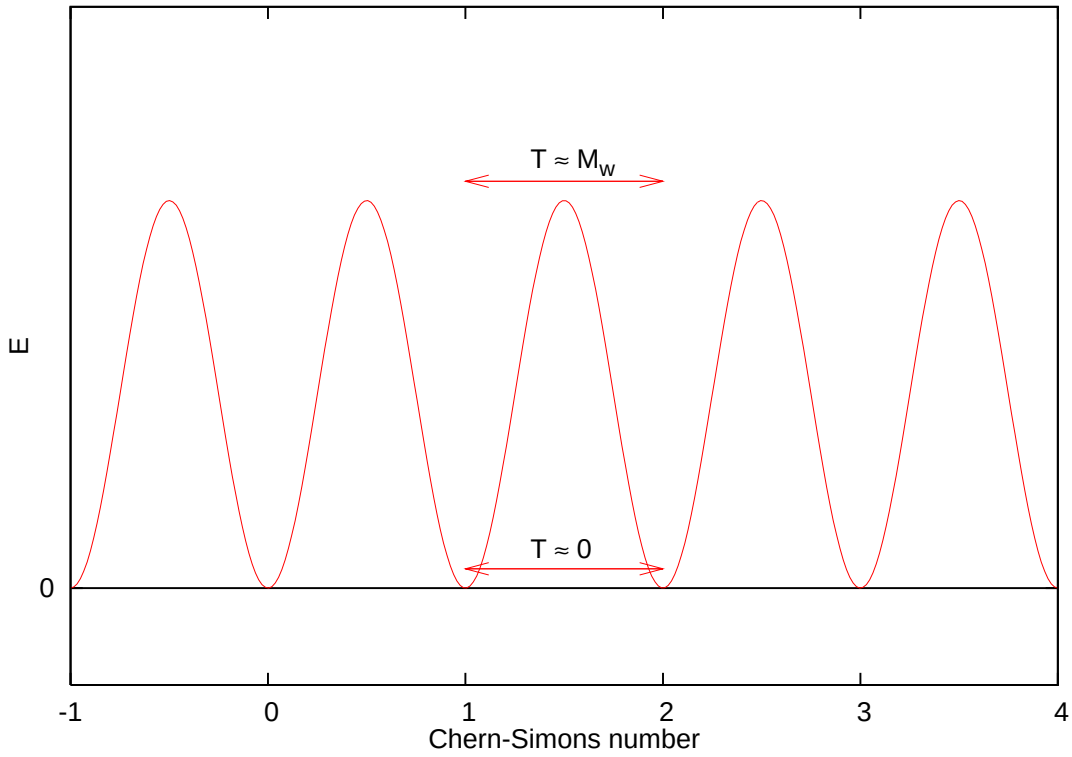

Figure 3.7: Sketch of the periodical vacuum structure in non-abelian gauge theories. For zero temperature tunneling transitions between different vacua labeled by the discrete Chern-Simons number are exponentially suppressed. In the standard model such processes are in thermal equilibrium if $T \gtrsim M_W$.

3.4.1 Electroweak Baryogenesis

In 1985 it was pointed out by Kuzmin, Rubakov and Shaposhnikov [92] that the standard model contains at least the first two ingredients for baryogenesis. Namely baryon number is violated by sphaleron processes, CP symmetry is violated for example in the decay of B-mesons. The third requirement would be departure from equilibrium at a point where the two other conditions are still fulfilled[34]. A widely discussed possibility was the electroweak phase transition in which three out of four massless electroweak gauge bosons acquire a mass via the Higgs mechanism and become the massive $W^{\pm}$ and Z^0 bosons while the photon stays massless.
However, lattice gauge theory calculations of the electroweak phase transition have shown that it is most likely a crossover for a Higgs mass of more than 80 GeV [93, 94, 95] while a standard model Higgs in that mass region is already excluded.

[34]This for example rules out the QCD phase transition in any case because both B and CP are conserved to a very high accuracy at $T \sim 200$ MeV.

Apart from this there is another problem, namely that electroweak baryogenesis in the standard model would only allow for a production of $\eta_B \sim 10^{-20}$ far below the necessary amount. In supersymmetric extensions to the standard model electroweak baryogenesis could be more effective and a first order phase transition is also possible in some models [96, 97].

3.4.2 Baryogenesis via Leptogenesis

As first pointed out by Fukugita and Yanagida in 1986 [98] baryogenesis might also be the result of a net lepton number being partially transformed into a net baryon number via sphaleron processes. The basic mechanism of baryogenesis via leptogenesis assumes the existence of right-handed neutrinos[35] with a very large Majorana mass $M \sim M_{GUT}$ which can also explain the smallness of the standard model neutrino masses via the seesaw mechanism. The left-handed neutrinos only acquire a mass due to off-diagonal terms in the neutrino mass matrix that arise from the interaction of the Higgs boson with left- and right-handed neutrinos. These interactions introduce new sources of CP-violation beyond those of the standard model. Once the temperature drops below the mass of the heavy right handed neutrinos they start to decay to left-handed neutrinos and the Higgs. These processes will automatically drop out of equilibrium once the decay rate becomes smaller than the Hubble constant thus the third Sakharov criterium is also met. The reader is referred to the extensive review by Buchmueller et al. [99] for more details.

3.4.3 Affleck-Dine Baryogenesis

The next question we need to address is if such a high initial baryon asymmetry is possible within one of the established baryogenesis mechanisms. For Affleck-Dine baryogenesis [100, 101] this is actually the case. In short the idea is that baryon- and lepton-number carrying scalar fields with very flat potentials can locally acquire very large expectation values. The Affleck-Dine mechanism can readily be incorporated into supersymmetric models [102], where squark- and slepton-fields play the role of the baryonic scalar fields. Once supersymmetry is broken the flat directions are lifted and the scalar-condensates become massive and roll down to the true minimum and thus decay to standard model particles leaving a finite baryon and lepton asymmetry. We will go through the basic mechanism of Affleck-Dine in the following without doing any quantitative calculation to see how the

[35] This violates lepton number even in very simple realizations [99].

mechanism fits into the Sakharov criteria.
A simple toy model[36] reads [103, 87]

$$\mathcal{L} = \frac{1}{2}\left(\partial_\mu\phi\right)\left(\partial^\mu\phi\right)^* + \lambda\left(|\phi|^4 - \frac{\phi^4+\phi^{*4}}{2}\right) = \frac{1}{2}\left(\partial_\mu\phi\right)\left(\partial^\mu\phi\right)^* - \lambda|\phi|^4\left(1-4\cos\theta\right) \tag{3.107}$$

where $\phi = |\phi|e^{i\theta}$ such that θ is the angle plane of the complex field. Because of the cosine term the potential is not rotationally invariant, i.e. the U(1) symmetry connected to the phase rotation

$$\Lambda_\alpha:\ \phi = |\phi|e^{i\theta} \quad\rightarrow\quad \phi' = |\phi|e^{i\theta}e^{i\alpha} = |\phi|e^{i(\theta+\alpha)} \tag{3.108}$$

is explicitly broken. In figure 3.8 the above potential is depicted, for a different power of the fields in the potential there may be more or less flat directions present. The potential in (3.107) has four flat directions at the angles $\theta = 0, \pi/2, \pi, 3\pi/2$ and it is usually assumed for Affleck-Dine baryogenesis that one of these directions was chosen by chance as a local initial condition set during the onset of inflation by quantum fluctuations. This state was then spread out over the whole present universe by the exponential expansion giving a common initial condition for baryogenesis[37]. A nonzero baryon asymmetry can even be created if all valleys are populated with similar probabilities if the potential prefers the production of baryon number over the production of antibaryon number. We will encounter such a situation with a slight extension of the above potential.
Remembering equation (2.16) we find the connected baryon charge

$$\begin{aligned}
B &= -i\int_V \frac{\partial\mathcal{L}}{\partial(\partial_0\Phi_\alpha)}\Omega^i_{\alpha\beta}\Phi^\beta d^3x = -i\int_V \frac{\partial\mathcal{L}}{\partial(\partial_0\Phi_\alpha)}\Omega^i_{\alpha\beta}\Phi^\beta d^3x \\
&= -i\int_V\left(\frac{\partial\mathcal{L}}{\partial(\partial_0\phi)}(-1)\phi + \frac{\partial\mathcal{L}}{\partial(\partial_0\phi^*)}(1)\phi^*\right)d^3x \\
&= \frac{i}{2}\int_V\left(\dot\phi^*\phi - \dot\phi\phi^*\right)d^3x \\
&= \frac{i}{2}\int_V\left(\left(|\dot\phi|e^{-i\theta} - i|\phi|\dot\theta e^{-i\theta}\right)|\phi|e^{i\theta} - \left(|\dot\phi|e^{i\theta} + i|\phi|\dot\theta e^{i\theta}\right)|\phi|e^{-i\theta}\right)d^3x \\
&= \int_V |\phi|^2\dot\theta d^3x
\end{aligned} \tag{3.109}$$

[36] More realistic models will not have flat directions with infinite extent. See for example the single complex field model in Ref. [103] where there is always an additional rotationally invariant term with the highest power.

[37] Thus there could be other Hubble volumes that consist entirely of antimatter in this approach.

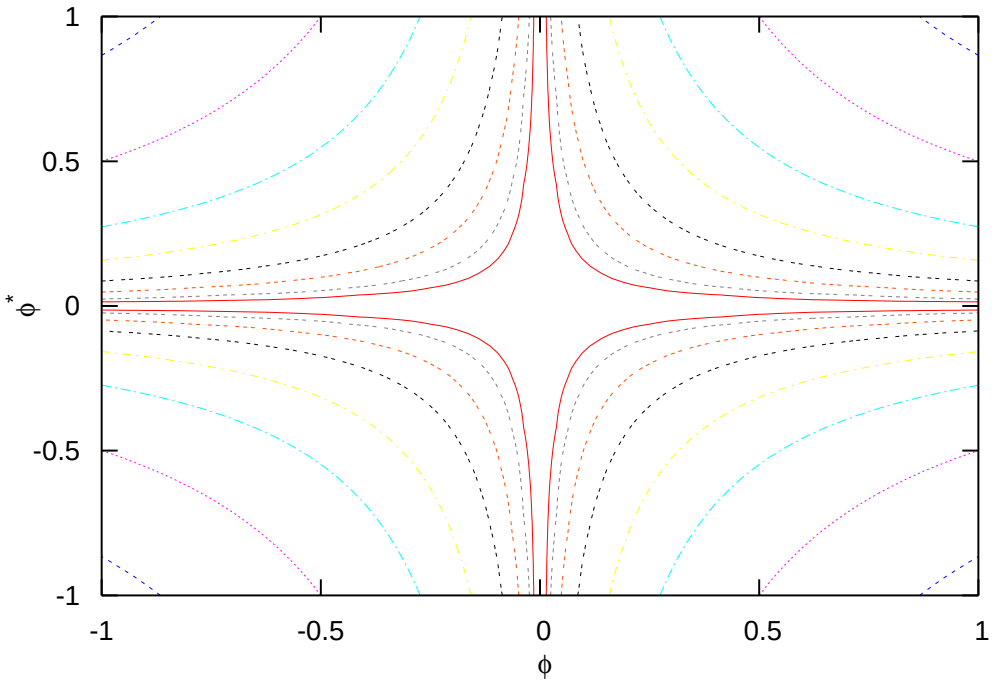

Figure 3.8: Baryon number violating scalar potential as given by (3.107). Such kind of potentials are present in many supersymmetric extensions of the standard model, where the scalar fields carrying baryon number are squark- and slepton-fields.

is not conserved. The result (3.109) means that the baryon number is given by the angular momentum of the field in the complex plane. Positive baryon number corresponds to the field rotating counterclockwise[38] and clockwise for negative baryon number. Thus the first Sakharov condition is already fulfilled by the Lagrangian (3.107).
The field obeys the equation of motion

$$\ddot{\phi} + 3H\dot{\phi} + \mathcal{U}'(\phi) = 0 \tag{3.110}$$

where the second term is a friction term due to the expansion of the universe. Thus if $\mathcal{U}$ is rotationally invariant then the last term only causes radial forces and the angular momentum is conserved as well known from Lagrange mechanics.

[38] note that the sign may differ depending on the definition of the U(1) transformation and the Noether charge

For the second Sakharov condition to be realized the potential has to be asymmetric with respect to the replacement of ϕ and ϕ^* that can be modeled for example by extending the potential in the following way by introducing a mass term

$$\begin{aligned}\mathcal{U} &= \lambda|\phi|^4\left(1-\cos\left(4\theta\right)\right)+m_\phi^2\left(|\phi|^2-\frac{\lambda_1\phi^2+\lambda_2\phi^{*2}}{2}\right)\\ &= \lambda|\phi|^4\left(1-\cos\left(4\theta\right)\right)+m_\phi^2|\phi|^2\left(1-\cos\left(2\theta+2\gamma\right)\right)\end{aligned} \tag{3.111}$$

If $\lambda_1 \neq \lambda_2$ then the phase γ will be non-zero and CP-symmetry is violated. The final ingredient, departure from equilibrium, is provided by the fact that some of the terms will actually be dependent on the Hubble parameter such that the minima at high field values will disappear at roughly the same time when the mass of the fields becomes large by breaking of supersymmetry[39]. Incorporating this into our toy model one may arrive at

$$\begin{aligned}\mathcal{U} &= \lambda|\phi|^6+|\phi|^4\left(A+a_H\frac{H}{M_p}\cos\left(4\theta\right)\right)\\ &+ |\phi|^2\left(m_\phi^2+c_HH^2\cos\left(2\theta+2\gamma\right)\right)\end{aligned} \tag{3.112}$$

Either $a_H < 0$ or $c_H < 0$ can cause a large initial vacuum expectation value to be set during inflation because at least local minima (or even global ones) will form at large field values. In Ref. [103] different mechanisms to acquire such negative terms within supersymmetric theories are discussed, where the Hubble dependent mass term will actually most likely be positive and both baryon number- and CP-conserving.

In figure 3.9 the potential is shown for $\gamma = -0.18\pi$, $a_HH/M_p = -2A$ and $c_HH^2 = 2m_\phi^2$ and excluding the $|\phi|^6$ term for simplicity. As one can see the potential is deformed as compared to (3.8), the valleys at $\theta = \pi/2, 3\pi/2$ are lifted and rotated clockwise while the valleys in the $\theta = 0, \pi$ directions are still pronounced and tilted counterclockwise. If the field starts out from one of the former valleys it will rotate clockwise creating negative baryon number while the latter valleys will lead to counterclockwise rotation and thus positive baryon number. It is rather obvious that even if all valleys were populated initially with equal probability[40] the "right" and "left" valley configurations will cause the field to acquire a higher angular momentum than the "upper" and "lower" valleys resulting globally in a net positive baryon number.

[39] i.e. the masses of the superpartners squarks and sleptons become much larger then the masses of their standard model counterparts.

[40] which is unlikely in the given example since there might not even be local minima present in the $\theta = \pi/2, 3\pi/2$ valleys for a wide range of parameters.

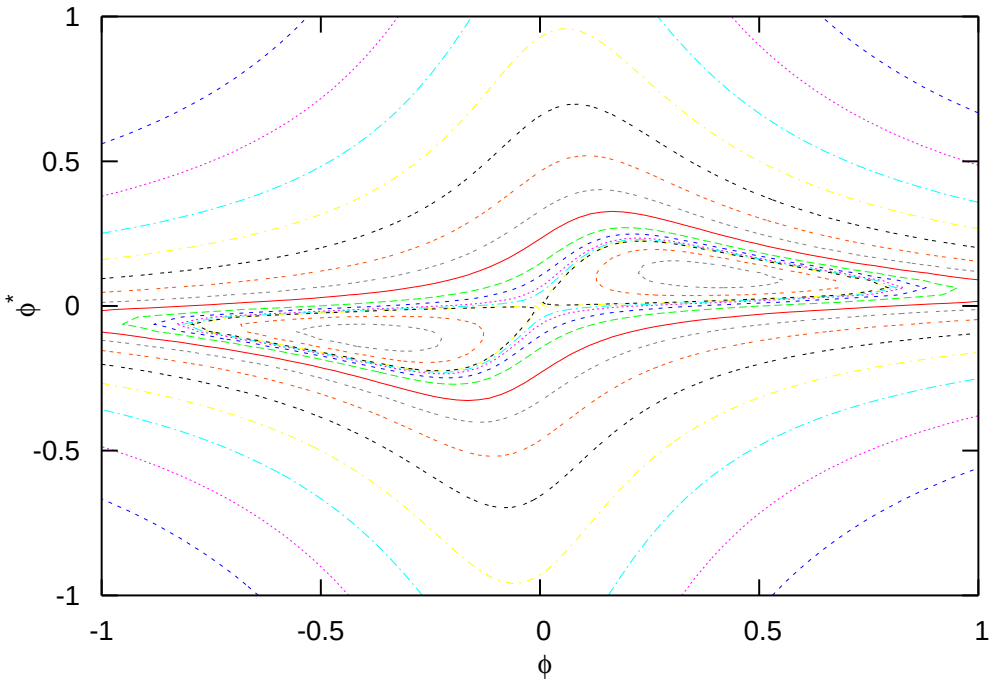

Figure 3.9: Potential according to 3.112 with a negative Hubble mass-term while $|c_H|H^2 \gtrsim m_\phi^2$ and the field starts to roll towards the origin in from either initial flat direction $\theta \sim 0, \pi$. Either starting condition will here lead to a preferred counterclockwise angular momentum and thus a positive baryon number. Once $|c_H|H^2 < m_\phi^2$ the global minimum is located in the origin.

Since H becomes smaller and smaller during the expansion of the universe the term responsible for the initially large vacuum expectation value will flip its sign and CP- and U(1)-symmetries become approximately conserved once the global minimum is located at $\phi = \phi^* = 0$. Finally the massive squark and slepton fields will spiral in around the origin while decaying to quarks and leptons transferring baryon (and lepton) number to the standard model sector.
In simple realizations the Affleck-Dine mechanism can easily produce a too high baryon asymmetry for the standard cosmological scenario, thus either models with multiple fields or more sophisticated coupling terms have to be introduced to limit the initial baryon number production or a subsequent reduction is necessary. The latter could be achieved, as mentioned earlier, by a large entropy release that di-

lutes the baryon to photon ratio to the right value observed today for example by an inflationary period (see e.g. ref. [101]). That being said Affleck-Dine baryogenesis can provide $\eta_B \sim \mathcal{O}(1)$, where this is probably an upper limit [101]. Still, this bound has not been explored any further after the estimates in the initial publications by Affleck, Dine and Linde for the obvious reason that an even higher baryon asymmetry was not desirable.

Chapter 4

A Little Inflation

...what I conclude is that a little inflation is a good thing.

– Nobel laureate in economy George Akerlof, in an interview about US fiscal policy in *Challenge* magazine in 2007.

4.1 QCD Phase Transition in Cosmology

The cosmological QCD phase transition from the quark-gluon plasma to a hadron gas happened about 10 microseconds after the big bang. In standard cosmology the baryon asymmetry is tiny $\eta_B = n_B/s \sim 10^{-9}$, with n_B being the net baryon density and s the entropy density, as deduced from later stages in the evolution of the universe. Improving lattice gauge theory calculations have shown in the last decade that at such conditions this transition was most probably only a rapid crossover [7, 8].

Therefore a first order QCD phase transition seemed very unlikely given the conditions. Still, the QCD phase diagram is for most parts terra incognita. The chiral and the deconfinement transition do not necessarily coincide but there are some indications from effective models [104] and lattice QCD calculations that there is at least a significant connection between the two. There has been recent progress in the attempt to include a finite baryon density on the lattice [20, 21] but effective models are still the method of choice to explore the uncharted regions of the QCD phase diagram [22]. Findings indicate that at finite baryon densities a first order phase transition can be expected as shown by chiral effective models of QCD [105] caused by to the melting of quark and/or gluon condensates or by color superconductivity [49]. A sketch of a possible QCD phase diagram is again depicted in figure 4.1 along with the commonly accepted path the universe took during and after the QCD-transition. The universe starts out in the upper left and moves along the temperature axis from the chirally symmetric quark gluon plasma through a crossover transition to the chirally broken hadron gas phase. Once protons and anti-protons stop to annihilate below 35 MeV the baryon chemical quickly shoots up from ~ 1 eV to the nucleon mass (see ref. [9] for more details). Effective models of QCD [32, 106] as well as lattice calculations [20] at finite baryon chemical potential give hints for the existence of a critical endpoint at $\mu_C = \mathcal{O}(1)T_C$.

Now let us finally come back to our initial question as outlined in the introduction. Could the cosmological QCD phase transition have been first order without violating the constraint of a small baryon asymmetry in the later evolution of the universe? On the one hand a large baryon asymmetry before the transition seems necessary for a first order phase transition to be possible. On the other hand we know that the baryon asymmetry was very small at later stages in the evolution of the universe[1].

[1] Already at BBN it must have been at the present day value as we have seen in section 3.1.

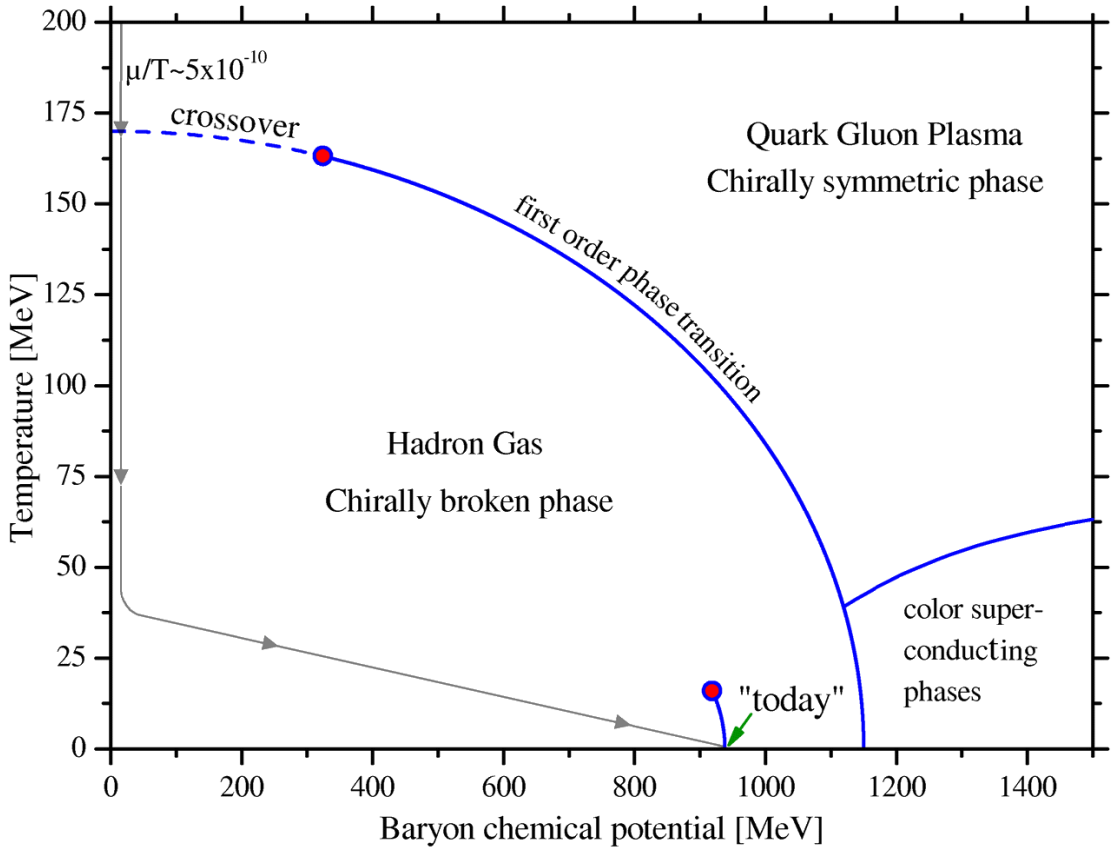

Figure 4.1: Sketch of a possible QCD-phase diagram with the commonly accepted standard evolution path of the universe as calculated e.g. in [9] depicted by the grey path.

These requirements can be met if the baryon asymmetry was reduced in the course of the phase transition for example by a large entropy release. Exactly this is the basic idea of the little inflation scenario: a large baryon asymmetry at earlier times allows a delayed strong phase transition that will trigger an entropy release which reduces the baryon asymmetry to the present day value.
In figure 4.2 I sketch the evolution path of the universe in the little inflation scenario. Here the universe starts out at a large baryon chemical potential and therefore crosses the first order phase transition line but stays in the deconfined chirally symmetric phase. The universe is trapped in the wrong QCD vacuum and undergoes a short period of inflation until the delayed phase transition takes place. The released vacuum energy then causes a large entropy release that dilutes the baryon asymmetry to the presently observed value. Afterwards the universe evolves along the standard path just as in figure 4.1.

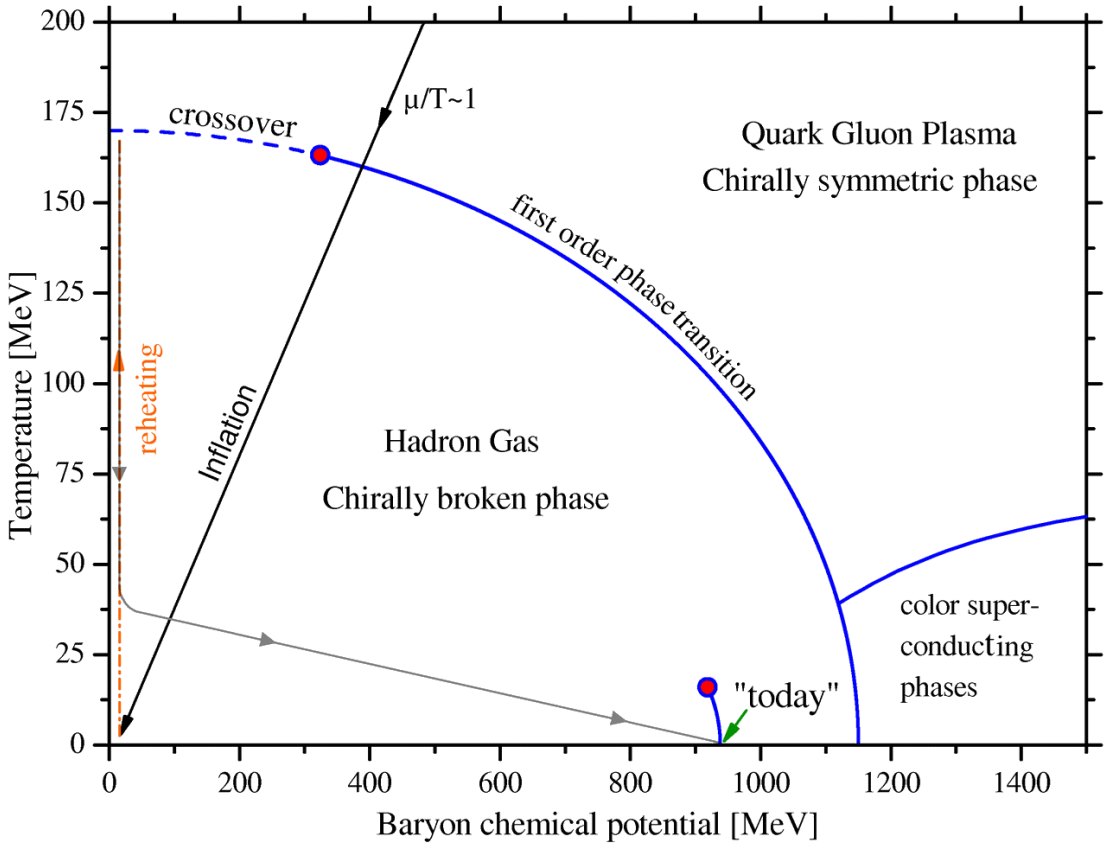

Figure 4.2: Sketch of a possible QCD-phase diagram with the commonly accepted standard evolution path of the universe as calculated e.g. in [9] depicted by the grey path.

The concept of a little inflation (or tepid inflation) at the QCD phase transition has been also introduced earlier by Kämpfer et al. [5, 107, 108, 109] and for a inflationary period of similar duration as discussed here later by Borghini et al. [110]. In both cases an initially higher net baryon density is diluted to the presently observed small value of the baryon-to-photon ratio in the course of the QCD phase transition. Still in both cases the most important aspects and The general idea of a short inflation to reduce a too high baryon asymmetry was mentioned even earlier by Linde in a publication on Affleck-Dine baryogenesis [101] but not explicitly in the context of the QCD phase transition.

4.2 Baryon asymmetry

4.2.1 Baryon Asymmetry

As we have seen one of the main requirements of such a short inflationary period at the QCD phase transition is a non-vanishing baryochemical potential $\mu_B/T \sim \mathcal{O}(1)$. Big bang nucleosynthesis calculations predict the observed primordial abundances of elements correctly only if the baryon asymmetry was tiny at a temperature of 1 MeV and below. The cosmic microwave background radiation as well as large scale structure observations predict very similar values and combining all these observations one finds a baryon asymmetry of $5.9 \cdot 10^{-10} < \eta_B < 6.4 \cdot 10^{-10}$ at 98% confidence [111].

Now we need to estimate how long such a little inflation has to be in order to start out with a sufficiently large ratio of μ_B/T. The net number of baryons in a comoving volume is conserved and can be estimated by $N_B \approx a_i^3 \mu_{Bi} T_i^2 \simeq a_f^3 \mu_{Bf} T_f^2$ where the index i refers to the initial values when the vacuum energy starts to dominate the energy budget of the universe and f to the final values after reheating. Therefore the initial ratio of the chemical potential to the temperature can be higher by

$$\frac{\mu_{Bi}}{T_i} \simeq \theta^3 \frac{\mu_{Bf}}{T_f} \left(\frac{T_f}{T_i} \right)^3 \tag{4.1}$$

with $\theta = a_f/a_i$. If the phase transition at the end of inflation transpires on a timescale much shorter than the Hubble time then the universe reheats back to the initial temperature at the start of inflation in good approximation $T_i \simeq T_f$. Then we can conclude from equation (4.1) that for $\theta \sim 10^3 \approx e^7$ the baryon asymmetry before inflation η_{Bi} and μ_i/T_i will be of order unity. The latter would, as we have seen, suffice to allow the QCD phase transition to be first order.

4.2.2 Chemical Potentials and the Duration of Inflation

Now we want to make the above estimates for the highest possible μ_B before such a little inflationary period a bit more quantitative taking $\eta_B = 1$ as an upper limit. To keep things simple we take all particles to be massless. The energy density,

pressure, entropy density and number density of a relativistic gas read

$$\rho = g\left(\frac{\pi^2}{30}T^4 + \frac{1}{7}\mu^2T^2 + \frac{1}{14\pi^2}\mu^4\right) \tag{4.2}$$

$$p = \frac{\rho}{3} = g\left(\frac{\pi^2}{90}T^4 + \frac{1}{21}\mu^2T^2 + \frac{1}{42\pi^2}\mu^4\right) \tag{4.3}$$

$$n = \frac{\partial p}{\partial \mu} = g\left(\frac{2}{21}T^2\mu + \frac{2}{21\pi^2}\mu^3\right) \tag{4.4}$$

$$s = \frac{\rho + p - \mu n}{T} = g\left(\frac{2\pi^2}{45}T^3 + \frac{2}{21}\mu^2T\right) \tag{4.5}$$

Here g is the effective number of bosonic helicity states, i.e. fermionic helicity states are weighted with a factor of $\frac{7}{8}$. For $\bar{n}_B$ we can directly use equation (4.4) with $g = g_q/3$ for the degrees of freedom[2]. The entropy density has contributions from particles with sizable chemical potential and from those without, therefore we label the quark degrees of freedom an index q and those that have a non-negligible chemical potential[3] with an index μ. This is necessary because both are not necessarily the same since leptons should most likely carry an asymmetry similar to the baryonic one.

$$s = g\frac{2\pi^2}{45}T^3 + g_\mu\frac{2}{21}\mu^2T \tag{4.6}$$

If we now combine both we arrive at an estimate for the baryon asymmetry

$$\eta_B = \frac{\frac{2g_q}{63}\left(T^2\mu + \frac{\mu^3}{\pi^2}\right)}{g\frac{2\pi^2}{45}T^3 + g_\mu\frac{2}{21}\mu^2T} = \frac{g_q 5\left(\frac{\mu}{T} + \frac{1}{\pi^2}\frac{\mu^3}{T^3}\right)}{g7\pi^2 + g_\mu 15\frac{\mu^2}{T^2}} \tag{4.7}$$

Interestingly this means that in the limit of $\mu \gg T$ as well as in the limit $\mu \ll T$ the baryon asymmetry is just proportional to μ/T. The limits can be directly read of to be

$$\eta_B \approx \begin{cases} \frac{g_q 5}{g7\pi^2}\frac{\mu}{T} & \mu \ll T \\ \frac{g_q}{g_\mu 3\pi^2}\frac{\mu}{T} & \mu \gg T \end{cases} \tag{4.8}$$

Here we assume for simplicity that all particle species with a non-zero chemical potential have the same chemical potential i.e. $\mu = \mu_q = \mu_\nu = \mu_e$ et cetera. In the end we assume that the equilibrium condition for the quark and baryon chemical

[2]This results from $\frac{7}{8} \cdot 2 \cdot 2 \cdot 2 \cdot 3/3$, i.e. the degrees of freedom are fermion weighting · spin · particle/antiparticle · flavor · color · the baryon number per quark.

[3]both are not necessarily the same since leptons should most likely carry an asymmetry similar to the baryonic one.

potential holds $\mu_B = 3\mu_q$. Note that one cannot treat baryons as fundamental degrees of freedom satisfying equation (4.4) with a charge of 1/3 within this simple estimate or there would be a contradiction to the chemical equilibrium condition $\mu_B = 3\mu_q$.
In figures (4.3) and (4.4) the results from (4.7) are shown for two particle compositions each for negligible lepton asymmetry and for equal baryon and lepton asymmetry. One can see that the influence from the particle composition is only a small effect, since the additional degrees of freedom contribute in a similar magnitude to numerator and denominator of η_B. On the other hand η_B is significantly suppressed at the same chemical potential when adding a equal lepton asymmetry. This can be easily understood since the lepton asymmetry only increases the entropy but not the baryon number. The limiting values for μ_B/T assuming $\eta_B = 1$ for the four cases are shown in table 4.1

	all particles g	quarks g_q	asym. particles g_μ	$\mu_B/T\|_{max}$ for $\eta_B = 1$
A	$e^\pm, \nu, u, d, \gamma, g$ 47.75	u, d 21	u, d 21	88.89
B	$e^\pm, \mu^\pm, \nu, u, d, s, \gamma, g$ 61.75	u, d, s 31.5	u, d, s 31.5	88.74
C	$e^\pm, \nu, u, d, \gamma, g$ 47.75	u, d 21	$u, d, e^\pm, \nu$ 29.75	125.2
D	$e^\pm, \mu^\pm, \nu, u, d, s, \gamma, g$ 61.75	u, d, s 31.5	$u, d, s, e^\pm, \mu^\pm, \nu$ 43.75	123.1

Table 4.1: Degrees of freedom in the 4 considered cases A-D correspond to the curves in figures 4.3 and (4.4) as well as the resulting maximum values for μ_B/T.

Now we can translate the limits on the initial chemical potential to temperature ratio to a constraint on the length of inflation. The baryon number in a comoving volume is conserved, i.e. $n_{Bi} = \theta^3 n_{Bf}$, therefore the length of inflation can be directly inferred from the ratio of baryon asymmetries before and after inflation

$$\theta = \left(\frac{\eta_{Bi} s_i}{\eta_{Bf} s_f}\right)^{1/3} = \left(\frac{\eta_{Bi}}{\eta_{Bf}}\right)^{1/3} \tag{4.9}$$

Note that this definition does not necessarily coincide with the period of exponential expansion as we shall see later. To evaluate this expression we only need to calculate the baryon asymmetry η_{Bi} because the two specific entropy densities s_i and s_f are by definition equal.

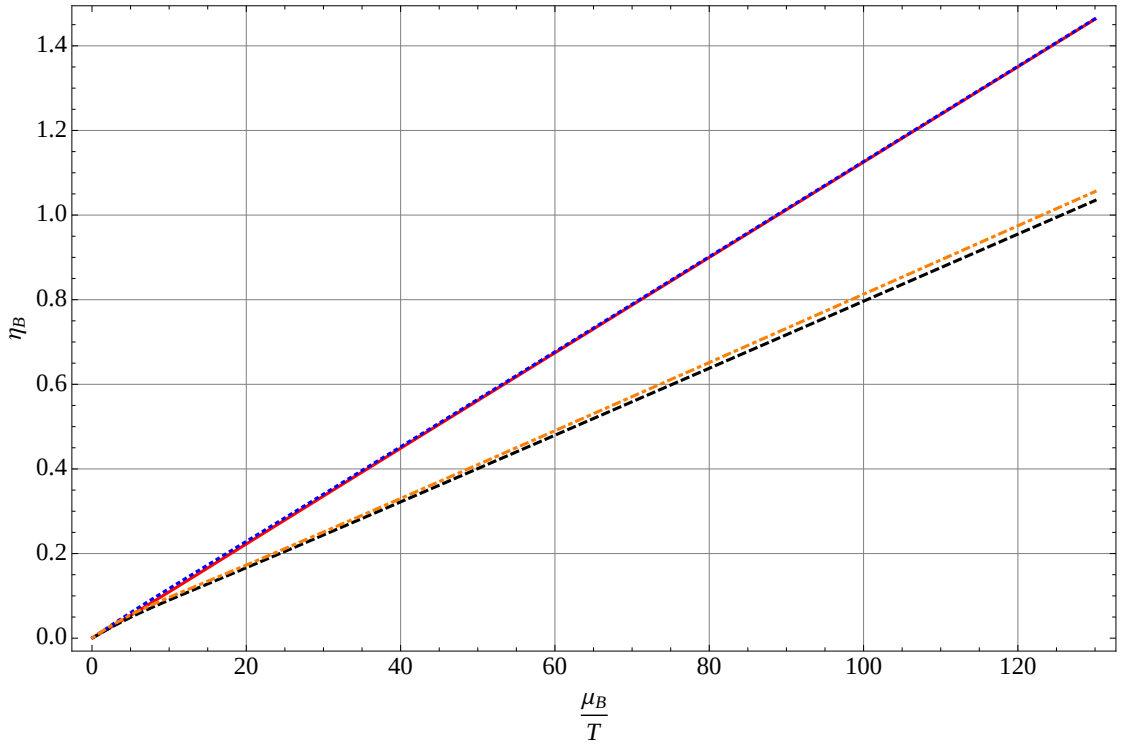

Figure 4.3: Here we plot the resulting baryon asymmetry from equation (4.7) as a function of μ_B/T for different cases. All curves include photons, three neutrino families, electrons and positrons, up and down quarks and eight gluons. Solid red (A) and dotted blue (B) curves assume a negligible lepton asymmetry while the latter also includes strange quarks and muons. The dashed black (C) and the dashed-dotted orange (D) lines include a lepton asymmetry and again the latter adds s-quarks and muons.

If we now make use of the experimental value for η_{Bf} we find the upper limit on the inflation length is given by

$$\theta_{max} = 1176\ \eta_{Bi}^{1/3} \tag{4.10}$$

independent of particle composition. In figure 4.5 we show the corresponding maximum dilution of baryon number by a delayed QCD phase transition in the little inflation scenario. This figure is part of the results of the dilaton quark meson model and the structure formation calculation in sections IV and V, respectively, but it is quite model independent apart from the value of the chosen value of the vacuum energy.

The period of exponential expansion could also be estimated for comparison and define the onset at the point where $p_V + p_R = 0$, but a simple estimate is rather lengthy and also not very accurate because for interesting inflation lengths the

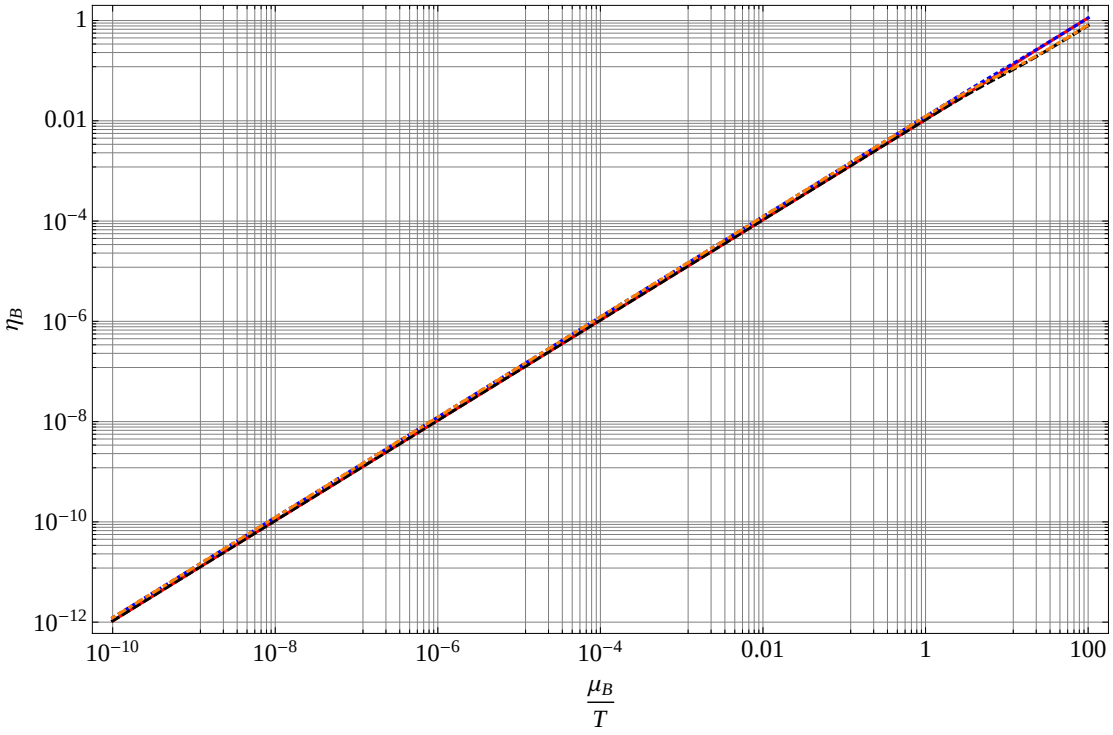

Figure 4.4: The same plot as figure (4.3) but on a wider double-log-scale. As one can see a general order of magnitude estimate for η_B is simply given by $0.01\frac{\mu_B}{T}$.

dark matter energy density is of similar magnitude of the vacuum and radiation energy densities. We will show the numerical results in section 4.4.

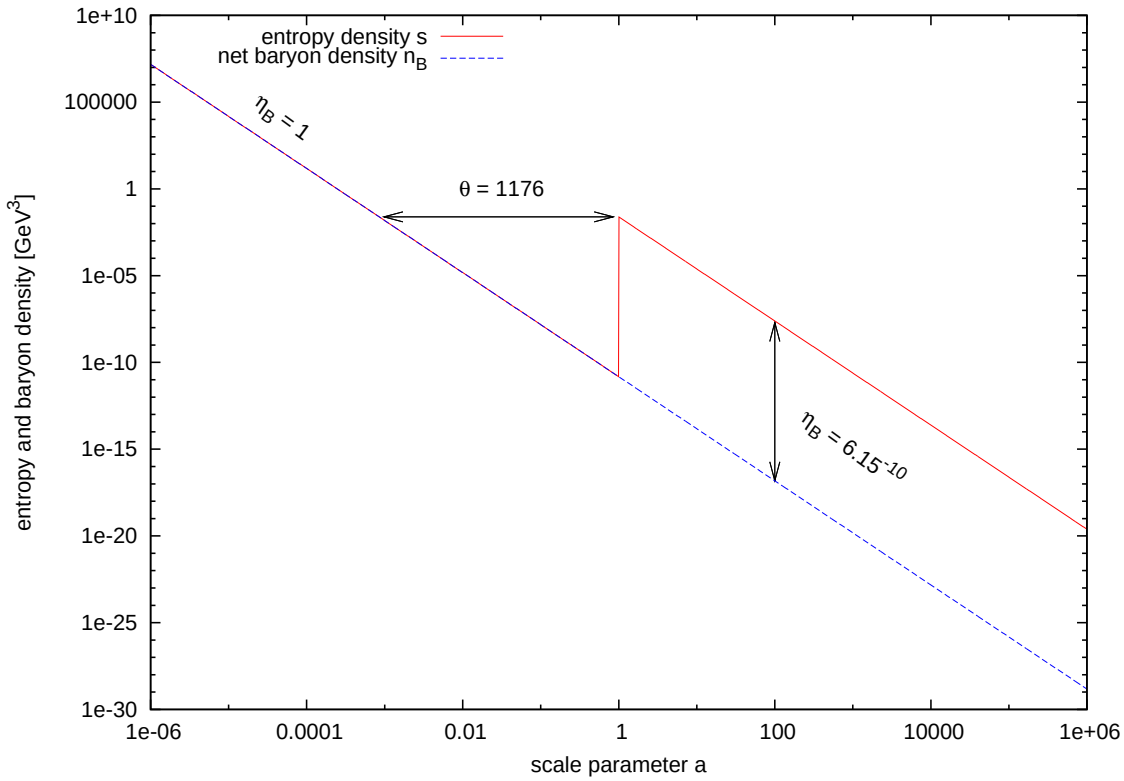

Figure 4.5: The reduction of η_B to the presently observed value

4.3 Nucleation

The next critical requirement of the little inflation scenario is a large supercooling or in other words if a sufficiently delayed phase transition is possible. This issue is directly connected to the stability and height of the barrier between the chirally broken phase and the chirally restored phase in the effective potential for sufficiently low temperatures. In chiral models of QCD including gluonic degrees of freedom in the form of a dilaton field the barrier only vanishes in the $T \to 0$ limit [47] thus strong supercooling is in principle possible and we will come back to this model later on.

First let us consider the nucleation rate Γ of the low temperature phase inside the high temperature phase

$$\Gamma = \Gamma_0 e^{-\Delta F_*/T} \tag{4.11}$$

where the functional form is that of a thermally activated process as found by Langer in the 60s and 70s, e.g. [112]. Γ_0 is in general a temperature dependent dynamical prefactor and ΔF_* is the free energy needed to produce a critical sized bubble of the new phase inside the old phase. What is meant by a critical sized

bubble in this context? If the temperature is smaller than the critical temperature $T < T_c$ the system becomes metastable and statistical fluctuations produce bubbles of the low temperature phase with a radius R and a free energy of

$$\Delta F = \frac{4\pi}{3} \left(p_H(T) - p_L(T) \right) R^3 + 4\pi R^2 \sigma_S \tag{4.12}$$

Here $p_H(T)$ and $p_L(T)$ is the pressure in the high and the low temperature phase, respectively, and σ_S is the surface tension. The first term describes the energy gained by transforming a spherical volume of radius R to the new phase while the second term gives the energy it costs to create the surface interface around the bubble. Since $p_L(T) > p_H(T)$ both terms have opposite sign and there is a critical radius R_* at which ΔF has a minimum

$$R_* = \frac{2\sigma_S}{p_L(T) - p_H(T)} \tag{4.13}$$

only bubbles larger than R_* can grow, for smaller ones it is energetically more favorable to shrink and disappear. One might just estimate Γ_0 by T^4 for dimensional reasons but Csernai and Kapusta [113] found Γ_0 in an effective field theory to be

$$\Gamma_0 = \frac{16}{3\pi} \left(\frac{\sigma_S}{3T} \right)^{3/2} \frac{\sigma_S \eta_H R_*}{\xi_H^4 (\Delta w)^2} \tag{4.14}$$

which can easily be a few orders of magnitude smaller than the naive estimate. Here η_H and ξ_H are the shear viscosity and the correlation length in the high T phase, respectively, and Δw is the difference in enthalpy density $w = \rho + p$ between the two phases.

The important ratio for the cosmological QCD phase transition is Γ/H, i.e. the rate of nucleation to the Hubble parameter. Once this ratio exceeds unity bubbles are produced abundantly and coalesce until the transition is complete. If Γ/H does not exceed one then bubbles of the low temperature phase will form and grow but the distance between bubbles increases so fast that the volume fraction of the new phase stays small.

We will in the following compare to work done by Csernai and Kapusta [114, 113] for the QCD phase transition within the bag model to find if the nucleation rate can be sufficiently small compared to the Hubble parameter such that the phase transition will initially fail. In ref. [114] the authors found that the transition is completed very quickly with only marginal supercooling of about 1% below the critical temperature. In fact this result depends strongly on the value of the surface tension σ_S which they took to be $\sim 50\text{MeV/fm}^2$. This number originates from an older work of Kajantie et. al [115] who calculated the surface tension at critical

temperature and zero density, for which the transition is found to be a crossover by all recent lattice calculations. As one can see from equation (4.11) Γ depends exponentially on the value of the surface tension as well as on the free energy difference between both phases and especially the former quantity is in principle unknown at non-zero baryon density.

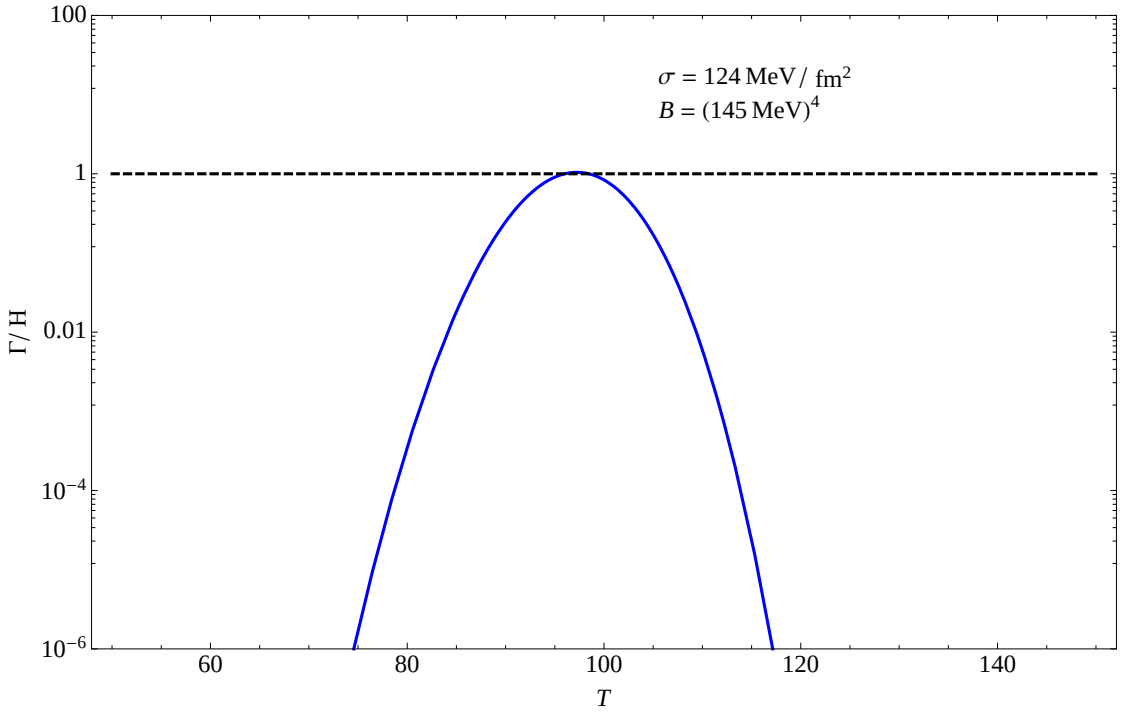

Figure 4.6: Nucleation rate over the Hubble parameter for the lowest value of the surface tension for which the phase transition would initially fail.

Using the bag model as outlined in section 2.7 with a critical temperature $T_c = 170$ MeV and the same parameters as used in [113] let us look for the lowest surface tension at which Γ/H does not exceed unity at least until its maximum at around $\sim T_c/2$. This might already be overstreching the applicability of (4.11) but it should still give a reasonable estimate of the surface tension needed for nucleation to fail. We find that the surface tension must indeed be very large and exceed 448 MeV/fm^2 $\sim 3.7\ T_c^3$ using their high value of the bag constant of $\mathcal{B} = (235$ MeV$)^4$. If we however go to the lower end of values found in the literature, i.e. the original number $\mathcal{B} = (145\text{MeV})^4$ found by the MIT group to fit hadron masses [37], we find that a significantly lower $\sigma_S = 124$ MeV/fm^2 suffices. The resulting Γ/H in that case is shown in figure 4.6. The surface tension for the QCD phase transition at non-zero baryon densities can only be estimated by effective models

since lattice gauge theory calculations for this case are still in its infancies. In ref. [116] a reasonable range of $\sigma_S = 50 - 150$ MeV/fm^2 is discussed but even smaller or larger values are not excluded in principle. If one considers very high densities the surface tension for the transition from color superconducting phases to nuclear matter could reach values of 300 MeV/fm^2 [117]. In figure 4.7 the minimal surface tension needed for nucleation to fail is shown for the commonly discussed range of the bag constant.

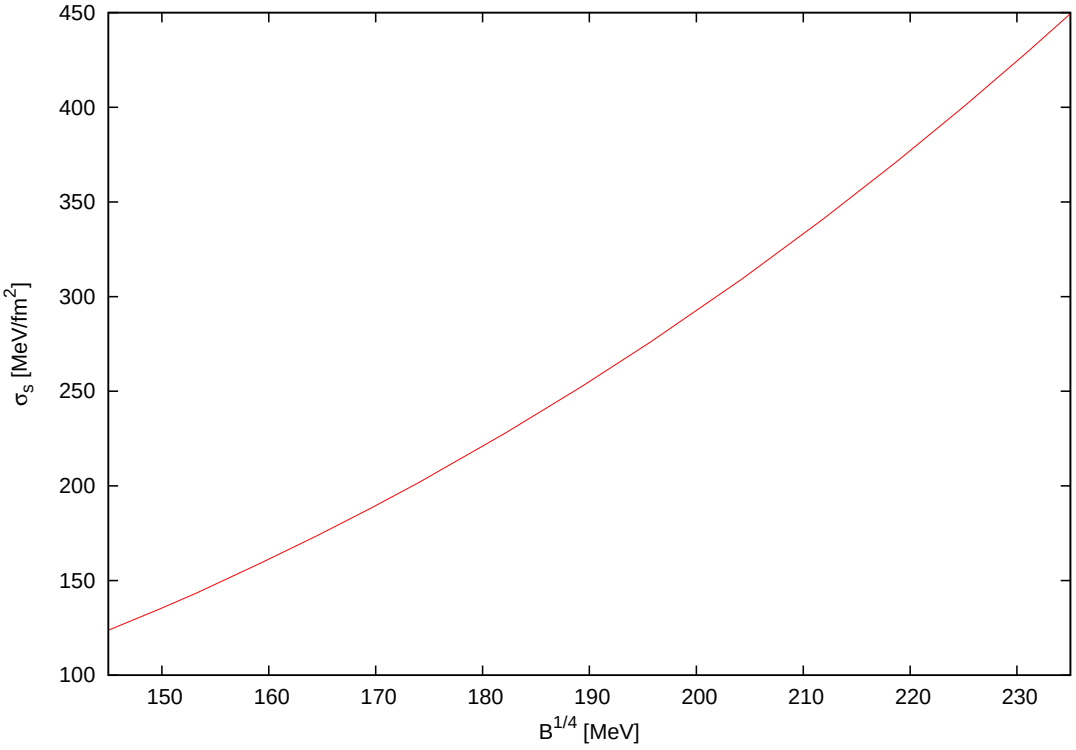

Figure 4.7: Minimum value of the surface tension as a function of the Bag constant at which Γ/H does not exceed unity.

This estimate only covers the initial failure to nucleate but it is clear that the phase transition has to occur after some limited supercooling (compared to ordinary inflation) of only about 7 e-foldings at most as we have seen. We stress that one should not take this estimate too far because both $\mathcal{B}$ and σ_S have to be temperature dependent in general since both will in a field theoretical approach originate from the relative height and the shape of the barrier between the two vacua in the effective potential. Finally Γ/H must exceed unity for inflation to end and the phase transition to proceed, for which the surface tension has to drop sufficiently fast such that fluctuations can easily overcome the barrier. Another possibility

would be the complete vanishing of the barrier and a spinodal decomposition as studied for example in [108] for a bag like model. Other authors have also discussed the strong sensitivity of nucleation rates for example in the context of neutron stars and core-collapse supernovae. There it was found that nucleation timescales can basically not be constrained and range from μs up to the age of the universe.
Also for heavy ion collisions strong supercooling is discussed for the "quench"-scenario, see e.g. [118]. There the chiral phase transition is delayed as the field is trapped in a metastable minimum and is only released to the true minimum in the T=0 limit.
The equation of state has to fulfill the usual condition $\rho + 3p < 0$ to enter an inflationary phase. In the bag model this would be the case below a temperature $T_{inf} = (30\mathcal{B}/(g\pi^2))^{1/4}$. In the linear-$\sigma$-model or the NJL-model this occurs when the thermal contributions to the energy density become smaller than the vacuum contributions like the quark condensate $\langle m_q q\bar{q}\rangle \approx f_\pi^2 m_\pi^2$ and the gluon condensate $\beta_{QCD}/(2g)\left\langle G^a_{\mu\nu}G^{\mu\nu}_a\right\rangle \approx 4B$ as we have discussed earlier.
We can conclude here that QCD at non-zero baryon densities is only poorly constrained and a delayed chiral phase transition is very well possible and has already been discussed for several other scenarios apart from the early universe.

4.4 Structure Formation

Next we will investigate the effect of a little inflationary period on primordial density perturbations. In particular dark matter perturbations are affected in several ways and on much larger scales than usual for the cosmological QCD phase transition. First of all the Hubble radius is roughly given by $R_H \sim g^{-1/2} m_{Pl} T_c^{-2} \sim 10$ km which encloses a total energy corresponding to about $1 M_\odot$. Since this epoch is long before matter radiation equality, i.e. $\rho_{DM} \sim (a_{QCD}/a_{EQ})\rho_R \sim 10^{-8}\rho_R$, the mass of dark matter in the same volume is smaller by the same factor resulting in a dark matter mass scale of approximately $10^{-8} M_\odot$. About ten years ago Schmidt, Schwarz and Widerin investigated the effect of the QCD phase transition on dark matter perturbations [119, 6]. They found that peaks and dips in the spectrum of dark matter perturbations may form for a first order phase transition but even for a crossover one could expect a boost for small scale perturbations. These effects were due to the reduction of the speed of sound c_s and equation of state $w = p/\rho$ of the radiation fluid during the phase transition. As the above estimate implies they only found these effects at very small mass scales below the Hubble scale. We shall examine the little inflation scenario with the same approach to density fluctuations, i.e. we work in uniform-expansion gauge as explained in section 3.3.5.

Basically all viable dark matter candidates are already chemically decoupled from the radiation fluid at the QCD phase transition, thus their numbers are not repopulated by reheating after inflation. Therefore the dark matter number density is diluted by the same factor θ^3 as the net baryon number. As stated before the dark matter mass enclosed inside the Hubble horizon is of the order of $10^{-8} M_\odot$ at $T_{QCD} \sim 170$ MeV, so any influence on perturbations inside dark matter would not have any consequences on larger scales. An inflationary period at the QCD-phase transition can change this in two ways, first of all the amount of dark matter enclosed inside the horizon must be larger by a factor θ^3 initially to match the present day dark matter density despite the dilution. For a short inflationary period, as discussed here, one encounters an additional effect on perturbations that have physical wavenumbers $k_{ph} \lesssim H$ at the beginning of inflation because an additional scale apart from H, namely $\dot{H}^{1/2}$, via equation (3.73) emerges. One may realize this by combining equations (3.11) and (3.12) to find that

$$\frac{\dot{H}}{H^2} = -\frac{2}{3}\frac{\rho + p}{\rho} = -\frac{2}{3}(1 + w) \tag{4.15}$$

so as long as w is not too close to -1 both scales coincide, but during an inflationary

phase this is no longer true. Let us do an estimate for a general mix of radiation, dark matter and vacuum energy, in this case

$$\dot{H} = -4\pi G \left[\frac{4}{3}\rho_{Ri}\left(\frac{a_i}{a}\right)^4 + \rho_{Mi}\left(\frac{a_i}{a}\right)^3\right] \propto \left(\frac{a_i}{a}\right)^q \tag{4.16}$$

where the subscripts refer to matter and radiation with $q = 3$ to 4, respectively, and the index i to the onset of inflation. Comparing this to the first Friedmann equation one finds that

$$H^2 = \frac{8\pi G}{3}\left[\rho_V + \rho_{Ri}\left(\frac{a_i}{a}\right)^4 + \rho_{Mi}\left(\frac{a_i}{a}\right)^3\right] \approx \frac{8\pi G}{3}\rho_V \tag{4.17}$$

As a consequence the two scales differ by $|\dot{H}/H^2|^{1/2} \simeq (1+\bar{w})^{1/2} \simeq \left(\frac{a_i}{a}\right)^{q/2}$, which would not play any role for a long inflationary period (i.e. with more than 50 e-foldings) because in this case $\dot{H}^{-1/2}$ is beyond the size of the observable universe, i.e. at the order of the infrared cutoff of the produced primordial spectrum. Summarizing, there should be two distinct scales in the spectrum dividing it into three regimes

$$\begin{aligned}
\left.\frac{k_{ph}}{H}\right|_i &> 1 && \text{(sub-hubble before inflation)} \\
1 > \left.\frac{k_{ph}}{H}\right|_i &> \left(\frac{a_i}{a_f}\right)^{q/2} && \text{(intermediate)} \\
\left.\frac{k_{ph}}{H}\right|_i &< \left(\frac{a_i}{a_f}\right)^{q/2} && \text{(unaffected)}
\end{aligned}$$

Translating this to the highest affected mass scale involved we estimate

$$M_{max} \sim 10^{-8} M_\odot \; \theta^{3q/2} \sim (10^5 - 10^9) M_\odot \tag{4.18}$$

at most for $\theta^{inf} \sim 640$.

4.4.1 Analytic Solutions

In section 3.3.6 we already derived the analytic super-horizon solutions for the radiation dominated case. These solutions set the initial conditions for all modes and are also applicable for any super-horizon mode after reheating when the universe is again dominated by ultra-relativistic particles. Now we want to additionally find the solutions for the inflationary phase in the different spectral regimes. For the inflationary regime it will be most important to examine the case of $q = 3$ because

radiation will be less abundant than matter soon after the onset of inflation for relevant inflation lengths. First of all we need the mean quantities

$$1+w \simeq \left(\frac{a_i}{a}\right)^3 \qquad \delta \simeq \delta_{DM}\left(\frac{a_i}{a}\right)^3 \qquad c_s^2 \simeq \frac{1}{3} \qquad w \simeq -1 \tag{4.19}$$

and we also need to remember that $k/\mathcal{H} \propto 1/a$ in the following. Now let us examine the two most relevant spectral regimes namely the intermediate and the unaffected regime. For the spectral range we will examine later on none of the modes will stay sub-Hubble sufficiently long during inflation to approach an analytic limit. This would only be the case for modes that stay similar or even below the Hubble frequency for they whole duration of the inflation. It turns out that the solutions in this case are combinations of Bessel functions that cannot be found by simple analytic means. Thus we skip a lengthy discussion for these modes and directly jump to the other two regimes that are more relevant and have analytic solutions that can be derived rather quickly.

Intermediate modes

These modes are defined by the condition $1 \gg \frac{k}{\mathcal{H}} \gg (1+w)^{1/2}$. Let us first examine the equations of motion for the dark matter perturbations

$$\alpha \simeq -3\left(\frac{\mathcal{H}}{k}\right)^2\left(\frac{a_i}{a}\right)^3\delta_{DM} \tag{4.20}$$

$$\delta'_{DM} \simeq -3\frac{\alpha}{a} = 9\left(\frac{\mathcal{H}}{k}\right)^2\frac{a_i^3}{a^4}\delta_{DM} \tag{4.21}$$

$$\hat{\psi}'_{DM} \simeq -\frac{1}{a}\hat{\psi}_{DM} \tag{4.22}$$

The solutions are easily found to be

$$\delta_{DM} = C_1 \exp\left[-9\left(\frac{\mathcal{H}}{k}\right)^2\left(\frac{a_i}{a}\right)^3\right] \tag{4.23}$$

$$\hat{\psi}_{DM} = \frac{C_2}{a} \tag{4.24}$$

with C_1 and C_2 being constants. This means that δ_{DM} will be frozen very quickly until the end of inflation[4] and quickly approaches a constant value. Now let us use

[4]Note that $(1+w)^{1/2}$ drops quicker than $\frac{k}{\mathcal{H}}$ so any mode that enters this regime stays there until the end of inflation.

these results to find the solutions for the radiation perturbations

$$\delta_R' \simeq -4\frac{\alpha}{a} = 12\left(\frac{\mathcal{H}}{k}\right)^2 \frac{a_i^3}{a^4}\delta_{DM} = \frac{4}{3}\delta_{DM}' \tag{4.25}$$

$$\hat{\psi}_R' \simeq -\frac{k}{\mathcal{H}}\frac{\alpha}{a} = 3\left(\frac{\mathcal{H}}{k}\right)\frac{a_i^3}{a^4}\delta_{DM} = \frac{1}{3}\frac{k}{\mathcal{H}}\delta_{DM}' \tag{4.26}$$

The solution to δ_R is thus directly found to be

$$\delta_R = \frac{4}{3}\delta_{DM} = C_1\frac{4}{3}\exp\left[-9\left(\frac{\mathcal{H}}{k}\right)^2\left(\frac{a_i}{a}\right)^3\right] \tag{4.27}$$

For $\hat{\psi}_R$ we may try the ansatz

$$\hat{\psi}_R = C_1\frac{1}{3}\frac{k}{\mathcal{H}}\exp\left[-9\left(\frac{\mathcal{H}}{k}\right)^2\left(\frac{a_i}{a}\right)^3\right] \tag{4.28}$$

$$\Rightarrow \hat{\psi}_R' = C_1\left(-\frac{1}{3}\frac{k}{\mathcal{H}a} + 3\frac{\mathcal{H}}{k}\frac{a_i^3}{a^4}\right)\exp\left[-9\left(\frac{\mathcal{H}}{k}\right)^2\left(\frac{a_i}{a}\right)^3\right] \tag{4.29}$$

The second term would solve equation (4.26) so we just need to get rid of the first term by adding a suitable counter term to the ansatz to find the right solution.

$$\hat{\psi}_R = C_1\left(\frac{1}{3}\frac{k}{\mathcal{H}} + \frac{1}{27}\left(\frac{k}{\mathcal{H}}\frac{a}{a_i}\right)^3\right)\exp\left[-9\left(\frac{\mathcal{H}}{k}\right)^2\left(\frac{a_i}{a}\right)^3\right] \tag{4.30}$$

$$\Rightarrow \hat{\psi}_R' = 3C_1\frac{\mathcal{H}}{k}\frac{a_i^3}{a^4}\exp\left[-9\left(\frac{\mathcal{H}}{k}\right)^2\left(\frac{a_i}{a}\right)^3\right] = \frac{1}{3}\frac{k}{\mathcal{H}}\delta_{DM}' \tag{4.31}$$

Thus (4.30) is the correct solution for $\hat{\psi}_R$.

Unaffected modes

Now let us turn to the unaffected modes that are given by the condition $1 \gg (1+w)^{1/2} \gg \frac{k}{\mathcal{H}}$. Again let us first examine the equations of motion for the dark matter perturbations

$$\alpha \simeq -\frac{2}{3}\delta_{DM} \tag{4.32}$$

$$\delta_{DM}' \simeq -\frac{3}{a}\alpha = \frac{2}{a}\delta_{DM} \tag{4.33}$$

$$\hat{\psi}_{DM}' \simeq -\frac{1}{a}\hat{\psi}_{DM} - \frac{k}{\mathcal{H}a}\alpha = -\frac{1}{a}\hat{\psi}_{DM} + \frac{2}{3}\frac{k}{\mathcal{H}a}\delta_{DM} \tag{4.34}$$

In this case the solution for δ_{DM} is quickly found to be

$$\delta_{DM} = Aa^2 \propto \left(\frac{\mathcal{H}}{k}\right)^2 \tag{4.35}$$

For $\hat{\psi}_{DM}$ we again need to make an educated guess

$$\hat{\psi}_{DM} = \frac{2}{3}\frac{k}{\mathcal{H}}Aa^2 + B\frac{1}{a} \tag{4.36}$$

$$\Rightarrow \hat{\psi}'_{DM} = \frac{2}{3}\frac{k}{\mathcal{H}}Aa - B\frac{1}{a^2} = \frac{4}{3}\frac{k}{\mathcal{H}a}\delta_{DM} - \frac{1}{a}\hat{\psi}_{DM} \tag{4.37}$$

This means we just need to change the ansatz slightly by dividing the first term by 2 to get the correct solution

$$\hat{\psi}_{DM} = \frac{1}{3}\frac{k}{\mathcal{H}}Aa^2 + B\frac{1}{a} \tag{4.38}$$

where A and B are again constants. The second term is a decaying solution that will quickly become subdominant. As before we will now use these solutions to find the solutions for the radiation perturbations

$$\delta'_R \simeq -4\frac{\alpha}{a} = \frac{8}{3a}\delta_{DM} = \frac{4}{3}\delta'_{DM} \tag{4.39}$$

$$\hat{\psi}'_R \simeq -\frac{1}{3}\frac{k}{\mathcal{H}a}\delta_R - \frac{4}{3}\frac{k}{\mathcal{H}a}\alpha = -\frac{1}{3}\frac{k}{\mathcal{H}a}\delta_R + \frac{8}{9}\frac{k}{\mathcal{H}a}\delta_{DM} \tag{4.40}$$

Again the solution for δ_R is proportional to δ_{DM}

$$\delta_R = \frac{4}{3}\delta_{DM} = \frac{4}{3}Aa^2 \tag{4.41}$$

Note that the solutions for δ_R and δ_{DM} are exactly the same solution as for the radiation dominated super-horizon case as found in section 3.3.6. We can immediately use this result for $\hat{\psi}_R$

$$\hat{\psi}'_R = -\frac{4}{9}\frac{k}{\mathcal{H}a}\delta_{DM} + \frac{8}{9}\frac{k}{\mathcal{H}a}\delta_{DM} = \frac{4}{9}\frac{k}{\mathcal{H}a}\delta_{DM} = \frac{4}{9}\frac{k}{\mathcal{H}}Aa = const. \tag{4.42}$$

Thus the dominant solution for $\hat{\psi}_R$ is also a linearly growing mode

$$\hat{\psi}_R = \frac{4}{9}\frac{k}{\mathcal{H}}Aa^2 \simeq \frac{4}{3}\hat{\psi}_{DM} \tag{4.43}$$

Comparing these results to the analytic super-horizon solutions in the radiation dominated universe we find that δ_{DM} and δ_R have the same growing mode[5] $\propto a^2$ while $\hat{\psi}_{DM}$ and $\hat{\psi}_R$ grow only linearly with the scale parameter[6]. This is actually necessary to keep the spectrum scale invariant on large scales [6] since this requires $\delta_i/\hat{\psi}_i \propto k/\mathcal{H}$. The latter keeps the amplitude at horizon entry independent of the wavenumber for large scales.

We will compare these analytic solutions in the following section to the results of a numerical calculation.

[5] Thus the naming of the spectral region as "unaffected" is justified.

[6] In contrast to a cubic growth in the radiation dominated super-Hubble case.

4.4.2 Numerical Results

For the numerical treatment I use the results from the WMAP 7 year data [71] for the dark matter density[7] $\Omega^0_{DM} = 0.227$ and the Hubble parameter $H_0 = 70.4$ km/s/Mpc. For the description of the radiation background I take the input from the dilaton-quark-meson model as described in section 2.10 and add a massless ideal gas of photons, gluons, $e^{\pm}$ and three neutrino families as in case C described in section 4.2.1. For the dark matter one may assume a decoupled pressureless non-relativistic gas with a vanishing speed of sound.

In figure 4.8 the evolution of the background densities is shown an inflation length

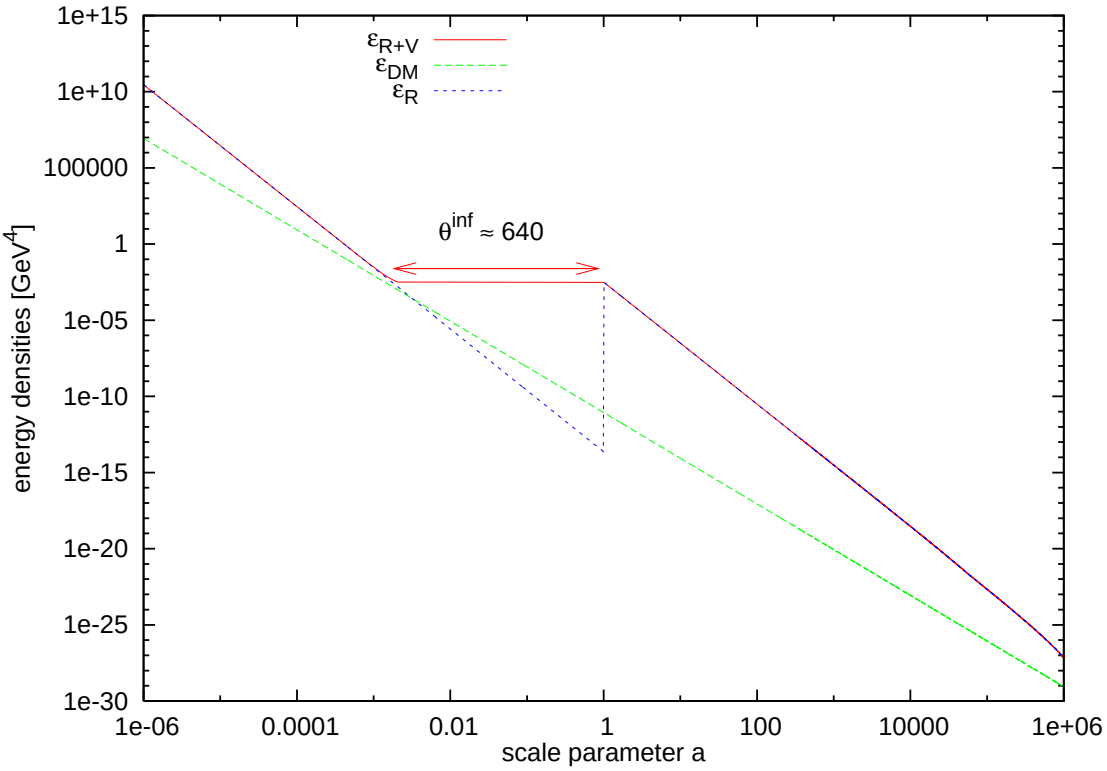

Figure 4.8: Evolution of the background energy densities of radiation plus vacuum contributions, dark matter and of radiation alone. As one can see the inflation length is only $\theta^{inf} \sim 640$ while the dilution factor is $\theta = 1176$.

of $\theta^{inf} = 640$ and a corresponding dilution factor of $\theta = 1176$. As one can see dark matter is in this case of the same order of magnitude as radiation at the onset of inflation. Furthermore one can see that dark matter is more abundant than the thermal radiation for almost the whole duration of the inflation in this case, thus

[7] The used parameter set is wmap7+bao+h0 for a flat ΛCDM model which includes results from baryon acoustic oscillations and independent measurements of the Hubble constant.

justifying the approximation made for the analytic solutions during inflation in (4.19).
For the density perturbations assume a scale invariant primordial Harrison-Zeldovich spectrum to be present before the phase transition. Each wavenumber k is followed separately from a point where is was sufficiently super-Hubble to apply the initial conditions for a radiation dominated universe given by the growing superhorizon modes [6, 82] as shown in section 3.3.6.

$$\delta_R = \frac{A}{6}\left(\frac{k}{\mathcal{H}}\right)^2 \qquad \hat{\psi}_R = \frac{A}{54}\left(\frac{k}{\mathcal{H}}\right)^3 \tag{4.44}$$

$$\delta_{DM} = \frac{3}{4}\delta_R \qquad \hat{\psi}_{DM} = \frac{9}{8}\hat{\psi}_R \tag{4.45}$$

The evolution of $\delta_R, \hat{\psi}_R, \delta_{DM}, \hat{\psi}_{DM}$ and k_{ph}/H is shown for three different wavelengths each corresponding to one of the three spectral regimes in the figures 4.9, 4.10 and 4.11. Radiation and dark matter perturbations are each evolved according

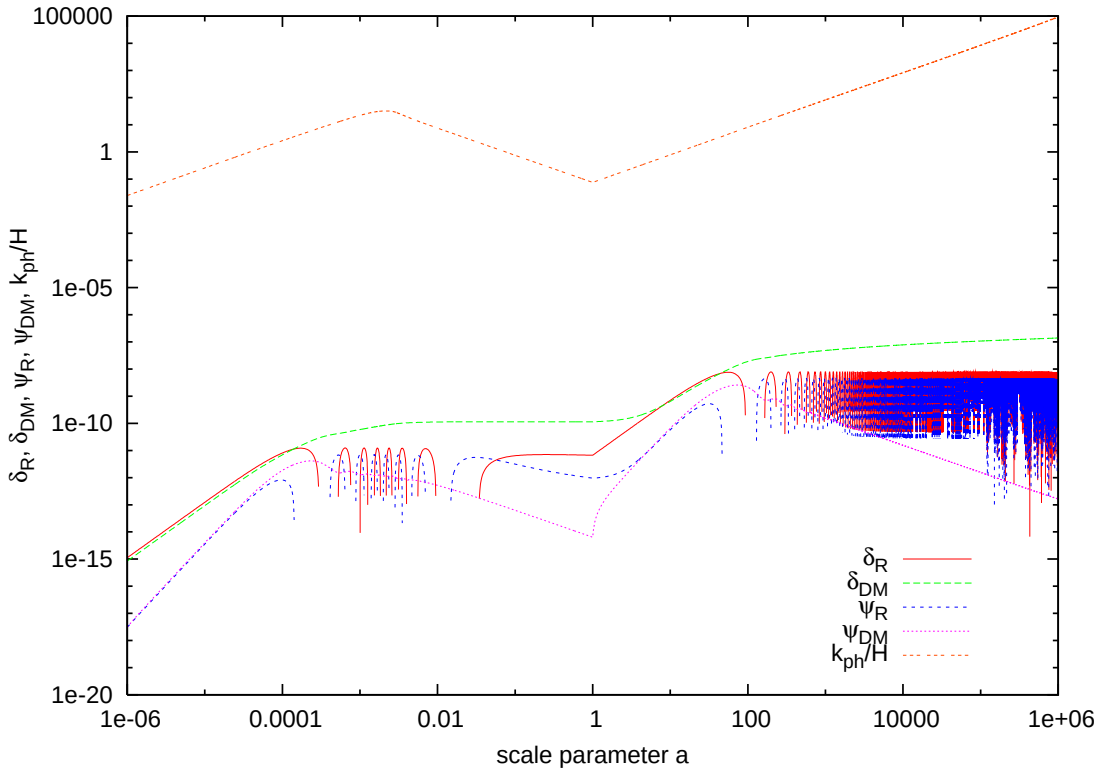

Figure 4.9: Evolution of $\delta_R, \hat{\psi}_R, \delta_{DM}, \hat{\psi}_{DM} = \hat{\psi}_R$ and k_{ph}/H for a comoving wavelength that encloses a dark matter mass of $10^{-2} M_\odot$.

to equations (3.74) and (3.75) coupled via the perturbation of the lapse α (3.76).

The scale parameter a is in each case normalized to the scale parameter at the end of inflation. As one can see the perturbations first follow the growing super-horizon solutions as given in (4.45). In figure 4.9 the modes enter the horizon at $a \sim 10^{-4}$ as visible by k_{ph}/H becoming larger than unity. Furthermore oscillations in δ_R and $\hat{\psi}_R$ start as well as the logarithmic growth in δ_{DM} according to the analytic solutions for sub-horizon modes during radiation domination, i.e. equations (3.99) and (3.104). At $a \sim 1/640$ the inflationary phase starts as visible in the turnaround of k_{ph}/H because H approaches a constant value. The mode is then pushed out of the horizon at $a \sim 0.1$ causing both δ_R and δ_{DM} to be frozen until the inflation ends at $a = 1$. This is just the behavior we have found in the previous section for intermediate modes in equations (4.27) and (4.23), i.e. the perturbations approach a constant value exponentially. Also for $\hat{\psi}_R$ and $\hat{\psi}_{DM}$ the behavior is as expected from (4.30) and (4.24), thus $\hat{\psi}_R$ approaches a $1/a$ solution while $\hat{\psi}_{DM}$ first decays as $1/a$ until it the asymptotically constant solution dominates. From this point on

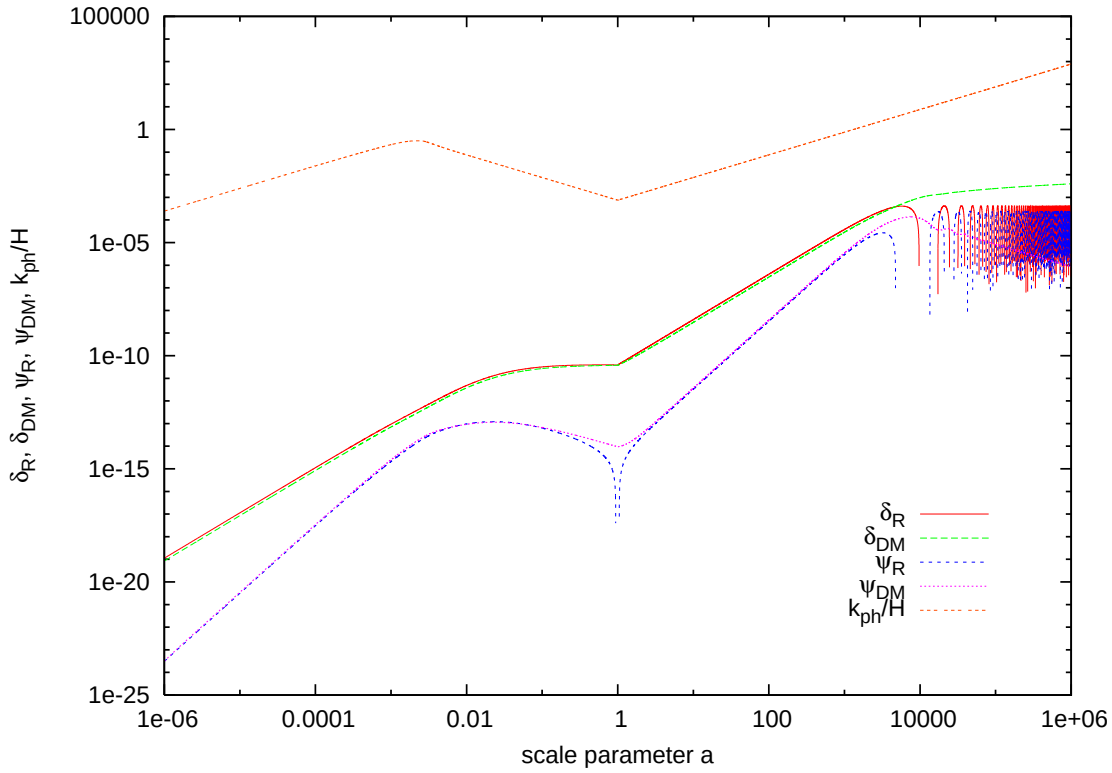

Figure 4.10: Same as figure 4.9 but for a wavelength that encloses a dark matter mass of $10^3 M_\odot$.

the mode switches again to the super-horizon solution for a radiation dominated universe until it reenters the horizon at $a \sim 100$. After that the fluctuations evolve

according to the solutions for a radiation dominated universe, i.e. oscillations at constant amplitude for δ_R and logarithmic growth for δ_{DM}. This mode is located in the part of the spectrum that is sub-Hubble before the onset of the inflationary phase.
The mode in figure 4.10 does not become sub-Hubble before the onset of inflation. It is first unaffected until $k_{ph}/\dot{H}^{1/2}$ exceeds unity and δ_R and δ_{DM} approach the constant super-horizon solution during inflation. The evolution of $\hat{\psi}_R$ is then again given by the asymptotic $1/a$ solution. $\hat{\psi}_{DM}$ in this case converges towards a negative value[8] which causes the seemingly sudden drop at $a \lesssim 1$ in the double-log-plot. In appendix 6.2.1 an example for this behavior is shown in a log-linear plot for another wave number where it is more clearly visible. Beyond $a = 1$ the behavior is similar to the previously discussed mode. Finally the long wavelength fluctu-

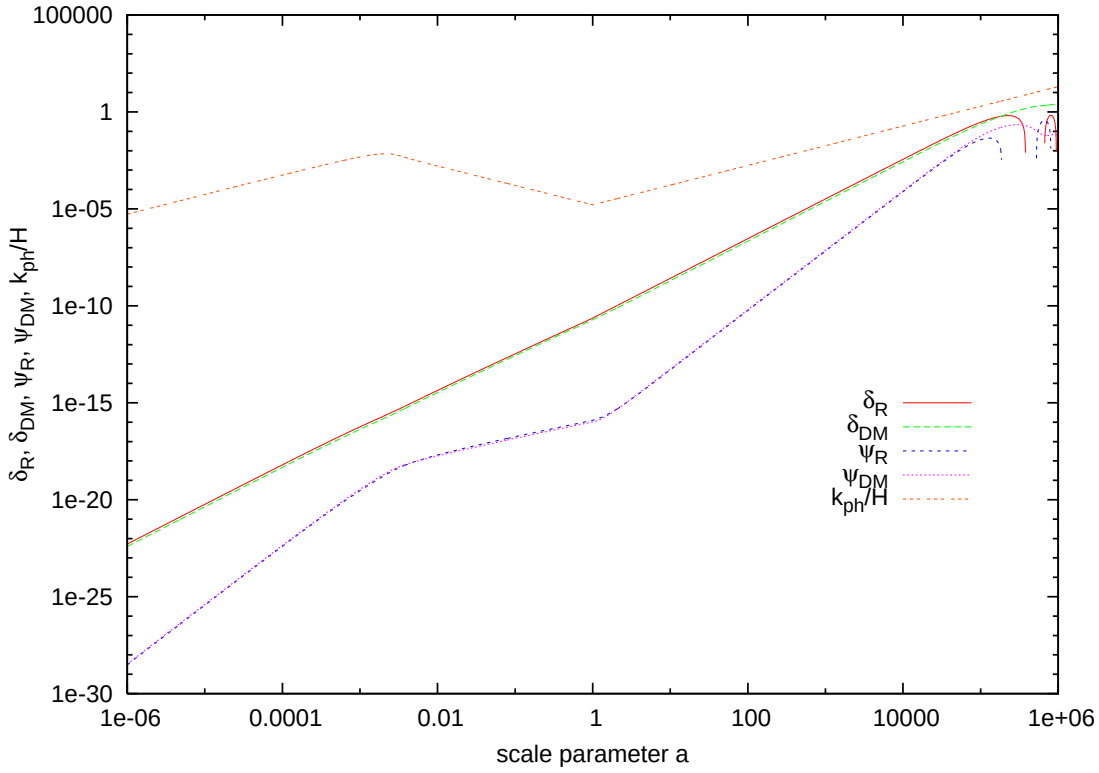

Figure 4.11: Same as figure 4.9 but for a wavelength that encloses a dark matter mass of $10^8 M_\odot$.

ation in figure 4.11 corresponding to a dark matter mass of $10^8 M_\odot$ is located in the unaffected region of the spectrum. For this mode neither k_{ph}/H nor $k_{ph}/\dot{H}^{1/2}$ exceed unity before or during inflation and thus it never enters the intermediate

[8] Note that all analytic solutions are only given up to a additive constant.

regime. δ_R and δ_{DM} behave as expected from the solutions (4.41) and (4.35) and thus grow $\propto a^2$. On the other hand $\hat{\psi}_R$ and $\hat{\psi}_{DM}$ show a reduced growth $\propto a$ according to (4.43) and (4.38) as we have discussed before.
The comparison between figure 4.10 and figure 4.11 shows that one may expect a relative suppression in the fluctuations below the unaffected part of the spectrum. In appendix 6.2.1 I additionally show a direct comparison of the evolution of δ_{DM} between different modes that may help to further clarify this point.
In figure 4.12 we show the resulting spectrum of primordial fluctuations after a little inflation in comparison to the spectrum as expected without little inflation. The spectrum is given in terms of the transfer functions defined in the following way

$$T_R(k) = \left(\frac{\delta_R^2(k) + \hat{\psi}_R^2(k)/c_{sR}^2}{\left(\delta_R^2 + \hat{\psi}_R^2/c_{sR}^2\right)_{in}} \right)^{1/2} \tag{4.46}$$

$$T_{DM}(k) = \left(\frac{\delta_{DM}^2(k)}{\delta_{DM,in}^2} \right)^{1/2} \tag{4.47}$$

The "*in*" quantities are evaluated at (final) horizon entry in the limit of small wavenumbers [6], i.e. in the unaffected part of the spectrum for the little inflation calculation[9]. The fluctuations are evolved for 12 orders of magnitude in a to ensure that the whole spectrum is super-horizon at the start of the calculation and is completely sub-horizon at the end[10]. Four orders of magnitude are needed due to the size of the spectrum, six orders of magnitude because inflation pushes the modes out of the horizon and they have to reenter again and finally one order of magnitude at the start and the end as a buffer.
All scales below $M_{max} \sim 10^6 M_\odot$ show a suppression, those below $M_H \sim M_\odot$ show additional features depending on their phase during horizon exit. Above this scale the spectrum of density perturbations is given by the primordial spectrum of density perturbations, e.g. a nearly scale invariant spectrum. The numerical result for the maximum mass scale is quite close to the lower bound in the above estimate (4.18) because dark matter has to be more abundant than radiation during almost the complete duration of the little inflation, which can be seen in figure 4.8. Still this mass scale is of cosmological interest as it is comparable to that of globular clusters (GC) which were the first objects to form during primordial

[9] Without little inflation this can just be evaluated at any arbitrary wavenumber since for a scale invariant spectrum by definition all modes enter at the same amplitude.
[10] The final temperature for the parameters used is $\sim 150\text{eV} \approx T_{reheat}/10^6$.

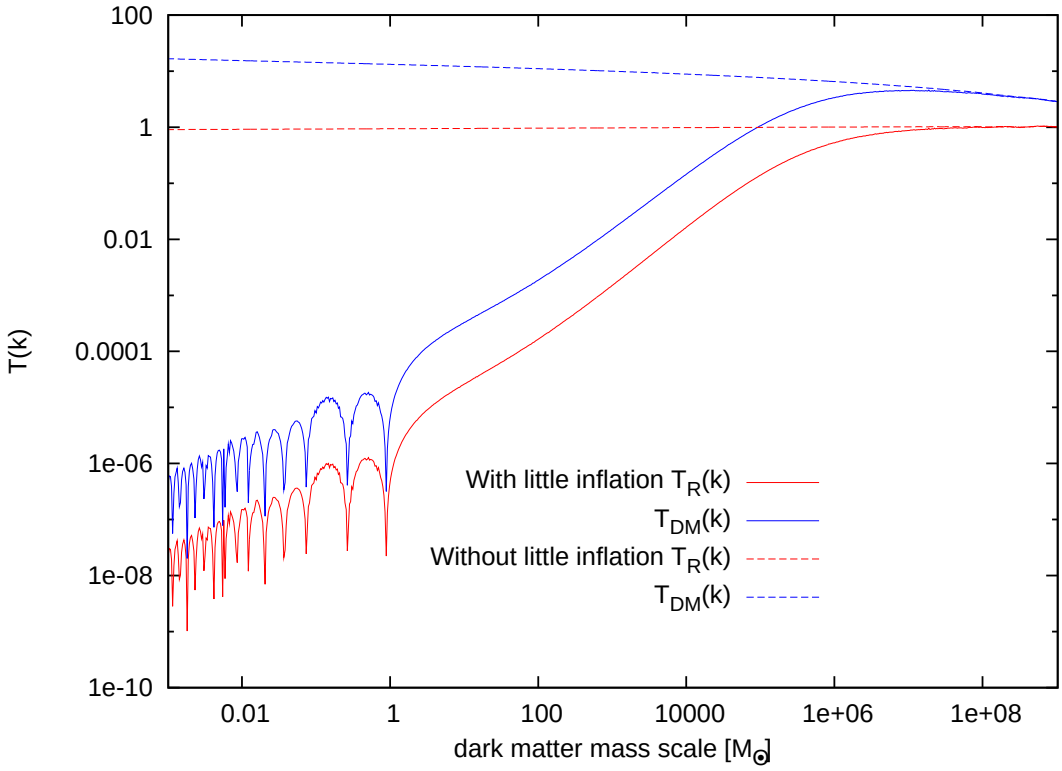

Figure 4.12: Spectrum of primordial fluctuations dependent on the dark matter mass scale in units of solar masses normalized to the amplitude at horizon entry.

galaxy formation[11]. Globular clusters are very compact star clusters of several hundred thousand to several million stars, with a radius of only ~ 10 pc. They are very metal poor objects and age estimates from stellar evolution models strongly suggest that they should already have been created during the formation of their host galaxy. Their mass function has a well defined peak at $M_{gc} \sim 2 \cdot 10^5 M_\odot$ in contrast to younger star clusters whose mass function shows a steep power law distribution between $10^4 M_\odot \lesssim M_{yc} \lesssim 10^7 M_\odot$ with an index of ≈ -2 [121]. There have been attempts to explain the preferred mass scale for GC by a higher Jeans mass at low metallicity that preferred more massive clusters to from at early times. Other explanations include disruptive processes (for low mass clusters) and mass loss due to stellar evolution (for high mass cluster) that might produce a preferred mass scale as seen in n-body simulations [122] starting from a steep mass function like the one of present young clusters. The latter point was dismissed by Vesperini et al. [123] whose simulations have shown that only very fine tuned initial conditions will result in GC properties that fit the observations if one assumes GC

[11] For a comprehensible overview of the topic the reader may have a look at the review by Harris [120]

formed just like clusters do today. On the other hand they showed that an initial mass function that was almost flat below the present peak mass scale succeeds in reproducing the observational data. Interestingly a power law cutoff in the dark matter fluctuations below a mass scale $10^{5-6}M_{\odot}$ as found in the little inflation scenario could thus help to explain this standing problem in galactic astrophysics. The suppression of the dark matter power spectrum below these scales could also be interesting to study because of its impact on the cuspy core density distribution of dark matter in small galaxies and the large number of halo structures seen in standard structure formation [124, 125, 126, 127]. A further possible influence could be on the emergence of the first generation of stars in the universe [128, 129]. These are believed to have triggered the reionization of the universe at the end of the dark ages and a initial suppression of low scale perturbations structures would thus probably delay reionization.

4.5 Dark Matter

Apart from the impact on small scale structure formation for dark matter the little inflation scenario has further direct consequences on properties of dark matter candidates. For cold dark matter the dilution of the energy and number densities leads to the possibility of a matter dominated phase before the inflationary phase since the dark matter energy density after reheating is basically fixed by the present day value. This can also be seen in figure 4.8 that displays the evolution of the different contributions to the energy density, wherein dark matter just starts to dominate right before the onset of inflation. To account for the different ratio of radiation and baryon densities before little inflation the dark matter density has to be larger by the same factor θ^3 as the baryon density. For $\theta \gtrsim 10^3$ the dark matter contribution actually becomes larger than the vacuum contribution which would in any case limit the maximum length of the exponential expansion to

$$\begin{aligned} \theta^{inf}_{max} &= \left(\frac{\mathcal{B}}{\rho_{DM}(a_f)}\right)^{1/3} \\ &\approx 900 \left(\frac{\mathcal{B}^{1/4}}{235\mathrm{MeV}}\right)^{4/3} \left(\frac{0.236}{\Omega_{DM0}}\right)^{1/3} \end{aligned} \tag{4.48}$$

where the bag constant $\mathcal{B}$ represents the vacuum contributions of QCD. Interestingly this limit and the previously discussed limit from the Affleck-Dine baryogenesis coincide by chance, while the latter actually limits the entropy release the former only limits the length of exponential expansion. As a side remark, to produce a complete spectrum of primordial fluctuations one would require $\theta \gtrsim 10^{10}$, far beyond both limits so little inflation cannot replace standard inflation.
Still figure 4.8 shows that the period of exponential expansion $\theta^{inf} \approx 640$ is even shorter than this estimate because the energy density of radiation increases so strongly with the baryon asymmetry at a fixed vacuum energy. This difference in θ and θ^{inf} is caused by the different dependencies of the entropy and the energy density on μ or rather n_B.

What does a larger dark matter density before the QCD scale mean for the properties of cold dark matter? For non-relativistic decoupling of dark matter the weak interaction cross section will no longer give the right amount of dark matter today. This is due to the fact that the dark matter annihilation cross section has to be much smaller, i.e.

$$\sigma^{annih}_{dm} \sim \frac{\sigma^{weak}}{\theta^3} \quad \text{because} \quad \Omega_{DM} \propto \frac{1}{\sigma^{annih}_{dm}}$$

where we ignore logarithmic dependencies on the dark matter mass. This allows more dark matter particles to survive annihilation before freeze-out and thus increases the CDM number density before little inflation. This gives the interesting prospect that the little inflation can be probed by ongoing and future collider experiments like the LHC since the discovery of a standard weakly interacting massive particle as the neutralino would exclude the scenario.
Another case would be thermally decoupled ultra-relativistic particles where the dilution of dark matter number densities can be incorporated in the ordinary temperature relation to the radiation background. Here little inflation leads to an effective shift in the temperature relation

$$T = T_{DM}\theta \left(\frac{g^s_{eff}(T_{Dec})}{g^s_{eff}(T)} \right)^{1/3} \tag{4.49}$$

This in turn modifies the relation of warm dark matter relic mass and decoupling degrees of freedom to match the present day density found for example in [69]

$$m^{max}_{DM} \approx 51\mathrm{eV}\theta^3 \left(\frac{4}{g_{DM}} \right) \left(\frac{g^s_{eff}(T_{Dec})}{106.75} \right) \left(\frac{\Omega^0_{DM}h^2}{0.116} \right) \tag{4.50}$$

This shifts the suitable mass of a thermal relic particle to a much higher value without the need for a large number of additional effective degrees of freedom at decoupling beyond those of the standard model.
There can also be effects for baryonic dark matter as discussed by Jedamzik [130]. During a first order phase transition the speed of sound vanishes and thus sufficiently nonlinear density fluctuations can collapse during that time. For an exponentially small fraction of Hubble volumes that are overdense enough primordial black holes (PBH) may form. The mass spectrum of these PBH will be strongly peaked around $1M_\odot$ which corresponds to the total (not just the dark matter) energy density inside the Hubble volume at the phase transition. The produced abundance of PBH depends on the spectral index and amplitude of the density fluctuation spectrum, which we have seen is different and in general more complicated in the little inflation scenario. Nevertheless it seems quite clear that the suppression of small scale density fluctuations will also strongly reduce the production of such primordial back holes during the phase transition at the end of a little inflation.
During the nucleation process lumps of quark matter or small quark stars could be produced but only with $M \sim 10^{-9}M_\odot$ as we argue that nucleation starts after the little inflationary epoch.

4.6 Magnetic Fields

A standing problem in astrophysics is the origin of large scale magnetic fields that have strengths of up to $B_\lambda^{obs} = 0.1\mu$G on extragalactic and up to 10 μG on galactic scales. To understand the existence of such magnetic fields with correlation lengths of typically 0.1 Mpc it is necessary to have an initial seed field generated before or during galaxy formation. The required strength of such seed fields varies strongly with the assumed amplification mechanism and may vary over many orders of magnitude $10^{-30}G \lesssim B_\lambda^{seed} \lesssim 10^{-10}$G, see [131] and references therein for an overview of the topic. The seed fields may be generated during ordinary inflation or at a first order phase transition. The latter has been discussed for the QCD phase transition by numerous authors [1, 2, 3] at a time when the phase transition at small baryon-asymmetry was still believed to be first order. The established mechanism for magnetic field production was the collision of hadronic bubbles during the phase transition [2]. Different masses of quarks and nucleons would lead to a diffusion of baryon number via the bubble walls and consequentially a baryon contrast close to the phase boundary would develop [1, 2]. This baryon contrast can be estimated by the ratio of the net baryon numbers in the two phases to be

$$R = \frac{\bar{n}_q^B}{\bar{n}_H^B} \tag{4.51}$$

Because muons and strange quarks are already slightly suppressed at the critical temperature T_c the baryon contrast would also cause a charge dipole layer at the phase boundary to develop. The resulting net positive charge density is

$$\rho_C^+ = e\,(2/3n_u - 1/3n_d - 1/3n_s) = \beta e n_B \tag{4.52}$$

where the indices u, d and s refer to the different quark flavors and the factor of proportionality β depends on the temperature, chemical potential and the masses of the particles. For a small η_B and reasonable strange quark and muon masses $\beta \sim 10^{-2} - 10^{-3}$. After a strong supercooling muons and strange quarks will be suppressed resulting in $\beta \approx 0.2$ for the little inflation case. Cheng et al. estimated the magnetic field generated by the collision the hadron gas bubbles to be

$$B_{QCD} \approx \frac{8\pi\rho_C\, r_d\, v}{3} = \frac{8\pi e R\,\beta\,\bar{n}_B\, r_{diff}^2\, H_{QCD}}{3} \tag{4.53}$$

due to turbulent charged flow. Here the flow parallel to the bubble walls was assumed to have velocities $v \sim r_n H_{QCD}$ giving the main contribution to the field generation. The thickness of the baryon excess layer r_d was estimated according to

results of [4] to be $r_d \approx r_{diff}^2/r_n$ with r_{diff} being the baryon diffusion length and r_n the mean separation of nucleation sites. $R\beta$ should be at least 0.3 with the above estimates up to values of $\sim 10 - 100$ if baryon number can be effectively piled up by the expanding bubble walls. Thus we arrive at magnetic fields of strength $B_{QCD} = 10^8 - 10^{10}$G for low baryon asymmetry, i.e. for the standard scenario assuming a first order phase transition. If the baryon contrast exceeds $R \sim 10$ then any initial field may be readily amplified by magneto-hydrodynamic (MHD) turbulence to the equipartition value (see [3] and refs. therein)

$$B_{eq} = \sqrt{8\pi T^4 v_f^2} \tag{4.54}$$

where v_f is the fluid velocity. Now we shall modify these estimates for the little inflation scenario. First of all the initial value of the baryon number contrast R between the two phases can be much higher because quarks are much more favorable carriers of baryon number than nucleons at such low temperatures of $T \sim 170\text{MeV}/\theta \sim 0.2\text{MeV}$ at the end of inflation. The diffusion length will also be larger because both baryon and antibaryon densities $n_B, n_{\bar{B}}$ will be additionally diluted by a factor θ^3 resulting in

$$r_{diff} \propto 1/\sqrt{n_B + n_{\bar{B}}} \sim 4\mu\text{m}\ \theta^{3/2} \sim 10\text{ cm} \tag{4.55}$$

for a random walk approximation. Thus development of MHD turbulence should be expected resulting in equipartition of the magnetic field with a strength of $B_{eq} \approx 10^{12}$G. The fluid velocities were taken to be $v_f \sim 1$ because the released latent heat is much larger than the thermal energy.

Next one may ask if such a strong magnetic field does not violate bounds for the total the energy density foremost from big bang nucleosynthesis, which is the next important milestone in the evolution of the universe after the QCD phase transition. Caprini and Durrer found that magnetic fields produced by a causal production mechanism (in contrast to magnetic fields produced during primordial inflation) can be strongly limited via their integrated energy density and the shape of the spectrum [132, 133]. They argued that the spectrum of the generated magnetic field must fall off with a steep power law for uncorrelated superhorizon scales, i.e. $B_\lambda^2 \propto \lambda^{-n}$ with $n \geq 2$. As stated earlier the typical comoving length scale of galactic magnetic fields is 0.1 Mpc which is comparable to the shortest magnetic field mode that survives plasma damping processes up to recombination [134, 135]. This scale is clearly much larger than the comoving horizon size $H^{-1} \sim 10$ pc at the QCD phase transition. Therefore even a relatively small field strength at the 0.1 Mpc scale requires a magnetic field at the 10 pc

scale that is larger by many orders of magnitude easily resulting in a very large integrated magnetic field energy density. We use the bound on an additional radiation energy density at big bang nucleosynthesis found by ref. [136] allowing at most 1.6 additional effective neutrino families at the 98% confidence level. The integrated magnetic energy density is thus bounded from above by $B_{QCD} = 5{\cdot}10^{13}$G which limits the strength of the comoving seed field to $B^{seed}_{0.1Mpc} < 10^{-22}$G. Our previous estimate of the generated magnetic field consequently does not violate this bound, but the field strength is very low and may not suffice to seed large scale magnetic fields if not enhanced sufficiently. In [137] it was found that an inverse cascade mechanism could transfer some field strength from small to larger scales thus partially escaping the effects of plasma damping. The inverse cascade mechanism requires a non-vanishing helicity of the primordial magnetic field, as one can expect in the presented scenario due to the large baryon asymmetry, thus one may still to successfully seed large scale magnetic fields fields at the QCD phase transition.

4.7 Gravitational Waves

The final signal of the QCD phase transition that we would like to discuss are gravitational waves. The process of nucleation and subsequent bubble collisions will stir hydrodynamic turbulence producing gravitational waves in the process [1, 138, 139, 140, 141]. Again the Hubble parameter gives an important scale for the spectrum [1, 140]. Since the production mechanism is causal a peak frequency has to greater or equal to the Hubble frequency, $\nu_{peak} \geq \nu_H$. By how much this peak scale differs will depend on the details of the production mechanism and most importantly on the relevant time- and lengthscales that might be significantly different from the Hubble frequency. Let us assume an exponential nucleation rate $\Gamma \propto \exp(t/\tau)$ with τ being the characteristic timescale for the nucleation process. Then the peak frequency of the spectrum due to the collision of bubbles will be given by

$$\nu^B_{peak} \approx 4.0 \cdot 10^{-8}\text{Hz} \left(\frac{0.1H^{-1}}{\tau}\right) \left(\frac{T^*}{150\text{MeV}}\right) \left(\frac{g^{eff}}{50}\right)^{1/6} \tag{4.56}$$

where T^* is the reheating temperature and the result is already redshifted to the present day frequency. It is common to denote a gravitational wave spectrum in terms of a characteristic strain amplitude which is defined in the following way

$$h_c(\nu) = 0.9 \cdot 10^{-18} \left(\frac{1\text{Hz}}{\nu}\right) \left(\frac{h_0}{0.7}\right) [\Omega_{gw}(\nu)]^{1/2} \tag{4.57}$$

With the above estimates one arrives at a peak strain amplitude for the bubble collision peak of

$$h_c(\nu^B_{peak}) = 4.7 \cdot 10^{-15} \left(\frac{\tau}{0.1H^{-1}}\right)^2 \left(\frac{150\text{MeV}}{T^*}\right) \left(\frac{50}{g^{eff}}\right)^{1/3}. \tag{4.58}$$

Bubble collisions will also create hydrodynamic turbulence that will stir gravitational waves with a slightly lower peak frequency

$$\nu^T_{peak} \simeq 0.3\, \nu^B_{peak} \tag{4.59}$$

but with a higher peak amplitude

$$h_c(\nu^T_{peak}) \simeq 2.1 h_c(\nu^B_{peak}) \tag{4.60}$$

for a strongly first order phase transition [140]. For frequencies lower than the Hubble frequency the spectrum should be uncorrelated white noise. The approximate shape of the strain amplitude spectrum is then given by

$$h_c(\nu) \propto \nu^{1/2} \quad \text{for} \quad \nu < H \tag{4.61}$$

$$h_c(\nu) \propto \nu^{-m} \quad \text{for} \quad \nu > \nu^B_{peak} \tag{4.62}$$

where the spectral index m should be at most 2 if the number of bubble collisions is low but could be close to 1 or even lower if multi-bubble collisions play an important role [139, 141].

The Parks Pulsar Timing Array (PPTA) measures timing residuals in pulsar signals to put upper bounds on a stochastic gravitational wave background in a relatively narrow frequency band around 10^-8 Hz [142, 143]. The PPTA results already allow to limit the nucleation timescale with the presently available data to $\tau/H^{-1} < 0.12$. This limit will improve to $\tau/H^{-1} < 0.06$ for the full data of the Parkes Pulsar Timing Array project [142]. This can be seen in figure 4.13 where the expected spectrum of gravitational waves for the former case is shown with three different high frequency slopes and the approximate sensitivity regions of existing and future detectors. The planned Square Kilometer Array (SKA) will improve

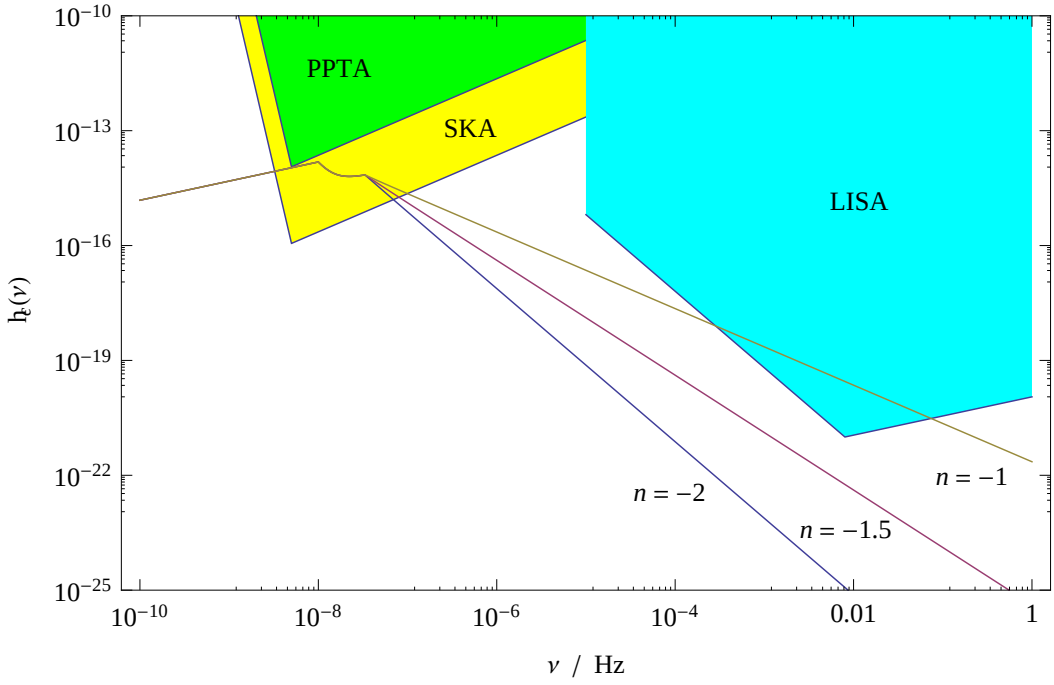

Figure 4.13: Largest strain amplitude spectrum still compatible with the data of the Parks Pulsar Timing Array. A shorter duration of the phase transition reduces the amplitude and shifts the peak to higher frequencies. Detection with LISA would only be possible if multi-bubble collisions play a significant role. For $\tau/H^{-1} < 0.005$ the signal would be unobservable with either SKA or LISA unless the high frequency spectral index is larger than -1.

the sensitivity in $\Omega_{gw}(\nu)$ by about four orders of magnitude [144]. Thus SKA will

lower the bound on τ/H^{-1} by about an order of magnitude as visible in figure 4.13. If multi-bubble collisions are important detection via the spaceborne Laser Interferometer Space Antenna (LISA) could also be possible if the high frequency spectral index $m \lesssim 1.4$ and $\tau/H^{-1} \gtrsim 10^{-2}$.

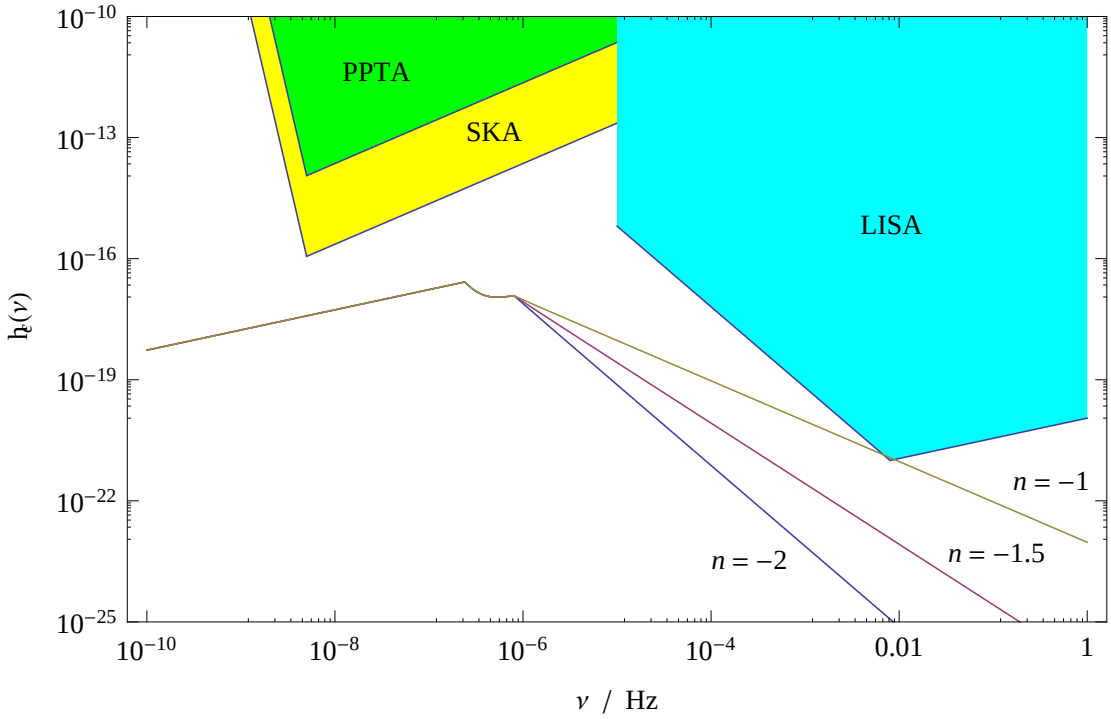

Figure 4.14: Same as figure 4.13 but for $\tau/H^{-1} = 0.005$ which is the limiting case for which not even a strong contribution from multi-bubble collisions (n=-1) would lead to an observable signal from the phase transition for any of the next generation gravitational wave detectors.

Furthermore it has been found that the QCD-phase transition will also leave a steplike imprint on the spectrum of primordial gravitational waves due to the strong reduction of the radiation degrees of freedom [145]. In [146] this result was confirmed also for several lattice equations of state. Furthermore the effect of a little inflationary phase on the primordial spectrum was examined and a strong power-law suppression for frequencies larger than the Hubble frequency at the QCD phase transition was found.

Chapter 5

Conclusion and Outlook

In this thesis I have explored the idea of a short inflationary period at the QCD phase transition in the early universe. The requirements both from particle physics and from cosmology have been discussed, most notably a strong mechanism of baryogenesis and the possibility of a delayed phase transition within effective models of QCD. Interesting cosmological implications were found such as the suppression of primordial density fluctuations up to dark matter mass scales of $M_{max} \sim 10^6 M_\odot$ relative to the large scale spectrum due to the change of the global equation of state. This could have interesting consequences for the physics of globular clusters and the emergence of the first stars and could also have an impact on the cuspy core density distribution of dark matter in small galaxies and the too large number of halo structures seen in standard structure formation. We also discussed the production of primordial magnetic fields that may be strong enough to seed the presently observed galactic and extragalactic magnetic fields. Furthermore we addressed the production of a spectrum of gravitational waves around a peak frequency of $4 \cdot 10^{-8}$ Hz that may be observable via pulsar timing in the future. Dark matter properties are also strongly affected as the annihilation cross section for cold dark matter has to be up to nine orders of magnitude lower to give the right amount of dark matter today, which can be probed for example at the LHC by detecting the neutralino with an unexpected low annihilation cross section. We have seen that the baryon density could actually be so large that one may even expect color superconducting phases to be present before the onset of the little inflation and this might pose an alternative route of investigation for the scenario. The conditions in such a cosmological phase transition would then be closer to the situation in heavy ion collisions or even the centre of neutron stars than to the standard QCD phase transition in the hot big bang scenario. Hence, the upcoming FAIR facility would actually for the little inflation scenario be a probe for the physics of the early universe.
The "little inflation" scenario still has many aspects that require further investigation. First of all some of the prerequisite have only been examined on a basic level and should be investigated further, these are

- The limit on the effectiveness of Affleck-Dine baryogenesis was taken from [101] to be $\eta_B = 1$. To my knowledge it not been examined any further later on and it would be important to investigate if this bound can be made more solid within the general Affleck-Dine mechanism or at least within realistic supersymmetric models.

- The initial failure to nucleate is a vital requirement of the mechanism and

is tightly linked to the value and the evolution of the surface tension during the onset of inflation. Nucleation has only be addressed here within the Bag model and should be studied also within more sophisticated effective models of QCD.

- We have seen that within the current approximations the universe could have entered the inflationary period from a color superconducting phase of QCD. This would allow a very different approach to the dynamics of the phase transition and might also alter some of the signals.

Understanding and quantifying these requirements would also allow to gain more insight into the expected signals. Several of the predictions of such a delayed cosmological QCD phase transition still have to be studied in more detail. Among them are

- Influences on low scale structure formation as indicated by the calculations on linear density perturbations done within this thesis. Especially the connection to the physics of globular clusters seems promising and should be addressed in more detail as well as implications for the first generation of stars.

- Changes of dark matter properties in the little inflation scenario should be studied in the context of different dark matter candidates. We have seen that the WIMP miracle does not lead to a viable dark matter candidate anymore within this scenario but there could be other parameter windows for the interaction cross section and particle mass opening up again. As stated before the discovery of a standard WIMP at the LHC would either completely rule out a little inflation or at least limit its duration severely. Thus this aspect is also very interesting from the point of view of testing the scenario.

- The predictions for the generated gravitational wave signals are yet based on the extrapolation of results from calculations for phase transitions without a previous inflationary period as done for example by Kosowski et al. [138]. The relevant peak frequency and amplitude of the gravitational wave spectrum then mostly depends on the duration of the phase transition and this might not be so simple in a more detailed calculation that also includes the inflationary phase and the reheating process.

- Although the supercooling in the little inflation scenario is much weaker than in the "long" primordial inflation the process of reheating is also relevant and

has not yet been addressed at all. This could alter several of the scenarios signals, i.e. the produced magnetic fields and gravitational waves could be modified and new scalar fluctuations below a dark matter mass scale of $\sim 1M_{\odot}$ could be generated. The latter point is mostly relevant if it would also result in substantial inhomogeneities in the spacial distribution of baryons because of their negative influence on BBN [147, 148].

Let me close this outlook by concluding that both the requirements and the signals of the little inflation scenario require further investigation and offer interesting connections to upcoming particle physics experiments like the LHC and FAIR and gravitational wave detectors like LISA and SKA.

Chapter 6

Appendix

6.1 Dilaton Quark Meson Model - Details

6.1.1 Speed of Sound

Now we have a more detailed look at the calculation of the speed of sound, especially for the dilaton-quark-meson-model. As a reminder, the speed of sound is calculated via

$$\left.\frac{\partial p}{\partial \epsilon}\right|_s = \frac{\left.\frac{\partial p}{\partial T}\right|_\mu \left.\frac{\partial s}{\partial \mu}\right|_T - \left.\frac{\partial p}{\partial \mu}\right|_T \left.\frac{\partial s}{\partial T}\right|_\mu}{\left.\frac{\partial \epsilon}{\partial T}\right|_\mu \left.\frac{\partial s}{\partial \mu}\right|_T - \left.\frac{\partial \epsilon}{\partial \mu}\right|_T \left.\frac{\partial s}{\partial T}\right|_\mu} = \frac{s \left.\frac{\partial s}{\partial \mu}\right|_T - n_B \left.\frac{\partial s}{\partial T}\right|_\mu}{\left.\frac{\partial \epsilon}{\partial T}\right|_\mu \left.\frac{\partial s}{\partial \mu}\right|_T - \left.\frac{\partial \epsilon}{\partial \mu}\right|_T \left.\frac{\partial s}{\partial T}\right|_\mu} \tag{6.1}$$

For this we first need the partial derivatives of ϵ and n_B with respect to temperature and chemical potential.

$$\left.\frac{\partial \epsilon}{\partial T}\right|_\mu = \frac{\nu_q}{2\pi^2 T^2}\int_0^\infty dp p^2 E_q \left[\frac{(E_q-\mu)e^{\beta(E_q-\mu)}}{(e^{\beta(E_q-\mu)}+1)^2} + \frac{(E_q+\mu)e^{\beta(E_q+\mu)}}{(e^{\beta(E_q+\mu)}+1)^2}\right] \tag{6.2}$$

$$\left.\frac{\partial \epsilon}{\partial \mu}\right|_T = \frac{\nu_q}{2\pi^2 T}\int_0^\infty dp p^2 E_q \left[\frac{e^{\beta(E_q-\mu)}}{(e^{\beta(E_q-\mu)}+1)^2} - \frac{e^{\beta(E_q+\mu)}}{(e^{\beta(E_q+\mu)}+1)^2}\right] \tag{6.3}$$

$$\left.\frac{\partial n_B}{\partial T}\right|_\mu = \frac{\nu_q}{2\pi^2 T^2}\int_0^\infty dp p^2 \left[\frac{(E_q-\mu)e^{\beta(E_q-\mu)}}{(e^{\beta(E_q-\mu)}+1)^2} - \frac{(E_q+\mu)e^{\beta(E_q+\mu)}}{(e^{\beta(E_q+\mu)}+1)^2}\right] \tag{6.4}$$

$$\left.\frac{\partial n_B}{\partial \mu}\right|_T = \frac{\nu_q}{2\pi^2 T}\int_0^\infty dp p^2 \left[\frac{e^{\beta(E_q-\mu)}}{(e^{\beta(E_q-\mu)}+1)^2} + \frac{e^{\beta(E_q+\mu)}}{(e^{\beta(E_q+\mu)}+1)^2}\right] \tag{6.5}$$

Now these can be used to calculate the derivatives of the entropy density

$$\left.\frac{\partial s}{\partial T}\right|_\mu = \frac{\frac{\partial \epsilon}{\partial T} + \frac{\partial p}{\partial T} - \mu\frac{\partial n_B}{\partial T}}{T} - \frac{\epsilon + p - \mu n_B}{T^2} = \frac{\frac{\partial \epsilon}{\partial T} - \mu\frac{\partial n_B}{\partial T}}{T} \tag{6.6}$$

$$= \frac{\nu_q}{2\pi^2 T^3}\int_0^\infty dp p^2 \left[\frac{(E_q-\mu)^2 e^{\beta(E_q-\mu)}}{(e^{\beta(E_q-\mu)}+1)^2} + \frac{(E_q+\mu)^2 e^{\beta(E_q+\mu)}}{(e^{\beta(E_q+\mu)}+1)^2}\right] \tag{6.7}$$

$$\left.\frac{\partial s}{\partial \mu}\right|_T = \frac{\frac{\partial \epsilon}{\partial \mu} + \frac{\partial p}{\partial \mu} - n_B - \mu\frac{\partial n_B}{\partial \mu}}{T} = \frac{\frac{\partial \epsilon}{\partial \mu} - \mu\frac{\partial n_B}{\partial \mu}}{T} \tag{6.8}$$

$$= \frac{\nu_q}{2\pi^2 T^2}\int_0^\infty dp p^2 \left[\frac{(E_q-\mu)e^{\beta(E_q-\mu)}}{(e^{\beta(E_q-\mu)}+1)^2} - \frac{(E_q+\mu)e^{\beta(E_q+\mu)}}{(e^{\beta(E_q+\mu)}+1)^2}\right] \tag{6.9}$$

Here one can make an interesting observation, namely that the isentropic speed of sound seems to be undefined at $\mu = 0$ since both numerator and denominator vanish in this limit. We will now show for the case of a massless fermi gas that this c_s^2 is actually well defined if one properly calculates $\lim_{\mu\to 0} c_s^2$.

The energy density, pressure, net number density and entropy density of a massless, free fermi gas at non-zero chemical potential reads (calculation can be found in [69])

$$\epsilon = \frac{7g\pi^2}{120}T^4 + \frac{g}{4}T^2\mu^2 + \frac{g}{8\pi^2}\mu^4 \tag{6.10}$$

$$p = \frac{\epsilon}{3} = \frac{7g\pi^2}{360}T^4 + \frac{g}{12}T^2\mu^2 + \frac{g}{24\pi^2}\mu^4 \tag{6.11}$$

$$n_B = \frac{\partial p}{\partial \mu} = \frac{g}{6}T^2\mu + \frac{g}{6\pi^2}\mu^3 \tag{6.12}$$

$$s = \frac{\epsilon + p - \mu n_B}{T} = \frac{7g\pi^2}{90}T^3 + \frac{g}{6}T\mu^2 \tag{6.13}$$

Furthermore we need the corresponding derivatives

$$\left.\frac{\partial \epsilon}{\partial T}\right|_\mu = \frac{7g\pi^2}{30}T^3 + \frac{g}{2}T\mu^2 \tag{6.14}$$

$$\left.\frac{\partial \epsilon}{\partial \mu}\right|_T = \frac{g}{2}T^2\mu + \frac{g}{2\pi^2}\mu^3 \tag{6.15}$$

$$\left.\frac{\partial s}{\partial T}\right|_\mu = \frac{7g\pi^2}{30}T^2 + \frac{g}{6}\mu^2 \tag{6.16}$$

$$\left.\frac{\partial s}{\partial \mu}\right|_T = \frac{g}{3}T\mu \tag{6.17}$$

Applying equation (6.1) we arrive at

$$\left.\frac{\partial p}{\partial \epsilon}\right|_s = \frac{\frac{-7g\pi^2}{180}T^4\mu - \frac{g}{30}T^2\mu^3 - \frac{g}{12\pi^2}\mu^5}{\frac{-7g\pi^2}{540}T^4\mu - \frac{g}{90}T^2\mu^3 - \frac{g}{36\pi^2}\mu^5} \tag{6.18}$$

Which obviously results in $\left.\frac{\partial p}{\partial \epsilon}\right|_s = \frac{1}{3}$ for $\mu \neq 0$. For $\lim_{\mu\to 0} c_s^2$ one has to apply l'Hôpital's rule, i.e. calculate the partial derivatives of numerator and denominator with respect to μ separately. If the ratio of these derivatives is well defined then it is the right limiting value, if not one has to do further partial derivatives until one ratio is well defined. In the given case already the first partial derivative yields a well defined ratio because of the first terms in numerator and denominator. The result is as it should be

$$\lim_{\mu\to 0}\left.\frac{\partial p}{\partial \epsilon}\right|_s = \lim_{\mu\to 0}\frac{\frac{-7g\pi^2}{180}T^4 - \frac{g}{10}T^2\mu^2 - \frac{5g}{12\pi^2}\mu^4}{\frac{-7g\pi^2}{540}T^4 - \frac{g}{30}T^2\mu^2 - \frac{5g}{36\pi^2}\mu^4} = \frac{1}{3} \tag{6.19}$$

6.1.2 Diagonalizing the Mass Matrix

Now we want to fill in the remaining gaps from section 2.10.3. The mass matrix had the form

$$M_{ij} = \left(\begin{array}{ccc} \frac{\partial^2 U}{\partial \pi^2} & 0 & 0 \\ 0 & \frac{\partial^2 U}{\partial \sigma^2} & \frac{\partial^2 U}{\partial \sigma \partial \chi} \\ 0 & \frac{\partial^2 U}{\partial \chi \partial \sigma} & \frac{\partial^2 U}{\partial \chi^2} \end{array} \right) \Bigg|_{vac} \tag{6.20}$$

for which we first need the corresponding derivatives. These read

$$\begin{aligned}
\frac{\partial U}{\partial \pi} &= \lambda \pi \left(\sigma^2 + \pi^2 \right) - k_0 \left(\frac{\chi}{\chi_0} \right)^2 \pi & (6.21)\\
\frac{\partial U}{\partial \sigma} &= \lambda \sigma \left(\sigma^2 + \pi^2 \right) - k_0 \left(\frac{\chi}{\chi_0} \right)^2 \sigma - f_\pi m_\pi^2 \left(\frac{\chi}{\chi_0} \right)^2 & (6.22)\\
\frac{\partial U}{\partial \chi} &= -k_0 \frac{\chi}{\chi_0^2} \left(\sigma^2 + \pi^2 \right) - 2 f_\pi m_\pi^2 \frac{\chi}{\chi_0^2} \sigma + 4 k_1 \frac{\chi^3}{\chi_0^4} + \chi^3 \left(1 + \ln \left(\frac{\chi^4}{\chi_0^4} \right) \right) & (6.23)\\
\frac{\partial^2 U}{\partial \pi^2} &= \lambda \left(\sigma^2 + 3\pi^2 \right) - k_0 \left(\frac{\chi}{\chi_0} \right)^2 & (6.24)\\
\frac{\partial^2 U}{\partial \sigma^2} &= \lambda \left(3\sigma^2 + \pi^2 \right) - k_0 \left(\frac{\chi}{\chi_0} \right)^2 & (6.25)\\
\frac{\partial^2 U}{\partial \chi^2} &= -\frac{k_0}{\chi_0^2} \left(\sigma^2 + \pi^2 \right) - \frac{2 f_\pi m_\pi^2}{\chi_0^2} + 12 k_1 \frac{\chi^2}{\chi_0^4} + \chi^2 \left(7 + 3 \ln \left(\frac{\chi^4}{\chi_0^4} \right) \right) & (6.26)
\end{aligned}$$

Thus we only need to find the solutions to the following eigenvalue problem

$$\left(\begin{array}{cc} \frac{\partial^2 U}{\partial \sigma^2} - m_\pm^2 & \frac{\partial^2 U}{\partial \sigma \partial \chi} \\ \frac{\partial^2 U}{\partial \chi \partial \sigma} & \frac{\partial^2 U}{\partial \chi^2} - m_\pm^2 \end{array} \right) \Bigg|_{vac} \left(\begin{array}{c} v_{\pm 1} \\ v_{\pm 2} \end{array} \right) = 0 \tag{6.27}$$

which can after some simple algebra found to be

$$m_\pm^2 = \frac{1}{2\chi_0} \left(G \pm \sqrt{G^2 - 4\chi_0^4 H} \right) \tag{6.28}$$

where G an H are given by

$$\begin{aligned}
G &= 2 f_\pi^2 m_\pi^2 + 2 f_\pi^4 \lambda + m_\pi^2 \chi_0^2 + 2 f_\pi^2 \lambda \chi_0^2 + 4 \chi_0^4 \\
H &= 2 f_\pi^2 m_\pi^4 + 6 f_\pi^4 m_\pi^2 \lambda + 4 m_\pi^2 \chi_0^4 + 8 f_\pi^2 \lambda \chi_0^4 & (6.29)
\end{aligned}$$

6.2 Structure Formation

6.2.1 Additional Results

In figure 6.1 the behavior of δ_{DM} is shown for several wavelengths corresponding to enclosed dark matter masses of $10^{-2}, 1, 10^2, 10^4$ and $10^6 M_\odot$. As one can see below $10^6 M_\odot$ the modes are frozen longer and longer and are thus stronger suppressed as compared to larger wavelengths.

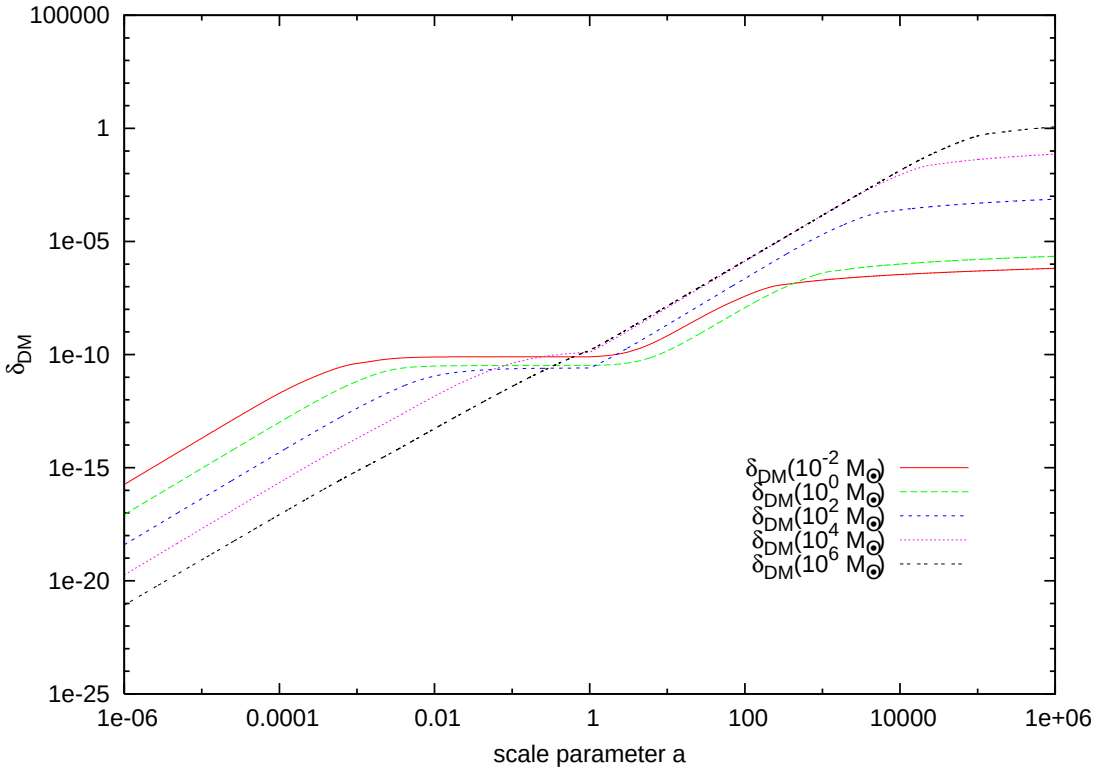

Figure 6.1: Evolution of δ_{DM} through the little inflationary phase for different wavelengths.

In figure 6.2 the behavior of $\hat{\psi}_R$ and $\hat{\psi}_{DM}$ during the little inflationary phase for an enclosed dark matter mass of $10^2 M_\odot$ is shown which corresponds to the intermediate regime in the spectrum. Before the onset of inflation both functions grow $\propto a^3$, then both approach a constant value $\propto 1/a$. $\hat{\psi}_R$ and converges towards a negative value in contrast to $\hat{\psi}_{DM}$. This also explains the apparent deviation from the expected $\propto 1/a$ behavior when shown in a log-log-plot as seen in figure 4.10 in section 4.4.2. After the end of inflation both functions again quickly converge towards the growing solutions proportional to a^3.

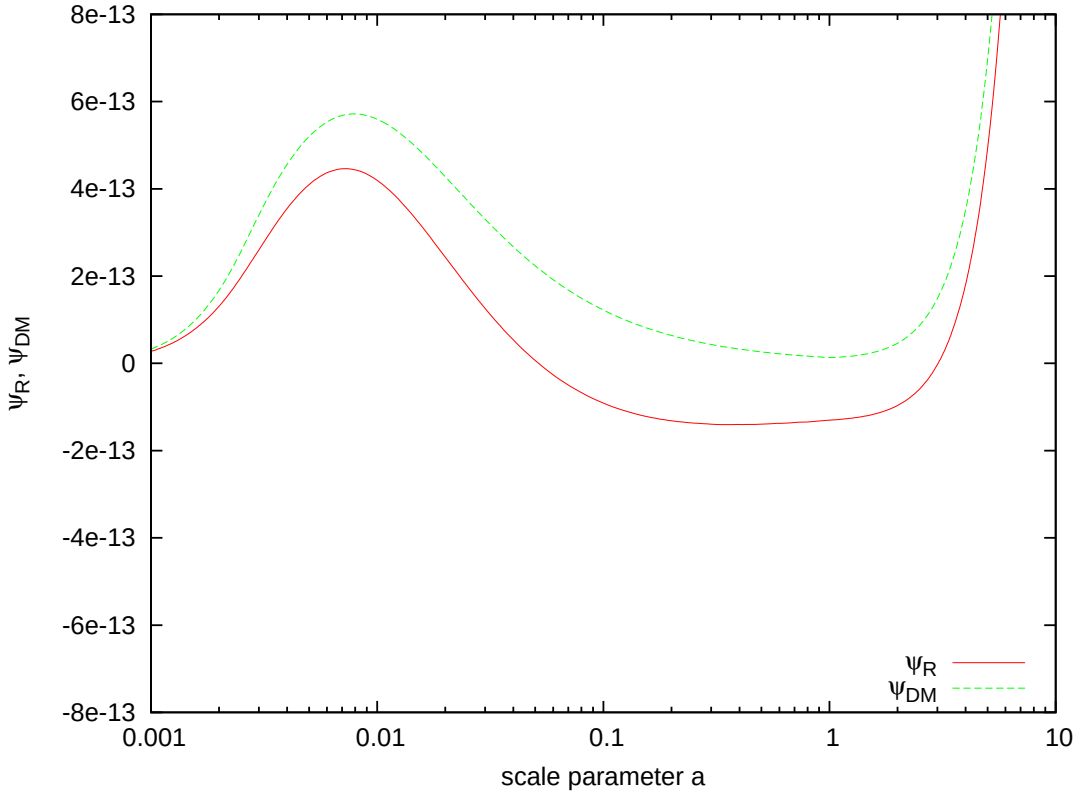

Figure 6.2: Evolution of $\hat{\psi}_R$ and $\hat{\psi}_{DM}$ through the little inflationary phase for an enclosed dark matter mass of $10^2 M_\odot$.

Bibliography

[1] E. Witten. Cosmic separation of phases. *Phys. Rev. D*, 30:272–285, July 1984.

[2] B. Cheng and A. V. Olinto. Primordial magnetic fields generated in the quark-hadron transition. *Phys. Rev. D*, 50:2421–2424, August 1994.

[3] G. Sigl, A. V. Olinto, and K. Jedamzik. Primordial magnetic fields from cosmological first order phase transitions. *Phys. Rev. D*, 55:4582–4590, April 1997.

[4] H. Kurki-Suonio. Baryon-number inhomogeneity generation in the cosmic quark-hadron phase transition. *Phys. Rev. D*, 37:2104–2110, April 1988.

[5] B. Kaempfer. Entropy production during an isothermal phase transition in the early universe. *Astronomische Nachrichten*, 307:231–234, 1986.

[6] C. Schmid, D. J. Schwarz, and P. Widerin. Amplification of cosmological inhomogeneities by the QCD transition. *Phys. Rev. D*, 59(4):043517–+, February 1999.

[7] Y. Aoki, Z. Fodor, S. D. Katz, and K. K. Szabó. The QCD transition temperature: Results with physical masses in the continuum limit. *Phys. Lett. B*, 643:46–54, November 2006.

[8] F. Karsch and the RBC-Bielefeld Collaboration. Transition temperature in QCD with physical light and strange quark masses. *J. Phys. G*, 34:627–+, August 2007.

[9] M. J. Fromerth and J. Rafelski. Hadronization of the Quark Universe. *ArXiv Astrophysics e-prints*, November 2002.

[10] T. Boeckel and J. Schaffner-Bielich. A Little Inflation in the Early Universe at the QCD Phase Transition. *Phys. Rev. Lett.*, 105(4):041301–+, July 2010.

[11] S. Schettler, T. Boeckel, and J. Schaffner-Bielich. The Cosmological QCD Phase Transition Revisited. *ArXiv e-prints*, December 2010.

[12] T. Boeckel and J. Schaffner-Bielich. *in preparation*, 2011.

[13] M. Gell-Mann. A schematic model of baryons and mesons. *Physics Letters*, 8(3):214 – 215, 1964.

[14] G Zweig. An su_3 model for strong interaction symmetry and its breaking; part i. *CERN theory reports*, CERN-TH-401:24 p, Jan 1964.

[15] G Zweig. An su_3 model for strong interaction symmetry and its breaking; part ii. *CERN theory reports*, CERN-TH-412:80 p, Feb 1964.

[16] M. Alford, D. Blaschke, A. Drago, T. Klähn, G. Pagliara, and J. Schaffner-Bielich. Astrophysics: Quark matter in compact stars? *Nature*, 445, January 2007.

[17] D. Boyanovsky, H. J. de Vega, and D. J. Schwarz. Phase Transitions in the Early and Present Universe. *Annual Review of Nuclear and Particle Science*, 56:441–500, November 2006.

[18] S. Bethke. Experimental tests of asymptotic freedom. *Progress in Particle and Nuclear Physics*, 58:351–386, April 2007.

[19] G. M. Prosperi, M. Raciti, and C. Simolo. On the running coupling constant in QCD. *Progress in Particle and Nuclear Physics*, 58:387–438, April 2007.

[20] Z. Fodor and S. D. Katz. Critical point of QCD at finite T and mu, lattice results for physical quark masses. *Journal of High Energy Physics*, 4:50–+, April 2004.

[21] C. R. Allton et al. QCD thermal phase transition in the presence of a small chemical potential. *Phys. Rev. D*, 66(7):074507–+, October 2002.

[22] R. D. Pisarski and F. Wilczek. Remarks on the chiral phase transition in chromodynamics. *Phys. Rev. D*, 29:338–341, January 1984.

[23] Walter Greiner and Berndt Mueller. *Quantum mechanics: symmetries. Original title 'Theoretische physik, Band 5:Quantenmechanik II, Symmetrien 3. Aufl.'; 2nd ed.* Springer, Berlin, 2nd edition, 1994.

[24] U. Mosel. *Fields, Symmetries and Quarks*. Springer, 2nd edition, 1999.

[25] Wolfgang Nolting. *Grundkurs Theoretische Physik*. Springer, Berlin, 7 edition, 2006.

[26] Walter Greiner and Berndt Mueller. *Quantum mechanics: symmetries. Original title 'Theoretische physik, Band 5:Quantenmechanik II, Symmetrien 3. Aufl.* Springer, Berlin, 2 edition, 1994. Includes examples.

[27] V. Koch. Aspects of Chiral Symmetry. *International Journal of Modern Physics E*, 6:203–249, 1997.

[28] W. Bentz, A. Arima, and H. Baier. Chiral symmetry and the axial current in nuclear matter. *Annals of Physics*, 200:127–189, May 1990.

[29] S. A. Coon. Chiral Symmetry and Low Energy Pion-Nucleon Scattering. *Czechoslovak Journal of Physics*, 49:1235–1271, September 1999.

[30] M. Gell-Mann and M. Levy. The axial vector current in beta decay. *Nuovo Cimento*, 415(4):486–+, 1960.

[31] P. Papazoglou, S. Schramm, J. Schaffner-Bielich, H. Stöcker, and W. Greiner. Chiral Lagrangian for strange hadronic matter. *Phys. Rev. C*, 57:2576–2588, May 1998.

[32] O. Scavenius, Á. Mócsy, I. N. Mishustin, and D. H. Rischke. Chiral phase transition within effective models with constituent quarks. *Phys. Rev. C*, 64(4):045202–+, October 2001.

[33] Á. Mócsy, I. N. Mishustin, and P. J. Ellis. Role of fluctuations in the linear σ model with quarks. *Phys.Rev.C*, 70(1):015204–+, July 2004.

[34] E. S. Bowman and J. I. Kapusta. Critical points in the linear σ model with quarks. *Phys. Rev. C*, 79(1):015202–+, January 2009.

[35] Jeremy Bernstein. Spontaneous symmetry breaking, gauge theories, the higgs mechanism and all that. *Rev. Mod. Phys.*, 46(1):7, Jan 1974.

[36] A. Chodos, R. L. Jaffe, K. Johnson, C. B. Thorn, and V. F. Weisskopf. New extended model of hadrons. *Phys. Rev. D*, 9:3471–3495, June 1974.

[37] T. Degrand, R. L. Jaffe, K. Johnson, and J. Kiskis. Masses and other parameters of the light hadrons. *Phys. Rev. D*, 12:2060–2076, October 1975.

[38] C. Itzykson and J.-B. Zuber. *Quantum Field Theory*. Dover, 1st (reprint) edition, 2005.

[39] Panajotis Papazoglou. *Chirale Beschreibung Seltsamer Hadronischer Materie in einem verallgemeinerten $SU_L(3) \times SU_R(3)-\sigma-$Modell, diploma thesis.* University of Frankfurt am Main, 1995.

[40] Lewis H Ryder. *Quantum field theory; 2nd ed.* Cambridge Univ. Press, Cambridge, 1996.

[41] M. A. Shifman. Anomalies in gauge theories. *Physics Reports*, 209(6):341 – 378, 1991.

[42] J. C. Collins, A. Duncan, and S. D. Joglekar. Trace and dilatation anomalies in gauge theories. *Phys. Rev. D*, 16:438–449, July 1977.

[43] I. Mishustin, J. Bondorf, and M. Rho. Chiral symmetry, scale invariance and properties of nuclear matter. *Nuclear Physics A*, 555(1):215 – 224, 1993.

[44] E. K. Heide, S. Rudaz, and P. J. Ellis. An effective lagrangian with broken scale and chiral symmetry applied to nuclear matter and finite nuclei. *Nuclear Physics A*, 571:713–732, May 1994.

[45] P. Papazoglou, J. Schaffner, S. Schramm, D. Zschiesche, H. Stöcker, and W. Greiner. Phase transition in the chiral σ-ω model with dilatons. *Phys. Rev. C*, 55:1499–1508, March 1997.

[46] L. Bonanno and A. Drago. Chiral Lagrangian with broken scale: Testing the restoration of symmetries in astrophysics and in the laboratory. *Phys. Rev. C*, 79(4):045801–+, April 2009.

[47] B. A. Campbell, J. Ellis, and K. A. Olive. Effective lagrangian approach to QCD phase transitions. *Phys. Lett. B*, 235:325–330, February 1990.

[48] A. I. Vaĭnshteĭn, V. I. Zakharov, and M. A. Shifman. Gluon condensate and leptonic decays of vector mesons. *Soviet Journal of Experimental and Theoretical Physics Letters*, 27:55–+, January 1978.

[49] M. G. Alford, A. Schmitt, K. Rajagopal, and T. Schäfer. Color superconductivity in dense quark matter. *Rev. Mod. Phys.*, 80:1455–1515, October 2008.

[50] E. Hubble. A Relation between Distance and Radial Velocity among Extra-Galactic Nebulae. *Proceedings of the National Academy of Science*, 15:168–173, March 1929.

[51] F. Zwicky. Die Rotverschiebung von extragalaktischen Nebeln. *Helvetica Physica Acta*, 6:110–127, 1933.

[52] F. Zwicky. On the Masses of Nebulae and of Clusters of Nebulae. *Astrophys. J.*, 86:217–+, October 1937.

[53] J. H. Oort. The force exerted by the stellar system in the direction perpendicular to the galactic plane and some related problems. *Bulletin of the Astronomical Institutes of the Netherlands*, 6:249–+, August 1932.

[54] Louise Volders. Neutral hydrogen in M 33 and M 101. *Bulletin of the Astronomical Institutes of the Netherlands*, 14:323–334, 1959.

[55] R. Alpher, H. Bethe, and G Gamov. The Origin of Chemical Elements. *Physical Review*, 73:803, 1948.

[56] E. M. Burbidge, G. R. Burbidge, W. A. Fowler, and F. Hoyle. Synthesis of the Elements in Stars. *Reviews of Modern Physics*, 29:547–650, 1957.

[57] Gary Steigman. Primordial nucleosynthesis: Successes and challenges. *Int. J. Mod. Phys.*, E15:1–36, 2006.

[58] V. C. Rubin and W. K. J. Ford. Rotation of the Andromeda Nebula from a Spectroscopic Survey of Emission Regions. *Astrophys. J.*, 159:379–+, February 1970.

[59] V. C. Rubin, N. Thonnard, and W. K. Ford, Jr. Rotational properties of 21 SC galaxies with a large range of luminosities and radii, from NGC 4605 /R = 4kpc/ to UGC 2885 /R = 122 kpc/. *Astrophys. J.*, 238:471–487, June 1980.

[60] http://www.astro.ucla.edu/ wright/intro.html.

[61] J. C. Mather, E. S. Cheng, R. E. Eplee, Jr., R. B. Isaacman, S. S. Meyer, R. A. Shafer, R. Weiss, E. L. Wright, C. L. Bennett, N. W. Boggess, E. Dwek, S. Gulkis, M. G. Hauser, M. Janssen, T. Kelsall, P. M. Lubin, S. H. Moseley, Jr., T. L. Murdock, R. F. Silverberg, G. F. Smoot, and D. T. Wilkinson. A preliminary measurement of the cosmic microwave background spectrum by the Cosmic Background Explorer (COBE) satellite. *Astrophys. J. Lett.*, 354:L37–L40, May 1990.

[62] http://lambda.gsfc.nasa.gov/product/cobe/.

[63] http://wmap.gsfc.nasa.gov/news/.

[64] R. Stiele, T. Boeckel, and J. Schaffner-Bielich. Cosmological implications of a dark matter self-interaction energy density. *Phys.Rev.D*, 81(12):123513–+, June 2010.

[65] Gregory D. Mack, John F. Beacom, and Bertone Gianfranco. Towards closing the window on strongly interacting dark matter: Far-reaching constraints from earth's heat flow. *Phys. Rev. D*, 76:043523, 2007.

[66] Lars Bergstrom and A Goobar. *Cosmology and particle astrophysics; 2nd ed.* Springer, Berlin, 2003.

[67] V. Mukhanov. *Physical Foundations of Cosmology*. Cambridge University Press, Cambridge, 1 edition, 2005.

[68] Tillmann Boeckel. *Cosmology of fermionic dark matter*. University of Frankfurt am Main, 2007.

[69] T. Boeckel and J. Schaffner-Bielich. Cosmology of fermionic dark matter. *Phys. Rev. D*, 76(10):103509–+, November 2007.

[70] Andrew R Liddle and David H Lyth. *Cosmological Inflation and Large-Scale Structure*. Cambridge Univ. Press, Cambridge, 2000.

[71] E. Komatsu, K. M. Smith, J. Dunkley, C. L. Bennett, B. Gold, G. Hinshaw, N. Jarosik, D. Larson, M. R. Nolta, L. Page, D. N. Spergel, M. Halpern, R. S. Hill, A. Kogut, M. Limon, S. S. Meyer, N. Odegard, G. S. Tucker, J. L. Weiland, E. Wollack, and E. L. Wright. Seven-year Wilkinson Microwave Anisotropy Probe (WMAP) Observations: Cosmological Interpretation. *Astrophys.J.Supp.*, 192:18–+, February 2011.

[72] A. H. Guth. Inflationary universe: A possible solution to the horizon and flatness problems. *Phys. Rev. D*, 23:347–356, January 1981.

[73] A. D. Linde. A new inflationary universe scenario: A possible solution of the horizon, flatness, homogeneity, isotropy and primordial monopole problems. *Physics Letters B*, 108:389–393, February 1982.

[74] A. H. Guth. Eternal inflation and its implications. *Journal of Physics A Mathematical General*, 40:6811–6826, June 2007.

[75] A. R. Liddle. An Introduction to Cosmological Inflation. In A. Masiero, G. Senjanovic, & A. Smirnov, editor, *High Energy Physics and Cosmology, 1998 Summer School*, pages 260–+, 1999.

[76] D. H. Lyth and A. Riotto. Particle physics models of inflation and the cosmological density perturbation. *Physics Reports*, 314:1–146, June 1999.

[77] A. H. Guth and S.-Y. Pi. Fluctuations in the new inflationary universe. *Physical Review Letters*, 49:1110–1113, October 1982.

[78] A. A. Starobinsky. Dynamics of phase transition in the new inflationary universe scenario and generation of perturbations. *Physics Letters B*, 117:175–178, November 1982.

[79] S. W. Hawking. The development of irregularities in a single bubble inflationary universe. *Physics Letters B*, 115:295–297, September 1982.

[80] James M. Bardeen. Gauge-invariant cosmological perturbations. *Phys. Rev. D*, 22(8):1882–1905, Oct 1980.

[81] V. F. Mukhanov, H. A. Feldman, and R. H. Brandenberger. Theory of cosmological perturbations. *Physics Reports*, 215:203–333, June 1992.

[82] J.-C. Hwang. Evolution of Ideal-Fluid Cosmological Perturbations. *Astrophys. J.*, 415:486–+, October 1993.

[83] J. M. Stewart. Perturbations of Friedmann-Robertson-Walker cosmological models. *Classical and Quantum Gravity*, 7:1169–1180, July 1990.

[84] J. M. Bardeen. Cosmology and Particle Physics. In L.-Z. Fang & A. Zee, editor, *Cosmology and Particle Physics,Proceedings of the CCAST (World Laboratory) Symposium/Workshop held at Nanjing University, Nanjing China, June 30 - July 2, 1988*, November 1988.

[85] Andrew G. Cohen and David B. Kaplan. Spontaneous baryogenesis. *Nuclear Physics B*, 308(4):913 – 928, 1988.

[86] M. Trodden. Electroweak baryogenesis. *Reviews of Modern Physics*, 71:1463–1500, October 1999.

[87] A. D. Dolgov. Cosmological Matter-Antimatter Asymmetry and Antimatter in the Universe. *ArXiv High Energy Physics - Phenomenology e-prints*, November 2002.

[88] A.D. Sakharov. Cp symmetry violation, c-asymmetry and baryonic asymmetry of the universe. *Pisma Zh. Eksp. Teor. Fiz.*, 5:32, 1967.

[89] G. 't Hooft. Symmetry breaking through bell-jackiw anomalies. *Phys. Rev. Lett.*, 37(1):8, Jul 1976.

[90] M. Dine and A. Kusenko. Origin of the matter-antimatter asymmetry. *Reviews of Modern Physics*, 76:1–30, December 2003.

[91] Sidney Richard Coleman. *Aspects of symmetry: selected Erice lectures*. Cambridge Univ. Press, Cambridge, 1985.

[92] V. A. Kuzmin, V. A. Rubakov, and M. E. Shaposhnikov. On anomalous electroweak baryon-number non-conservation in the early universe. *Physics Letters B*, 155:36–42, May 1985.

[93] K. Kajantie, M. Laine, K. Rummukainen, and M. Shaposhnikov. Is There a Hot Electroweak Phase Transition at mH ¿ mW? *Physical Review Letters*, 77:2887–2890, September 1996.

[94] F. Karsch, T. Neuhaus, A. Patkós, and J. Rank. Critical Higgs Mass and Temperature Dependence of Gauge Boson Masses in the SU(2) Gauge-Higgs Model. *Nuclear Physics B Proceedings Supplements*, 53:623–625, February 1997.

[95] M. Gürtler, E.-M. Ilgenfritz, and A. Schiller. Where the electroweak phase transition ends. *Phys.Rev.D*, 56:3888–3895, October 1997.

[96] D. Bödeker, P. John, M. Laine, and M. G. Schmidt. The 2-loop MSSM finite temperature effective potential with stop condensation. *Nuclear Physics B*, 497:387–414, February 1997.

[97] M. Carena, M. Quirós, and C. E. M. Wagner. Electroweak baryogenesis and Higgs and stop searches at LEP and the Tevatron. *Nuclear Physics B*, 524:3–22, July 1998.

[98] M. Fukugita and T. Yanagida. Barygenesis without grand unification. *Physics Letters B*, 174:45–47, June 1986.

[99] W. Buchmüller, R. D. Peccei, and T. Yanagida. Leptogenesis as the Origin of Matter. *Annual Review of Nuclear and Particle Science*, 55:311–355, December 2005.

[100] I. Affleck and M. Dine. A new mechanism for baryogenesis. *Nucl. Phys. B*, 249:361–380, 1985.

[101] A. D. Linde. A new mechanism of baryogenesis and the inflationary Universe. *Phys. Lett. B*, 160:243–248, 1985.

[102] M. Dine, L. Randall, and S. Thomas. Baryogenesis from flat directions of the supersymmetric standard model. *Nucl. Phys. B*, 458:291–323, January 1996.

[103] S. Kasuya and M. Kawasaki. Towards the robustness of the Affleck-Dine baryogenesis. *Phys. Rev. D*, 74(6):063507–+, September 2006.

[104] J. Braun, L. M. Haas, F. Marhauser, and J. M. Pawlowski. Phase Structure of Two-Flavor QCD at Finite Chemical Potential. *Physical Review Letters*, 106(2):022002–+, January 2011.

[105] M. Stephanov, K. Rajagopal, and E. Shuryak. Signatures of the Tricritical Point in QCD. *Phys. Rev. Lett.*, 81:4816–4819, November 1998.

[106] S. Rößner, C. Ratti, and W. Weise. Polyakov loop, diquarks, and the two-flavor phase diagram. *Phys. Rev. D*, 75(3):034007–+, February 2007.

[107] V. G. Boiko, L. L. Enkovskii, B. Kaempfer, and V. M. Sysoev. Mini-inflation prior to the cosmic confinement transition? *Astronomische Nachrichten*, 311:265–269, August 1990.

[108] L. L. Jenkovszky, V. M. Sysoev, and B. Kämpfer. On the expansion of the universe during the confinement transition. *Zeitschrift fur Physik C Particles and Fields*, 48:147–150, September 1990.

[109] B. Kämpfer. Cosmic phase transitions. *Annalen der Physik*, 9:605–635, September 2000.

[110] N. Borghini, W. N. Cottingham, and R. V. Mau. Possible cosmological implications of the quark-hadron phase transition. *J. Phys. G*, 26:771–785, June 2000.

[111] V. Simha and G. Steigman. Constraining the early-Universe baryon density and expansion rate. *JCAP*, 6:16–+, June 2008.

[112] J. S. Langer. Statistical theory of the decay of metastable states. *Ann. Phys.*, 54:258–275, 1969.

[113] L. P. Csernai and J. I. Kapusta. Nucleation of relativistic first-order phase transitions. *Phys. Rev. D*, 46:1379–1390, August 1992.

[114] L. P. Csernai and J. I. Kapusta. Dynamics of the QCD phase transition. *Phys. Rev. Lett.*, 69:737–740, August 1992.

[115] K. Kajantie, L. Kärkkäinen, and K. Rummukainen. Interface tension in QCD matter. *Nuclear Physics B*, 333:100–119, March 1990.

[116] D. N. Voskresensky, M. Yasuhira, and T. Tatsumi. Charge screening at first order phase transitions and hadron quark mixed phase. *Nucl. Phys.*, A723:291–339, 2003.

[117] M. Alford, K. Rajagopal, S. Reddy, and F. Wilczek. Minimal color-flavor-locked-nuclear interface. *Phys. Rev. D*, 64(7):074017–+, October 2001.

[118] O. Scavenius and A. Dumitru. A first-order chiral phase transition may naturally lead to the 'quench' initial condition and strong soft-pion fields. *Phys. Rev. Lett.*, 83:4697–4700, 1999.

[119] C. Schmid, D. J. Schwarz, and P. Widerin. Peaks above the Harrison-Zel'dovich Spectrum due to the Quark-Gluon to Hadron Transition. *Phys. Rev. Lett.*, 78:791–794, February 1997.

[120] W. E. Harris. Globular cluster systems in galaxies beyond the Local Group. *Ann. rev. of astron. and astrophys.*, 29:543–579, 1991.

[121] J. L. Prieto and O. Y. Gnedin. Dynamical Evolution of Globular Clusters in Hierarchical Cosmology. *Astrophys. J.*, 689:919–935, December 2008.

[122] S. M. Fall and Q. Zhang. Dynamical Evolution of the Mass Function of Globular Star Clusters. *Astrophys. J.*, 561:751–765, November 2001.

[123] E. Vesperini, S. E. Zepf, A. Kundu, and K. M. Ashman. Modeling the Dynamical Evolution of the M87 Globular Cluster System. *Astrophys. J.*, 593:760–771, August 2003.

[124] A. Klypin, A. V. Kravtsov, O. Valenzuela, and F. Prada. Where Are the Missing Galactic Satellites? *Astrophys. J.*, 522:82–92, September 1999.

[125] G. Gentile, P. Salucci, U. Klein, D. Vergani, and P. Kalberla. The cored distribution of dark matter in spiral galaxies. *MNRAS*, 351:903–922, July 2004.

[126] B. Moore, S. Ghigna, F. Governato, G. Lake, T. Quinn, J. Stadel, and P. Tozzi. Dark Matter Substructure within Galactic Halos. *Astrophys. J. Lett.*, 524:L19–L22, October 1999.

[127] P. Salucci. The mass distribution in Spiral galaxies. In J. Davies & M. Disney, editor, *IAU Symposium*, volume 244 of *IAU Symposium*, pages 53–62, May 2008.

[128] P. C. Clark, S. C. O. Glover, R. S. Klessen, and V. Bromm. Gravitational Fragmentation in Turbulent Primordial Gas and the Initial Mass Function of Population III Stars. *Astrophys. J.*, 727:110–+, February 2011.

[129] P. C. Clark, S. C. O. Glover, R. J. Smith, T. H. Greif, R. S. Klessen, and V. Bromm. The Formation and Fragmentation of Disks Around Primordial Protostars. *Science*, 331:1040–, February 2011.

[130] K. Jedamzik. Primordial black hole formation during the QCD epoch. *Phys. Rev. D*, 55:5871–+, May 1997.

[131] Lawrence M. Widrow. Origin of galactic and extragalactic magnetic fields. *Rev. Mod. Phys.*, 74(3):775–823, Jul 2002.

[132] Chiara Caprini and Ruth Durrer. Gravitational wave production: A strong constraint on primordial magnetic fields. *Phys. Rev. D*, 65(2):023517, Dec 2001.

[133] R. Durrer and C. Caprini. Primordial magnetic fields and causality. *J. Cosmol. Astropart. Phys.*, 11:10–+, November 2003.

[134] K. Subramanian and J. D. Barrow. Magnetohydrodynamics in the early universe and the damping of nonlinear Alfvén waves. *Phys. Rev. D*, 58(8):083502–+, October 1998.

[135] K. Jedamzik, V. Katalinić, and A. V. Olinto. Damping of cosmic magnetic fields. *Phys. Rev. D*, 57:3264–3284, March 1998.

[136] R. H. Cyburt, B. D. Fields, K. A. Olive, and E. Skillman. New BBN limits on physics beyond the standard model from ^{4}He ; (note that we used the pure ^{4}He results for ΔN_ν from this reference that were prefered by the author to the results from other light elements, personal communication with H.Cyburt). *Astropart. Phys.*, 23:313–323, April 2005.

[137] C. Caprini, R. Durrer, and E. Fenu. Can the observed large scale magnetic fields be seeded by helical primordial fields? *J. Cosmol. Astropart. Phys.*, 11:1–+, November 2009.

[138] Arthur Kosowsky, Michael S. Turner, and Richard Watkins. Gravitational waves from first-order cosmological phase transitions. *Phys. Rev. Lett.*, 69(14):2026–2029, Oct 1992.

[139] M. Kamionkowski, Arthur Kosowsky, and Michael S. Turner. Gravitational radiation from first-order phase transitions. *Phys. Rev. D*, 49(6):2837–2851, Mar 1994.

[140] T. Kahniashvili, A. Kosowsky, G. Gogoberidze, and Y. Maravin. Detectability of gravitational waves from phase transitions. *Phys. Rev. D*, 78(4):043003–+, August 2008.

[141] S. J. Huber and T. Konstandin. Gravitational wave production by collisions: more bubbles. *J. Cosmol. Astropart. Phys.*, 9:22–+, September 2008.

[142] F. A. Jenet et al. Upper Bounds on the Low-Frequency Stochastic Gravitational Wave Background from Pulsar Timing Observations: Current Limits and Future Prospects. *Astrophys.J.*, 653:1571–1576, December 2006.

[143] G. Hobbs, A. Archibald, Z. Arzoumanian, D. Backer, M. Bailes, N. D. R. Bhat, M. Burgay, S. Burke-Spolaor, D. Champion, I. Cognard, W. Coles, J. Cordes, P. Demorest, G. Desvignes, R. D. Ferdman, L. Finn, P. Freire, M. Gonzalez, J. Hessels, A. Hotan, G. Janssen, F. Jenet, A. Jessner, C. Jordan, V. Kaspi, M. Kramer, V. Kondratiev, J. Lazio, K. Lazaridis, K. J. Lee, Y. Levin, A. Lommen, D. Lorimer, R. Lynch, A. Lyne, R. Manchester, M. McLaughlin, D. Nice, S. Oslowski, M. Pilia, A. Possenti, M. Purver, S. Ransom, J. Reynolds, S. Sanidas, J. Sarkissian, A. Sesana, R. Shannon, X. Siemens, I. Stairs, B. Stappers, D. Stinebring, G. Theureau, R. van Haasteren, W. van Straten, J. P. W. Verbiest, D. R. B. Yardley, and X. P. You. The International Pulsar Timing Array project: using pulsars as a gravitational wave detector. *Classical and Quantum Gravity*, 27(8):084013–+, April 2010.

[144] M. Kramer et al. Strong-field tests of gravity using pulsars and black holes. *New Astron. Rev.*, 48:993–1002, December 2004.

[145] D. J. Schwarz. Evolution of Gravitational Waves Through the Cosmological QCD Transition. *Modern Physics Letters A*, 13:2771–2778, 1998.

[146] S. Schettler, T. Boeckel, and J. Schaffner-Bielich. Imprints of the QCD Phase Transition on the Spectrum of Gravitational Waves. *ArXiv e-prints*, October 2010.

[147] H. Kurki-Suonio and R. A. Matzner. Effect of small-scale baryon inhomogeneity on cosmic nucleosynthesis. *Phys. Rev. D*, 39:1046–1053, February 1989.

[148] H. Kurki-Suonio, R. A. Matzner, K. A. Olive, and D. N. Schramm. Big bang nucleosynthesis and the quark-hadron transition. *Astrophys.J.*, 353:406–410, April 1990.